

LONG TERM TRENDS IN LAKE MICHIGAN WAVE CLIMATE

A Thesis

Submitted to the Faculty

of

Purdue University

by

Nicholas R. Olsen

In Partial Fulfillment of the

Requirements for the Degree

of

Master of Science in Civil Engineering

May 2019

Purdue University

West Lafayette, Indiana

THE PURDUE UNIVERSITY GRADUATE SCHOOL
STATEMENT OF APPROVAL

Dr. Cary Troy, Chair

Lyles School of Civil Engineering

Dr. Dennis Lyn

Lyles School of Civil Engineering

Dr. Venkatesh Merwade

Lyles School of Civil Engineering

Approved by:

Dr. Dulcy M. Abraham

Chair of the Burke Graduate Program

To my parents.

ACKNOWLEDGMENTS

Thank you, Dr. Cary Troy, for coming up with an interesting research question and advising me along the way.

Dr. Dennis Lyn whose classes led me towards the statistical analysis I needed to answer my questions.

Dr. Venkatesh Merwade for serving on my committee.

Dr. Robert Jensen and the United States Army Corps of Engineers for providing me with so much data and making so much amazing material free to everyone online.

David Cannon for his practical knowledge of the the lake and always being there to add to the speculation on why my results looked the way they did.

My girlfriend, Alex Christensen, for her knowledge on coding, being a graduate student, and being there every night.

Finally to Draconian, Ashbury Heights, Delain, and Amorphis for music that moved me to jump up and dance around while writing.

TABLE OF CONTENTS

	Page
LIST OF TABLES	vii
LIST OF FIGURES	viii
ABSTRACT	xv
1 INTRODUCTION	1
1.1 Background	1
1.1.1 Long-term Trends in the Great Lakes	4
1.2 Research Questions and Hypotheses	6
1.2.1 Have waves in Lake Michigan increased in size over the 36-year NDBC record?	6
1.2.2 Has storm frequency or duration increased over the 36-year ND- BC record?	7
1.2.3 Has the direction of the waves changed?	7
1.2.4 Is the increasing lake level related to the size of the waves?	7
2 METHODS	8
2.1 Buoy Background	8
2.2 WIS Background	10
2.3 Identifying Trends	11
2.3.1 Data Cleaning	11
2.3.2 Have waves in Lake Michigan increased in size over the 36-year NDBC record?	12
2.3.3 Has storm frequency or duration increased over the 36-year ND- BC record?	18
2.3.4 Has the direction of the waves changed?	21
2.3.5 Is the increasing lake level related to the size of the waves?	21
3 RESULTS	23
3.1 Lake Michigan's Wave Climate	23
3.2 Have waves in Lake Michigan increased in size over the 36-year NDBC record?	27
3.2.1 Annual Means	27
3.2.2 Mean of Largest Five Independent Wave Heights	32
3.2.3 Mann-Kendall Test Results on Monthly Wave Height Means	35
3.2.4 Seasonal Dependence in Wave Height	35
3.2.5 Removing Seasonality from Wave Height Data	35

	Page
3.2.6 Removing Temporal and Spatial Dependence from Wave Height Data	42
3.3 Has storm frequency or duration increased over the 36-year NDBC record?	49
3.3.1 Trends in Storm Metrics	49
3.3.2 Shifting Extreme Value Distribution	53
3.4 Has the direction of the waves changed?	64
3.4.1 Trends in Annual Wave Frequency by Direction	64
3.4.2 Kernel Density Estimates of Wave Direction	68
3.5 Is the increasing lake level related to the size of the waves?	71
4 DISCUSSION	77
4.1 Have waves in Lake Michigan increased in size over the 36-year NDBC record?	77
4.2 Has storm frequency or duration increased over the 36-year NDBC record?	80
4.3 Has the direction of the waves changed?	83
4.4 Is the increasing lake level related to the size of the waves?	84
5 SUMMARY	85
6 RECOMMENDATIONS	87
REFERENCES	88
A DIRECTIONAL TRENDS	92
B DATA CLEANING	98
C EXTREME VALUE AND PARETO DISTRIBUTIONS	102
D SEASONAL MANN-KENDALL RESULTS FOR DIRECTIONAL BINS	111
E TRENDS IN STORM PARAMETERS	113

LIST OF TABLES

Table	Page
2.1 Buoy 45007's hull type history. [32]	9
2.2 Buoy 45007's electronic payload history. [32]	9
3.1 Summary of trends. Format: Median(95%CI)	31
3.2 Pearson's R correlation coefficients and p values (R-value, p-value) for paired lake level and wave height series.	74
B.1 Data removal and justification.	99
B.2 Value ranges of raw data.	100
B.3 Value ranges of data with officially recognized error values removed. . . .	101

LIST OF FIGURES

Figure	Page
2.1 Data available from Buoy 45007 in Lake Michigan's southern basin with the May-October cut-off shown in red [37].	13
2.2 Data available from Buoy 45002 in Lake Michigan's northern basin with the May-October cut-off shown in red [37].	13
2.3 Map of Lake Michigan and surrounding region indicating the position of the buoys and the corresponding extracted WIS data as well as nearshore station 94463, chosen for comparison [37,38].	14
3.1 Wave climate at the location of Buoy 45007 in Lake Michigan's southern basin separated in 10-degree directional bins. [37,38].	25
3.2 Wave climate at the location of Buoy 45002 in Lake Michigan's northern basin separated in 10-degree directional bins [37,38].	26
3.3 Yearly mean wave heights for waves $\geq 0.25m$. Buoy and WIS series restricted to the months of May-October. Significant trends, found only in the buoy series, are depicted. [37,38]	29
3.4 Yearly mean wave heights for complete WIS hindcast series. No significant trends were detected. [38]	29
3.5 Trends in the annual mean of hourly significant wave heights (1979-2014) including full year and waves of all sizes) at all of the WIS nearshore stations on Lake Michigan [38]. Stations in gray do not have significant Theil-Sen regression slopes.	30
3.6 The annual series of the mean of the five largest independent wave heights was tested for trends using Theil-Sen regression slopes. No significant trends were detected in the data. For compatibility between series all data was limited to waves $\geq 0.25m$, occurring between May and October. [37,38].	33
3.7 The annual series of the mean of the five largest independent wave heights was tested for trends using Theil-Sen regression slopes. No significant trends were detected in the data. This analysis of the WIS data did not limit the series by height or season. [38].	33

Figure	Page
3.8 Trends in the annual mean of the five largest independent wave heights (1979-2014) at all of the WIS nearshore stations [38]. Stations in gray do not have significant Theil-Sen regression slopes. This analysis of the WIS data did not limit the series by height or season. No significant trends were detected.	34
3.9 Monthly mean wave heights from the WIS model at Lake Michigan's buoy locations. No monotonic trends were detected by the modified Mann-Kendall statistic for autocorrelated series [38].	36
3.10 Adjusted Mann-Kendall test results for monotonic trends in the monthly mean wave heights at all Lake Michigan nearshore stations [38].	37
3.11 Seasonal Mann-Kendall test results for monotonic trends in the monthly mean wave heights at all Lake Michigan nearshore stations. [38].	38
3.12 Periodograms and autocorrelation results indicate a 12-month seasonal pattern in the WIS wave model [38]. The periodograms were performed on the monthly means of the entire WIS dataset and show a peak frequency of 1/12. The autocorrelation function was taken of the monthly means and shows a 12-step or 12-month period. These results indicate seasonal dependence in wave height series.	39
3.13 Yearly mean wave heights of hourly deseasoned data (May-October, $H_s > 0.25\text{m}$). Series were tested for trends using 95% confidence interval of Theil-Sen regression slopes. No significant trends were detected. [37, 38]	41
3.14 Yearly mean wave heights of hourly deseasoned data (all year, all heights). Series were tested for trends using 95% confidence interval of Theil-Sen regression slopes. No significant trends were detected. [38]	41
3.15 Comparison of wave-height trend results for annual means using (A) Theil-Sen regression confidence intervals, (B) Mann-Kendall test with Theil-Sen regression, and (C) seasonally differenced series with Theil-Sen confidence intervals on WIS nearshore stations [38]. Significant trends were not detected at stations shown in gray.	43
3.16 Comparison of wave-height trend results for monthly means using (A) Theil-Sen regression confidence intervals, (B) adjusted Mann-Kendall test with Theil-Sen regression, and (C) seasonally differenced series with Theil-Sen confidence intervals on WIS nearshore stations [38]. Significant trends were not detected at stations shown in gray.	44

Figure	Page
3.17 Comparison of wave-height trend results for annual means separated into 30-degree bins using (A) Theil-Sen regression confidence intervals, (B) Mann-Kendall test with Theil-Sen regression, and (C) seasonally differenced series with Theil-Sen confidence intervals on WIS nearshore stations [38]. Significant trends were not detected at stations shown in gray. .	45
3.18 Comparison of wave-height trend results for monthly means separated into 30-degree bins using (A) Theil-Sen regression confidence intervals, (B) adjusted Mann-Kendall test with Theil-Sen regression, and (C) seasonally differenced series with Theil-Sen confidence intervals on WIS nearshore stations [38]. Significant trends were not detected at stations shown in gray.	46
3.19 Comparison of Lake Ontario wave-height trend results for annual means separated into 30-degree bins using (A) Theil-Sen regression, (B) modified Mann-Kendall test with Theil-Sen regression, and (C) seasonally differenced series with Theil-Sen confidence intervals on WIS nearshore stations [38]. Significant trends were not detected at stations shown in gray. .	47
3.20 Comparison of Lake Ontario wave-height trend results for monthly means separated into 30-degree bins using (A) Theil-Sen regression, (B) modified Mann-Kendall test with Theil-Sen regression, and (C) seasonally differenced series with Theil-Sen confidence intervals on WIS nearshore stations [38]. Significant trends were not detected at stations shown in gray. .	48
3.21 Annual storm parameter values using the WIS model at Lake Michigan buoy locations applied to entire year of WIS data. Tested for long term trends using 95% Theil-Sen slope confidence intervals. [38]	50
3.22 Annual storm parameter values using the WIS model at Lake Michigan buoy locations applied to May-October series of buoy and WIS data. Tested for long term trends using 95% Theil-Sen slope confidence intervals. [37,38]	51
3.23 Annual storm parameter values using all Lake Michigan WIS nearshore stations applied to entire year of WIS data. Tested for long term trends using 95% Theil-Sen slope confidence intervals. Significant trends were not detected at stations shown in gray. [38].	52
3.24 Probability of receiving a wave 5m or greater at the three WIS sites in a year, from the generalized extreme value distribution determined by a growing window of annual maxima after the first decade [38].	56
3.25 Probability of receiving a wave 5m or greater at the three WIS sites in a year, from the generalized extreme value distribution determined by moving decadal window of annual maxima [38].	56

Figure	Page
3.26 Slope of Theil-Sen regression on probability of receiving a wave larger than 5m for full WIS model of Lake Michigan [38]. Probabilities determined from an extreme value distributions generated from a growing window of yearly maxima.	57
3.27 Slope of Theil-Sen regression on probability of receiving a wave larger than 5m for full WIS model of Lake Michigan [38]. Probabilities determined from an extreme value distributions generated from a moving window of yearly maxima.	58
3.28 Slope of Theil-Sen regression on probability of receiving a wave larger than 5m for full WIS model of Lake Ontario [38]. Probabilities determined from an extreme value distributions generated from a growing window of yearly maxima.	59
3.29 Slope of Theil-Sen regression on probability of receiving a wave larger than 5m for full WIS model of Lake Ontario [38]. Probabilities determined from an extreme value distributions generated from a moving window of yearly maxima.	60
3.30 Slope of Theil-Sen regression on probability of receiving a wave larger than 5m for publicly available WIS wave model nearshore stations in Lake Michigan [38]. Probabilities determined from an extreme value distributions generated from a growing window of yearly maxima.	61
3.31 Slope of Theil-Sen regression on probability of receiving a wave larger than 5m using WIS model at buoy locations and a southern basin nearshore station [38]. Probabilities determined from Pareto distributions generated from a growing yearly window of peak $> 2m$ event heights. 95% confidence intervals developed by bootstrapping.	62
3.32 Slope of Theil-Sen regression on probability of receiving a wave larger than 5m using WIS model at buoy locations and a southern basin nearshore station [38]. Probabilities determined from Pareto distributions generated from a moving decadal window of peak $> 2m$ event heights. 95% confidence intervals developed by bootstrapping.	63
3.33 Annual trends in hourly frequency for wave approach direction in 30-degree bins from the WIS model at Buoy 45007. Significant Theil-Sen trends are indicated by depicting the slope as a red line. [38]	65
3.34 Annual trends in hourly frequency for wave approach direction in 30-degree bins from the WIS model at Buoy 45002. Significant Theil-Sen trends are indicated by depicting the slope as a red line. [38]	66

Figure	Page
3.35 Annual trends in hourly frequency for wave approach direction in 30-degree bins from the WIS model at all WIS nearshore stations. [38]	67
3.36 Annual trends in hourly frequency for wave approach direction in 30-degree bins from the WIS model at all WIS nearshore stations in Lake Ontario. [38]	67
3.37 Kernel-Density Estimate of probability distributions functions of wave directions for Buoy 45007, divided by month. A 40% data completeness threshold was required to generate a plot.	69
3.38 Integration of annual PDFs of wave approach direction to determine the annual trends in Buoy 45007's probability of receiving a wave from 90-degree bins centered on the four cardinal directions. No significant trends were detected. A 40% data completeness threshold within a month was required to generate a point.	70
3.39 Monthly wave height means from WIS at Buoy 45007 and the USACE lake level record. [38, 43]	72
3.40 60-month moving averages of monthly wave height mean from WIS at Buoy 45007 and the USACE lake level record. [38, 43]	72
3.41 Monthly wave height maxima from WIS at Buoy 45007 and the USACE lake level record. [38, 43]	73
3.42 Change in Pearson's R with increasing moving average range. These coefficients were all found to be significant with $P < 0.05$.	73
3.43 Identifying seasonality in Lake Michigan water level records using periodogram and autocorrelation function results. A peak frequency is seen at 12 months in the periodogram with lower frequency cycling. The autocorrelation function shows sinusoidal decay with a period of 12 months.	75
3.44 Monthly means of deseasoned wave height at Buoy 45007 and USACE lake level. Non-significant correlation of -0.1 directly, 0.06 with six-month lag. [38, 43]	75
3.45 Monthly max of deseasoned wave heights and deseasoned USACE lake levels. Correlation of -0.32 directly, 0.34 with six-month lag. [38, 43]	76
A.1 Directional trends in annual wave heights at all WIS nearshore stations.	93
A.2 Directional trends in annual wave heights at all WIS nearshore stations in Lake Ontario.	93
A.3 Directional trends in annual wave time at buoy 45007.	94
A.4 Directional trends in annual wave time at buoy 45002.	94

Figure	Page
A.5 Directional trends in annual wave time at buoy 45007. Summer Only. . . .	95
A.6 Directional trends in annual wave time at buoy 45002. Summer Only. . . .	95
A.7 Directional trends in annual wave time at buoy 45007. Summer Only. . . .	96
A.8 Directional trends in annual wave time at buoy 45002. Summer Only. . . .	96
A.9 Directional trends in annual wave spatial frequency at all WIS nearshore stations.	97
A.10 Directional trends in annual wave spatial frequency at all WIS nearshore stations in Lake Ontario.	97
C.1 Slope of Theil-Sen regression on probability of receiving a wave larger than 5m between May and October for full WIS model of Lake Michigan [38].	103
C.2 Slope of Theil-Sen regression on probability of receiving a wave larger than 5m between May and October for full WIS model of Lake Michigan [38].	104
C.3 Probability of receiving a wave 5m or greater at the three WIS sites in a year, from the generalized extreme value distribution determined by a growing window of annual maxima after the first 10 years [38]. Confidence intervals determined by bootstrapping from annual maxima.	105
C.4 Probability of receiving a wave 5m or greater at the three WIS sites in a year, from the generalized extreme value distribution determined by moving 10-year window of annual maxima [38]. Confidence intervals de- termined by bootstrapping from annual maxima.	105
C.5 Probability of receiving a wave 5m or greater at the three WIS sites in a year, from the generalized extreme value distribution determined by a growing window of annual maxima after the first 12 years [38].	106
C.6 Probability of receiving a wave 5m or greater at the three WIS sites in a year, from the generalized extreme value distribution determined by moving 12-year window of annual maxima [38].	106
C.7 Probability of receiving a wave 5m or greater at the three WIS sites in a year, from the generalized extreme value distribution determined by a growing window of annual maxima after the first 15 years [38].	107
C.8 Probability of receiving a wave 5m or greater at the three WIS sites in a year, from the generalized extreme value distribution determined by moving 15-year window of annual maxima [38].	107

Figure	Page
C.9 Slope of Theil-Sen regression on probability of receiving a wave larger than 5m using WIS model at buoy locations and a southern basin nearshore station [38]. Generalized Pareto distributions generated from a growing yearly window of peak $> 2m$ event heights after the first 15 years.	108
C.10 Slope of Theil-Sen regression on probability of receiving a wave larger than 5m using WIS model at buoy locations and a southern basin nearshore station [38]. Generalized Pareto distributions generated from a moving 10-year window of peak $> 2m$ event heights after the first 15 years.	108
C.11 Slope of Theil-Sen regression on probability of receiving a wave larger than 5m using WIS model at buoy locations and a southern basin nearshore station [38]. Generalized Pareto distributions generated from a growing yearly window of peak $> 3m$ event heights after the first 10 years.	109
C.12 Slope of Theil-Sen regression on probability of receiving a wave larger than 5m using WIS model at buoy locations and a southern basin nearshore station [38]. Generalized Pareto distributions generated from a moving 10-year window of peak $> 3m$ event heights after the first 10 years.	109
C.13 Slope of Theil-Sen regression on probability of receiving a wave larger than 5m using WIS model at buoy locations and a southern basin nearshore station [38]. Generalized Pareto distributions generated from a growing yearly window of peak $> 3m$ event heights after the first 15 years.	110
C.14 Slope of Theil-Sen regression on probability of receiving a wave larger than 5m using WIS model at buoy locations and a southern basin nearshore station [38]. Generalized Pareto distributions generated from a moving 15-year window of peak $> 3m$ event heights after the first 15 years.	110
D.1 Seasonal Mann-Kendall test results for monotonic trends in the monthly mean wave heights at all Lake Michigan nearshore stations for isolated 30-degree directional bins. [38].	112
E.1 Annual storm ($H_s > 3m$) parameter values from WIS model at Lake Michigan buoy locations using entire year of WIS data tested for long term trends using 95% Theil-Sen slope confidence intervals [38].	114

ABSTRACT

Olsen, Nicholas R. MSCE, Purdue University, May 2019. Long Term Trends in Lake Michigan Wave Climate. Major Professor: Cary Troy.

Waves are a primary factor in beach health, sediment transport, safety, internal nutrient loading, and coastal erosion, the latter of which has increased along Lake Michigan's western coastline since 2014. While high water levels are undoubtedly the primary cause of this erosion, the recent losses may also be indicative of changes in the lake's wind-driven waves. This study seeks to examine long-term trends in the magnitude and direction of Lake Michigan waves, including extreme waves and storm events using buoy measurements (National Data Buoy Center Buoys 45002 and 45007) and the United States Army Corps of Engineers Wave Information Study (USACE WIS) wave hindcast.

Tests show significant long-term decreases in annual mean wave height in the lake's southern basin (up to -1.5mm/yr). When wave-approach direction was removed by testing directional bins for trends independently, an increase in the extent of the affected coast and rate of the shrinking waves was found (up to -4mm/yr). A previously unseen increasing trend in wave size in the northern basin (up to 2mm/yr) was also revealed.

Data from the WIS model indicated that storm duration and peak wave height in the southern basin has decreased at an averaged rate of -0.085hr/yr and -5mm/yr, respectively, from 1979 to 2017. An analysis of the extreme value distribution's shape in the southern basin found a similar pattern in the WIS hindcast model, with the probability of observing a wave larger than 5 meters decreasing by about $-0.0125yr^{-1}$. In the northern basin, the probability of observing a wave of the same size increased at a rate of $0.0075yr^{-1}$.

The results for trends in the annual means revealed the importance of removing temporal- and spatial-within-series dependencies, in wave-height data. The strong dependence of lake waves on approach direction, as compared to ocean waves, may result from the relatively large differences in fetch length in the enclosed body of water. Without removal or isolation of these dependencies trends may be lost. Additionally, removal of the seasonal component in lake water level and mean wave-height series revealed that there was no significant correlation between these series.

1. INTRODUCTION

1.1 Background

Surface waves are a fundamental consideration in any coastal or marine engineering project because of their role in nearshore processes including shoreline erosion and undercutting of infrastructure. Therefore, engineers typically design for the largest subset of expected waves to minimize risk to structures and human life.

The Intergovernmental Panel on Climate Change (IPCC) has determined that there exists a changing wind climate around the world [1]. As the primary cause behind formation of surface waves in large water bodies many researchers have hypothesized that there exists a corresponding change in the world's wave climate as well. Studies looking for long-term trends in wave climate have shown increased hurricane wave sizes [2] in the Atlantic, as well as an increasing annual mean wave height in the Pacific [3,4].

Long-term wave climate studies prior to the 1990s used a wide variety of datasets, varying in quality and instrumentation, including shipborne wave recorders, ocean weather stations, and visual observations to look for long-term trends [5]. However, these datasets were often recorded inconsistently and left records that were difficult to compare. Most measurements, recorded by sailors, were typically taken relatively far from the coast, limiting their utility to coastal engineers. Nonetheless, a 1990 review of the early work on wave-climate trends suggested that there was an overall agreement on an increasing trend in the mean wave heights observed in the North Atlantic [5].

More recent studies have primarily relied on long-term records of coastal wave heights, recorded by the United States' National Oceanographic and Atmospheric Administration National Data Buoy Center (NOAA NDBC) [2-4, 6], which began

placing buoys along the U.S. coastline during the 1970s and 1980s. These buoys transmit hourly wave spectral data from internal accelerometers. Typical wave parameters, such as significant wave height, direction, period, etc., are derived from the spectra and published online. Their use continues with periodic updates in measurement hardware and software.

The significant wave height (H_s), calculated from the buoy's results, is the primary wave parameter used in studies of wave climate. H_s attempts to capture the wave size that a person watching the ocean's surface over a period of time might report as the wave size. The probability distribution function (PDF) of all wave heights over this time interval is expected to follow the Rayleigh distribution, which is strongly right skewed [7]. H_s is calculated from this distribution by taking the mean of the largest third of the waves. A similar parameter, H_{m0} , differs from H_s only by a small percentage typically, is determined using $4\sqrt{M_0}$ where M_0 is the zeroth moment of the wave spectra recorded over an interval of time.

In 2000, Komar and Allen showed a temporally increasing wave height trend in four NOAA NDCB buoys along the Pacific coast [3]. This study looked at the annual mean of all waves and the annual mean of the winter (October-March waves) and required a 90% data availability within each month for inclusion in the regression. The p-value of these trends is not given. Komar and Allen (2000) reported a relationship between storm frequency and El Niño events, but no increasing trend in storm frequency was found to explain the overall increasing trends in the mean wave heights [3].

This study was followed in 2010 by Ruggiero et al. [4] using NOAA NDBC Buoy 46005, off the coast of Alaska, to examine trends in the significant wave heights in that region from 1976 to 2007. Further analysis was performed to study how these increasing annual means influenced the probability distributions of the waves approaching the coast. By sub-sampling the hourly NDBC data based on mean storm duration to obtain independent values, an estimated PDF of wave heights over the

last decade was shown to have shifted towards larger wave-height values, indicating an increased probability of receiving larger waves [4].

In 2011, the results of studies using the NOAA NDCB records were questioned over the quality and consistency of the data [6]. Hardware and software changes over the buoys' 46-year history led to questions about the record's utility in determining the presence of long-term trends, without adjustment to the values [6]. The RHtestV3 statistical software, developed by Wang and Feng [8] to find changepoints in long-term environmental datasets, was used to determine the presence of step changes in buoy wave-height records. Gemmrich et al. (2011) determined that if these step changes were adjusted for in the raw data record, the significant trends previously found in the Pacific were eliminated [6].

By using historical wave data for coastal design engineers make an assumption of stationarity: that the distribution each wave is drawn from remains the same and that the covariance of two values in series is independent of their temporal position. In the long-term data may lead to under- or overestimates of wave parameters if climate trends exist. Since wave behavior is highly seasonal, the annual series are often not stationary and these seasonal effects may mask underlying long-term trends if they exist.

Complications from the statistical assumptions of the mean and regression led Vanem and Walker (2013) to work on wave trend analysis using statistical techniques developed specifically for dependent time series analysis [9]. This work used the ERA-40 wave dataset for the North Atlantic developed by the European Centre for Medium-Range Weather Forecasts instead of buoy data [9]. The use of seasonal differencing to create a "deseasoned" dataset, now with stationary annual series, showed an increasing trend in the waves of the North Atlantic driven by waves that occurred during the winter season [9]. Removal of seasonality is often used in studies of climate to focus on trends rather than regular seasonal variation [10–12]. This study also applied the Theil-Sen regression technique to limit the impact that outliers have on the least-squares regression [9].

1.1.1 Long-term Trends in the Great Lakes

Prior work on long-term climate trends in the Laurentian Great Lakes have looked into ice-cover [13], wind [14], and temperature [15]. Each of these studies concluded that changes had occurred. Surface waves are also studied in the Laurentian Great Lakes system, because they are found to drive many natural phenomena such as the production of aerosols [16, 17], the transport of sediment [18], and the orientation of deltaic zones [19]. However, long-term trends in the surface waves have not been examined.

Coastal aerosol production is attributed to breaking waves in large freshwater lakes [16]. Aerosolized particles are expected to play a role in local climate forcings given their light-scattering properties [16]. The particles generated on Lake Michigan have been anticipated to influence the climate around the lake, and are hypothesized to generate higher particle concentrations with greater regularity than atmospheric mechanisms in the area [16].

Sediment plumes resulting from coastal and benthic erosion caused by waves have been shown to have significant impacts on water quality and ecosystem structure [20]. Areas within large sediment plumes have been shown to resemble more eutrophic systems than regions outside the plume [20]. Sediment transport is dependent on wave height to the $5/2$ power meaning that over a span of time it is the larger waves that result in the majority of sediment suspension [7]. Coastal longshore currents, generated by waves breaking at an angle to shore, move sediment plumes along a coast in the prevailing wave direction [21].

Many areas of research have found evidence of long-term changes in and around Lake Michigan [22,23]. Changes in the lake's trophic structure have been dramatically influenced by the introduction of invasive species, notably *Dreissena rostriformis bugensis* [22]. Declines in phytoplankton productivity and seasonal diatom blooms have contributed to a decreasing trend in lake productivity [22].

Long-term work on Lake Michigan's water quality has also shown declines in chlorophyll and nutrient uptake [23]. These changes are attributed to the presence of the dreissenid mussels [23]. These filter-feeding organisms have reduced populations of plankton and algae that previously utilized the lake's excess nitrate [23]. With *Dreissena rostriformis bugensis* concentrated along the lake's coast [24], wave suspended sediments and coastal erosion could influence their long-term impact on the lake's ecosystem.

Work showing long-term changes in the Laurentian Great Lakes has shown decreasing annual ice-cover [13] and increasing water temperature in Lake Superior. In 2002, Waples and Klump showed that shifts in wind strength and direction had occurred across the entire Laurentian Great Lakes region [14]. From the 1980s to the 1990s they found an easterly shift in wind direction.

In 2017, articles describing increasing beach erosion around Lake Michigan began appearing in the popular media. The erosion, encroaching on private homes as well as public works, has been increasing in rate since 2014 [25]. The increasing rate of erosion, the changing wind climate, and numerous studies indicating significant changes in the ocean's wave climate led to questions about the possibility of long-term trends existing in Lake Michigan. The Lake Michigan coast is home to several major cities and ports which serve as international shipping hubs. Changes in the already hazardous wave climate may be a serious economic concern to the region's residents.

The waves in Lake Michigan are generated by wind acting on the surface of the water. A change in wind direction is expected to directly impact the direction of wave travel. Compared to ocean waves, the Great Lakes have much greater relative differences in fetch length as direction changes. The enclosed lake waves are more likely to be fetch-limited than ocean waves. With primarily wind-driven waves across the lake, a shift in wind direction can indirectly impact the wave height by changing the fetch direction and therefore the height the wave builds to in a fetch-limited,

enclosed water body. Previous studies have largely ignored the question of wave direction likely due to the primarily duration-limited ocean wave environment.

Lake Michigan's water level has been higher than its mean level since 2015 and continues to trend upwards [26]. Higher water levels will lead to coastal erosion, beach recession, and mass failure, similar to the effect of large wave events [7]. While the lake level will be responsible for a component of the erosion, a 1997 paper by Meadows et al. suggested that there was a strong correlation between Lake Michigan's monthly mean water levels and the wave heights [27]. Pearson correlation coefficients of 0.69 and 0.73 (with a one-year lag applied to the water level) were determined after applying a 60-month moving average to the data to remove within-series dependence on season. This contrasts with a 2012 report published by the United States Army Corps of Engineers, which showed no correlation between extreme wave events and the water level of the lake [28]. If the water level is related to wave climate in multi-year series of monthly means, the recent erosion may be impacted by both phenomena.

1.2 Research Questions and Hypotheses

This review indicating the existence of long-term changes in the physical climate of the Great Lakes as well as increasing trends in wave height around the world led to questions about the possibility of these trends in Lake Michigan. Currently, there is no work examining the long-term wave climate in the Laurentian Great Lakes. Lake Michigan, with two NOAA NDBC buoys measuring waves heights since 1981, and serving as important economic resource to Chicago and Milwaukee, makes it an important place to examine changes in the wave climate.

1.2.1 Have waves in Lake Michigan increased in size over the 36-year NDBC record?

This study hypothesized that long term increasing trends will be found in Lake Michigan's waves. This hypothesis is motivated by prior studies indicating increases in wave heights around the world [3–5, 9], as well as the increasing erosion reported

regionally [25]. While studies have been conducted in the ocean, as a large body of water, Lake Michigan might be anticipated to show similar trends.

1.2.2 Has storm frequency or duration increased over the 36-year NDBC record?

This study hypothesizes that storm frequency and duration will show increasing trends. Again, prior research in the world's oceans has indicated that storm behavior has shown increasing trends [2]. Climate change, generally, is expected to increase extreme weather behavior [29]. Additionally, the coastal erosion noticed by the public around the lake could be indicative of increasing storms since beach profiles are expected to be determined by large events that remove material from the shore [30].

1.2.3 Has the direction of the waves changed?

From the IPCC's prediction of Earth's changing wind climate and Waples and Klump's 2002 result indicating directional shifts in wind over the Great Lakes, we hypothesized that the approach direction of Lake Michigan's waves would show trends in annual frequency [1, 14]. Lake Michigan's waves are driven primarily by wind over the lake so it is expected that disturbance to the spatial pattern of the wind will be reflected in the waves [31].

1.2.4 Is the increasing lake level related to the size of the waves?

After visualizing the homogenizing effect of the 60-month moving average applied by Meadows et al. (1997) and the lack of a relationship found by the USACE between lake level and extreme wave events [27, 28] we hypothesized that wave climate would not be related to the lake level.

2. METHODS

2.1 Buoy Background

Two NDBC buoys exist in Lake Michigan, located in the northern (45002 45.344N, 86.411W) and southern (45007 42.674N, 87.026W) basins. The two buoys have taken hourly measurements of wave properties since 1979 and 1981, respectively. The NDBC buoy program collects data from these and hundreds of other buoys around the coastal United States as part of a safety network for water users and planners. In recent years, researchers have begun to use these buoys to study trends in the wave climate as they form one of the most consistent long-term records of wave properties to date.

In the Great Lakes, due to the danger posed by winter ice, buoys must be retrieved before winter each year. This leads to larger and more frequent gaps in the Lake Michigan buoys than are typically found in the ocean-deployed buoys. With winter waves generally observed to be larger than those in the summer, the NDBC datasets do not include measurements of the lake's largest waves. This limitation severely impacts the utility of buoy data for coastal engineers since it is the largest waves that constrain coastal design.

Since their original deployment, most of the buoys in the NDBC network have seen periodic upgrades throughout their lifetime. Changes involve buoy hull design and size, as well as electronic and software updates. Tables 2.1 and 2.2 indicate the available history of hull types and electronic payloads used by Buoy 45007 in Lake Michigan.

Table 2.1. Buoy 45007's hull type history. [32]

Deployment Date	Hull Type
3/88	6N (6 meter NOMAD)
3/89	3D (3 meter discus)
4/07	3DV (3 meter discus)

Table 2.2. Buoy 45007's electronic payload history. [32]

Deployment Date	Electronic System
3/88	DACT (Data Acquisition and Control Telemetry)
4/90	DACT/DW (Directional Waverider)
3/92	DACT/MO-DW (Magnetometer-Only - Directional Waverider)
3/98	DACT DWA/MO (Directional Wave Analyzer)
10/07	DACT DWA (DWA/Magnetometer-Only configuration)
4/10	AMPS/DDWM (Digital Directional Wave Module)
5/15	AMPS/DDWM SMART

2.2 WIS Background

The USACE WIS hindcast utilizes three wave models to determine wave heights along the coastal United States [33]. The Great Lakes region uses the WAM discrete spectral model, which applies an energy balance to a 2-D wave field driven by wind [33]. The WAM model uses wind fields generated from land-based stations, operated by several agencies [34]. This collection of point-source meteorological data is combined into a regional wind field using the natural neighbor interpolation algorithm [34].

The model has options to include water body geometry, wind fields, time step, changing water depths, and the earth's curvature [35]. While the model utilizes and produces the wave spectra at each grid point at each time step, it also outputs wave height, wave period, and mean wave direction for general use [35]. The USACE WIS online database provides the general public with the model results at coastal stations. Hourly data from the nearshore stations is available from 1979 to 2014. Users must place requests with the USACE for access to the entire gridded dataset or more recent data.

Data produced by the WIS model in Lake Michigan is validated by comparison with data collected by NOAA NDBC buoys 45007 and 45002, described above and used in this study as well [34]. Time series of significant wave height, peak wave period, mean wave period, wave direction, wind speed, and wind direction are compared [34]. The validation study concluded that errors in the model are likely due to errors made interpolating wind fields and that the natural neighbor interpolation did not capture the strongest north/south winds [34]. Studies have found good agreement between the WIS hindcast and data ($R^2=0.64$) from field instrumentation, with the WIS model predicting wave heights approximately 30% larger than measured [36]. In the most extreme events ($H_{mo} \approx 4-$ to 6-meter) the WIS model under-predicted wave height [34, 36].

There are also concerns regarding the quality of the buoy data against which the WIS hindcast was validated [34]. Buoy meta-data is not well recorded, and other studies have shown that sensor package and hull history can influence records of wave parameters [6, 34].

2.3 Identifying Trends

2.3.1 Data Cleaning

Historical hourly data from NOAA’s NDBC buoys 45007 and 45002 were downloaded on 12/24/2017. The annual data files were imported as floating point arrays into python without headers, which were imported separately to look for changes in the structure of the files. In 2005, a new column was added to indicate the minute of each data point’s collection. For 2007, a second header row was added to indicate the units of measurement in each column.

Histograms were then plotted for wind direction, wind speed, gust speed, wave height, dominant wave period, average wave period, mean wave direction, air temperature, and water temperature. This was to allow a qualitative look at the distribution of the data set and the prevalence of error values. The range of values in each of these data sets was printed.

Rather than remove errors across all parameters, these values, officially indicated by a 99 or 999 (used when 99 was a viable data point, ie, direction), were replaced with the NaN indicator. This value, recognized by Python, can easily be managed or removed from analysis later. The separate year, month, day, and hour values were then merged to create a single date-time variable. Each cleaned dataset was then plotted against time.

These plots were examined for apparently erroneous data. This was determined by looking for rapid fluctuations of the water temperature and consistently similar readings of air and water temperature. These fluctuations were hypothesized to indicate that the buoy had been activated before deployment and represented transport to the

field. Particular attention was paid to the early and late season when the buoy was just deployed or prepared for removal. If this was concluded based on temperature data all parameters were removed from the cleaned data. Table B.1 in Appendix B describes the position of the removed data and the justification for removal.

To complement the buoy data, the WIS hindcast was utilized as well. The points on Lake Michigan corresponding to the buoy locations were extracted from the complete lake's model, as well as one of the nearshore stations available from the USACE WIS website. This nearshore station was included to visualize temporal cycles or patterns that may be hidden on plots including trends in all of the nearshore stations. The data from these three WIS stations are used as a comparison to buoy data for accuracy, and to extend the analysis into the winter months. Figure 2.3 indicates the location of the NDBC buoys as well as the nearshore station.

2.3.2 Have waves in Lake Michigan increased in size over the 36-year NDBC record?

Annual Means

An initial subsample was created by clipping each year to the same beginning and ending day, regardless of actual data availability. The cutoff days were chosen as the start and end of May and October, respectively. This subsample was generated to eliminate seasonal weighting in yearly means due to variability in the dates of buoy deployment and retrieval. The available data range and the results of the clipping can be seen in figures 2.1 and 2.2.

In 2008, the buoy appeared to stop recording small waves as zero meters in height and began using error values instead. During the same year, the wave height threshold seemed to have been lowered, before recording the value as an error or zero. No longer including zero-height waves in the analysis had the apparent effect of artificially reducing the mean wave size in the years following that change. Therefore the series was again resampled to removed wave height measurements of smaller than 0.25 meters.

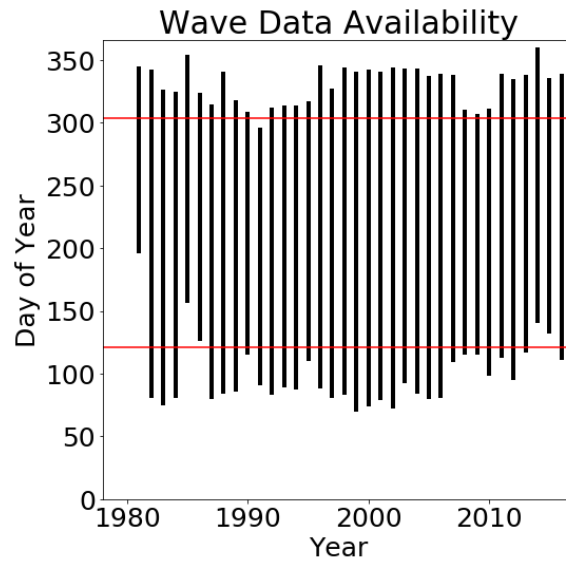


Figure 2.1. Data available from Buoy 45007 in Lake Michigan's southern basin with the May-October cut-off shown in red [37].

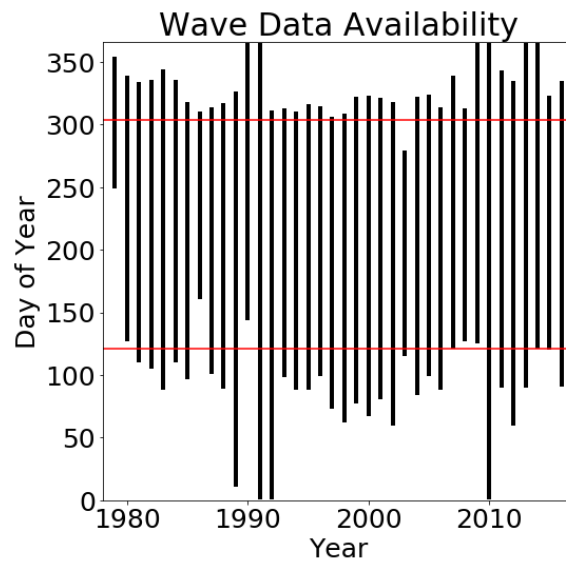


Figure 2.2. Data available from Buoy 45002 in Lake Michigan's northern basin with the May-October cut-off shown in red [37].

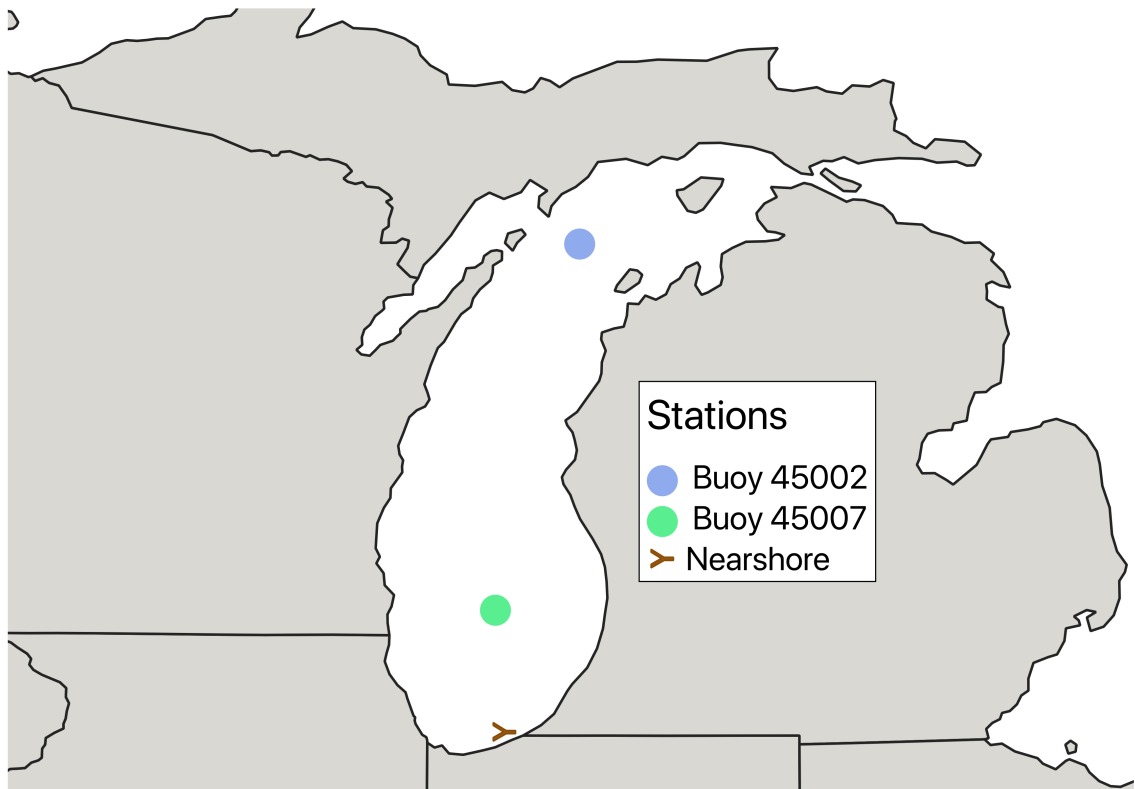


Figure 2.3. Map of Lake Michigan and surrounding region indicating the position of the buoys and the corresponding extracted WIS data as well as nearshore station 94463, chosen for comparison [37, 38].

Three locations from the WIS model were selected, two corresponding to the NDBC buoy locations and a third, nearshore station 94463, located in the southern basin.

For comparability to the buoy data the WIS model's wave heights were also subsampled to waves 0.25 meters and larger occurring between May and October. Separate analyses were performed on the complete WIS dataset. Data points occurring during ice coverage are removed in all analyses.

To explore long-term trends in the described series, Theil-Sen regressions were applied to annual wave height means from each of the series described above. Theil-Sen regressions were used in this study instead of least-squares to reduce the impact of outliers on the results. The SciPy `stats.mstats.theilslopes` method was used to obtain all the Theil-Sen slope and its 95% confidence interval. Theil-Sen results that did not contain zero within the 95% confidence interval for the regression slope were accepted as significant. The accepted trend results are depicted as lines on plots or colored points on maps. Rejected trends are not shown on scatter plots and are depicted as grayed-out points on maps.

Mean of Largest Five Independent Wave Heights

Each of the five data series was subjected to a peaks-over-threshold subsample by selecting the peak wave height within each event for which the wave height series exceeded two meters. The two meter threshold was chosen due to the USACE definition for a storm wave [39]. The events isolated by the peaks-over-threshold method are assumed to be independent of each other in this analysis.

To examine the trend in wave heights during the largest storms of each year, the yearly mean was taken of each year's five largest waves from these independent storm events.

Mann-Kendall Test Results on Monthly Wave Height Means

Results from the augmented Dickey-Fuller test indicate that hourly wave data series are not independent ($p < 0.05$) and that the hourly wave data series had an autoregressive unit root. This means that the hourly wave heights were influenced by prior wave heights.

Autocorrelation within the residuals of a data series can impact results of regression analyses [40]. The Mann-Kendall test is a statistical test for trends in time series, but typically assumes that each data point is independently sampled and has been shown to have been influenced by autocorrelated data [40]. However, to overcome this common concern Hamed and Rao (1998) developed a modified Mann-Kendall test that accounts for the presence of autocorrelation in a series [40].

Hourly wave data are expected to have a positive autocorrelation, which can lead to increases in the detection rate of non-existent trends [40] which led me to use of the modified Mann-Kendall test on the WIS data at the buoy locations and the nearshore stations for series of monthly means in this study. Only the WIS model was used in these tests due to the lack of gaps in the available data. To apply Hamed and Rao's (1998) adjusted Mann-Kendall test to monthly wave-height means, the `mkTrend` method from R's `fume` package was utilized [41]. The same method and package were applied to annual means to obtain Mann-Kendall results for the non-autocorrelated annual wave-height means [41].

Finally, to avoid problems with the autocorrelated nature of the monthly means and the Mann-Kendall's test on the monotonicity of a trend, the seasonal Mann-Kendall was applied as well using the `smk.test` method from R's `trend` package. Where necessary, data gaps were filled using `auto.arima` to generate an ARIMA time series model from the complete portion of the series. The missing values are fit from the ARIMA using a Kalman filter (`KalmanRun`, from R's `forecast` package).

Seasonal Dependence in Wave Height

Another method for dealing with autocorrelation within a time series is to remove it by using backwards differencing. Subtracting prior values can remove the dependence of the series on the time of year or season, a contributing factor to the autocorrelation in the wave series.

To determine the seasonality of the wave climate, a periodogram and autocorrelation function of the WIS model at both buoy locations was generated using Python's SciPy `signal.periodogram` and R's `acf` methods, respectively. Only the WIS model was used because of the completeness of the data which overcame the limitations associated with the buoy removal and deployment. The large gaps in the buoy's data prevented finding temporal patterns longer than the period over which the data was collected. Filling these gaps with an ARIMA model was not considered because of the expected strong seasonality leading to non-stationary wave behavior across seasons.

The peak frequencies appearing in the periodograms period of the autocorrelation function of the data could be used to remove the within-series dependence on the time of year.

Removing Seasonality from Wave Height Data

To apply the seasonality result, the 12-month season was used to generate new datasets in which the hourly wave heights were subtracted from the wave height 365 days prior. These "deseasoned" datasets were then used to develop "deseasoned" annual means and corresponding Theil-Sen regression slopes.

Removing Temporal and Spatial Dependence from Wave Height Data

A deseasoned dataset was developed by subtracting each monthly mean from the monthly mean of the previous year. To check the comparability of the main analyses used in this study: the Theil-Sen slope confidence interval, the modified Mann-

Kendall test, seasonal Mann-Kendall test, and Theil-Sen slope confidence interval of the newly generated deseasoned series, all tests were applied to series of annual and monthly means at all of the WIS nearshore stations on Lake Michigan.

While the seasonal differencing scheme may be appropriate for oceans, where the fetch in any particular direction is sufficiently large that it can be assumed not to impact the size of waves approaching from different directions, we can see from the wave climate figures in the next section (Figures 3.1 and 3.2) that this is not the case in Lake Michigan, which is longitudinally stretched. Waves approaching from the north-south are not comparable to waves approaching from the east-west. To overcome this issue, a two-dimensional differencing scheme was developed. Monthly means were developed for the WIS model of waves approaching from 30-degree bins. The dependence on wave direction was examined by testing all the above techniques with annual and monthly mean wave heights subdivided into 30-degree directional bins.

The deseasoned data was not applied to tests of the annual mean of the largest five waves because the individual storm peaks are assumed to be independent of one another.

2.3.3 Has storm frequency or duration increased over the 36-year NDBC record?

Trends in Storm Metrics

To examine the long-term trends in storm behavior over the lake, several storm metrics were developed. These were annual mean storm length, annual total time storming, annual number of storms, and the annual storm wave peak height mean. These metrics were calculated alongside the peaks-over-threshold subset of the hourly wave height data described above. Each time span exceeding the threshold was counted to develop the mean storm duration and total yearly time spent with waves >2m. (Results for a threshold of >3m can be seen in Appendix E) The final peaks-

over-threshold dataset was used to develop the number of storms and the peak wave means.

To examine storms and extreme events, annual values for these metrics were tested with the 95% confidence interval for slope of Theil-Sen regressions. This analysis was performed on buoy data from Lake Michigan, the WIS hindcast at the buoy locations, and the WIS hindcast at nearshore station 94463 in the southern basin.

Shifting Extreme Value Distribution

To further study storm behavior, the largest wave from each year was selected from the WIS data at the buoy locations. These annual series of wave maxima were used to generate generalized extreme value probability distribution (GEVD) functions for the WIS model datasets. This technique of applying the GEVD to annual maxima is referred to as Gumbel's approach [42].

To study the long-term trends in the GEVD, the first decade of each extreme event dataset was taken. Maximum likelihood analysis was used to fit the GEVD parameters to the first 10 values of the yearly data series. With these parameters, the integration of the fitted GEVD was performed to determine the probability of receiving a wave between the sizes of 5 and 8 meters (inclusive). With this value recorded, the same analysis was performed again, now using the initial 11 years of the series. This process continued until the probability of receiving a wave between 6 and 8 meters was determined for the full time series of annual extreme values. A 95% confidence interval for each of the annual probabilities was determined by bootstrap sampling of the extreme wave height annual values. The GEVD was estimated using maximum likelihood by SciPy's `stats.genextreme.fit` command and the bootstrapped confidence intervals for the annual probabilities were calculated with R's `boot` package and the `boot.confint` tool.

By increasing the size of the extreme value subset in each step of the previous analysis, the assumption is made that the process that creates these waves is un-

changing. Considering Waples and Klump's (2002) result indicating a shift in wind direction over the Great Lakes region and the results from the growing window analysis above, a similar analysis was performed in which the collection of annual wave height maxima was maintained at a 10yr long moving sample [14]. This adjustment to a moving decadal window assumes that the process generating waves in the lake may be changing in time.

In both procedures, the probability series generated were subjected to a Theil-Sen regression to look for significant trends in the data. These analyses were performed using data from the WIS model at both buoy locations, all available nearshore stations, and the full lake model from WIS.

To reduce the confidence intervals on the integrated extreme wave GEVD returned from the Gumbel approach, the peaks-over-threshold approach was applied as well. This approach uses the maxima of all runs over some threshold (2 and 3 meter thresholds applied) to generate a Generalized Pareto Distribution (GPD) using maximum likelihood analysis. The inclusion of more data points is expected to decrease the range of the 95% confidence interval, again predicted from bootstrap sampling for both the growing and moving windows (10, and 15 year windows applied). This analysis was performed using the WIS model data at the buoy locations as well as nearshore station 94463. This approach was also applied to waves selected from both a yearly growing and moving window of for comparison. The GPD was estimated using maximum likelihood by SciPy's `stats.genpareto.fit` command and the bootstrapped confidence intervals for the annual probabilities were calculated with R's `boot` package and the `boot_confint` tool.

Due to the distinctive north-south orientation of Lake Michigan, the whole lake analysis was expanded to Lake Ontario, an east-west oriented lake, to examine for any spatial patterns that might emerge.

2.3.4 Has the direction of the waves changed?

Trends in Annual Wave Frequency by Direction

In addition to changes in the size of the waves coming from each direction, the amount of time waves spent coming from each direction was considered as well. For 10- and 30-degree bins the number of measurements taken within each bin was counted for each year in the buoys and their WIS model locations. Buoy data was subsampled to data between May and October with wave heights measuring of 0.25 meters or larger. All available WIS data were utilized.

Kernel Density Estimates of Wave Direction

In addition to studying the number of waves coming from a particular direction each year, a kernel density estimate was also used to generate a probability distribution function (PDF) of wave directions for each month. These PDFs were generated using the density command in R and a bandwidth of 29 for all estimations. The PDF of waves can be integrated for any range to determine the probability of receiving a wave from that direction range in that particular month. These monthly PDFs were first generated using the first and last three, four, and five years of directional wave data. These plots were compared for stable changes in directional probability.

Changes that appeared stable across the three time spans were then investigated by generating annual PDFs for the months where sufficient data were available (40% monthly data availability criteria). These PDFs could then be integrated in the apparent region of change and studied using Theil-Sen regression for significant trends in the probability of receiving a wave from that direction.

2.3.5 Is the increasing lake level related to the size of the waves?

Previous work [27, 28] has examined the relationship between wave heights and the water surface level of Lake Michigan. It has been hypothesized that the two

parameters may be related by the effect of storms occurring in the lake vicinity. This work proposed that the wind and rain associated with these events could lead to increases in wave height and lake level, respectively [27]. Furthermore, a lag between the effect of the wind on wave height and rain on water level was hypothesized due to surface hydrology delaying precipitation from reaching the lake [27].

Meadows et al. (1997) recognized the need to remove the within-series dependence on season from the two time series and subsequently applied a 60-month moving-average to both the lake level and the monthly mean wave heights [27]. This long moving average window smoothed out higher-frequency oscillations in lake levels and wave heights associated with seasonal lake trends. The 60-month moving averaged series showed a strong, significant correlation coefficient (0.69) between the monthly mean wave-height hindcast by WIS and USACE lake level [27]. With a one-year lag between the wave height and the lake level, a stronger coefficient of 0.73 was found.

To avoid the influence of the moving average window size on the correlation result and still eliminate the influence of seasonality on the relationship, this study removes seasonality from the monthly series by using backwards differencing. To determine the period of the lake level data series, a periodogram and autocorrelation function were built from the monthly means. Results for peak frequencies in the lake level series can be used to determine the time span to difference the data over and remove the effect of season on the lake level. Seasonality will be removed from the wave height data according to the same season found previously in the annual mean wave height study above.

After seasonality is removed from both series, the correlation coefficient between the monthly mean and monthly maxima is determined for both unlagged and one-year lagged lake level series.

3. RESULTS

The results from this analysis of Lake Michigan waves using the NOAA buoys and WIS datasets are presented below. Theil-Sen results that did not contain zero within the 95% confidence interval for the regression slope were accepted as significant and included as dashed lines on the corresponding scatter plots. Rejected trends are not shown on annual or monthly scatter plots and are depicted as gray points on nearshore station trend maps.

3.1 Lake Michigan's Wave Climate

With reliable buoy data existing only from May to October (Figures 3.1 and 3.2), it appears that the smallest mean wave heights occur in June in both the northern and southern basins. Both buoys show steady increases in mean wave height until October. A similar trend is seen in the annual large wave mean heights.

Data from NDBC Buoy 45007 indicates that the southern basin of Lake Michigan experiences a median of 14 storms each year during the May-October period with a median peak storm wave height of 3.7 meters. The same analysis (Period: May-October, $H_s \geq 2\text{m}$) indicated a median of 16.5 storms each year with a median peak storm wave height of 3.7 meters in the northern basin (NDBC Buoy 45002). These values were determined from a peaks-over-threshold subset of the buoy's data using a threshold of 2 meters. Appendix E plots the same storm metrics using a threshold of 3 meters.

Figure 3.1 characterizes the monthly wave behavior in the vicinity of Buoy 45007 using the WIS model and the collected buoy data. The mean wave heights in the southern basin vary little with respect to the approach direction. The mean of the five largest waves in each direction shows greater dependence on approach angle, with

the largest waves typically arriving from the north or south, from May to July. In the later months, the five largest waves also begin to show less dependence on approach direction, until October when the largest waves come from the north.

The vast majority of waves approach from either nearly due north or south. Only a small minority of waves come from the east or west in the southern basin.

Figure 3.2 characterizes the monthly wave behavior in the vicinity of Buoy 45002 using the WIS model and the collected buoy data. In the northern basin, the mean wave height has a greater directional dependence. Waves approaching from the south have both greater overall mean height and greater mean large wave height. This holds true for the entire May-October buoy season.

Wave approach direction in the north is dominated by south-southwesterly waves (170-200 degrees).

To obtain the autocorrelation lag time for the wave data, all uninterrupted data runs of at least 10 days were sampled from the complete data set. Each hourly wave height in these runs was subtracted from the closest value 365 days prior. The closest value was only considered acceptable if it was within 12 hours of the 365-day difference.

The stationarity of each annually differenced run was checked using the augmented Dickey-Fuller test. Approximately four fifths of these runs were found to be stationary. These stationary runs were then tested using the autocorrelation function. Inspection of the autocorrelation results showed a sinusoidal decay behavior, indicative of an autoregressive behavior in the waves. This autoregressive behavior was tested using the partial autocorrelation function and found to have a partial autocorrelation lag time of 3 hours in most of the runs. This autoregressive behavior in the hourly time series indicates that any significant wave height is, on average influenced by the non-seasonal variation in the significant wave heights that have occurred over the prior three hours.

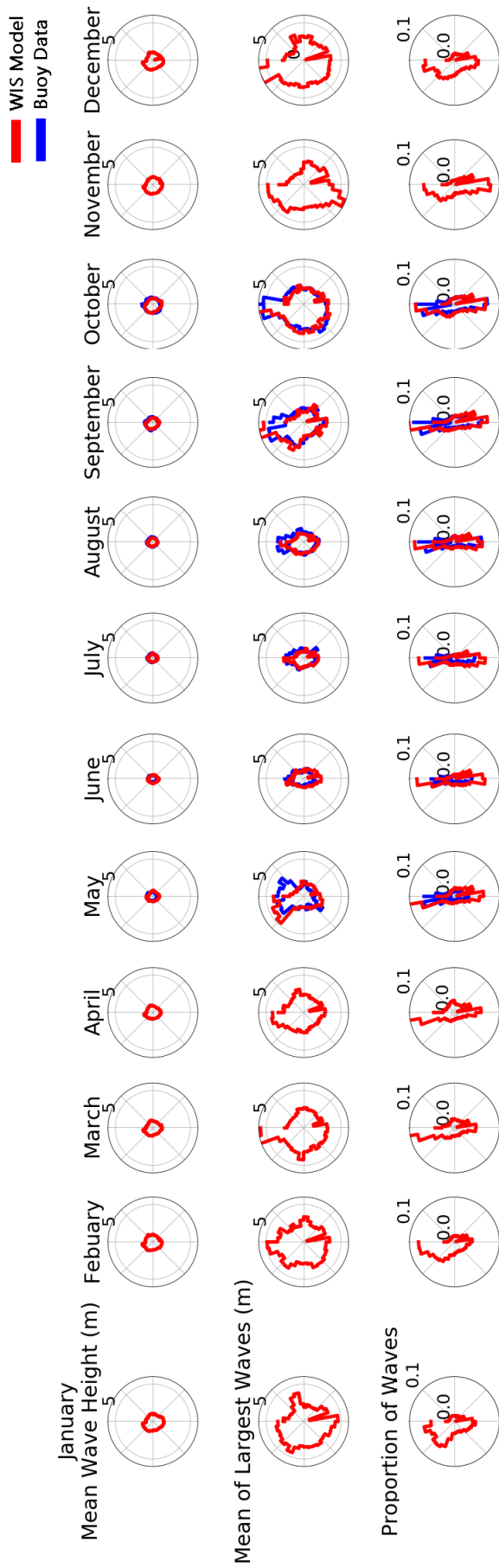


Figure 3.1. Wave climate at the location of Buoy 45007 in Lake Michigan's southern basin separated in 10-degree directional bins. [37, 38].

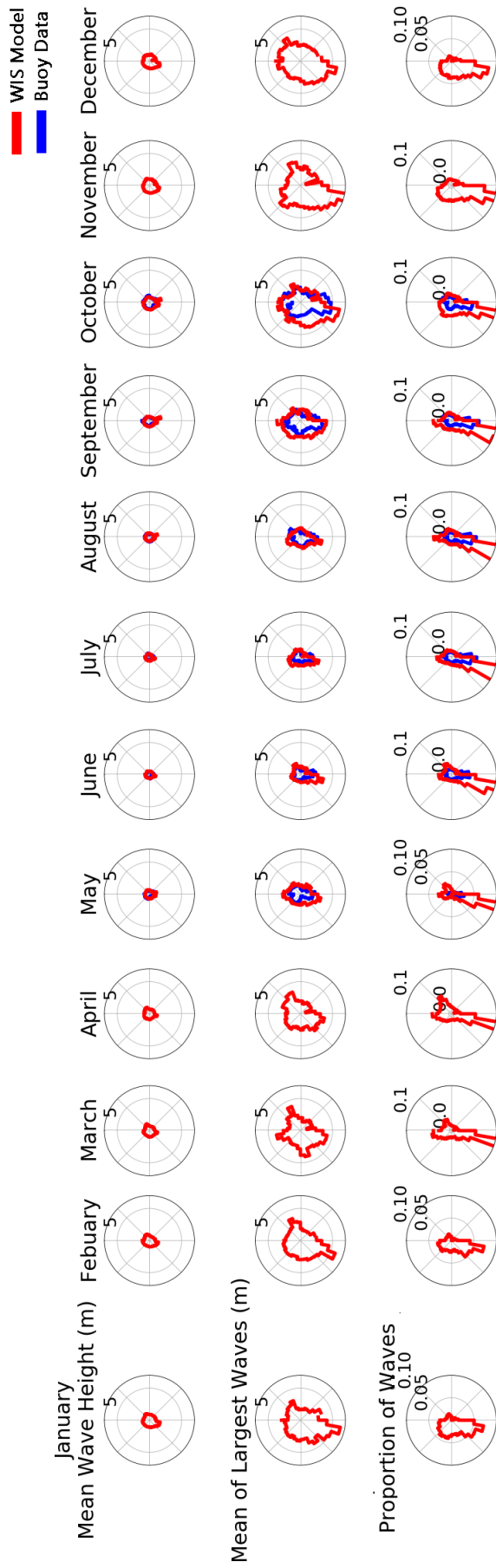


Figure 3.2. Wave climate at the location of Buoy 45002 in Lake Michigan's northern basin separated in 10-degree directional bins [37, 38].

3.2 Have waves in Lake Michigan increased in size over the 36-year ND-BC record?

3.2.1 Annual Means

The annual mean height of waves greater than 0.25 meters occurring from May to October in Lake Michigan is plotted in Figure 3.3. The Theil-Sen slopes and 95% confidence intervals for Buoy 45007 and Buoy 45002 are -1.5 mm/yr (-3.0 - -0.01mm/yr) and -3.8 mm/yr (-4.6 - -2.8mm/yr), respectively. The other series did not have significant trends. This is an indication that the waves may be decreasing rather than increasing in Lake Michigan, though further investigation is necessary due to the discrepancy between the buoy and WIS data despite identical season (May-October) and height ($> 0.25m$) requirements to allow comparability between series. Results for these trends are summarized in Table 3.1.

In 75% of the years, the buoy-measured annual mean wave height in the northern basin was larger than the southern. The mean of the difference between the series was 3.1 cm. Annual mean wave heights ranged from approximately 0.7 to 1.1m. Both the largest and smallest mean annual wave height occurred in the northern basin.

The mean difference between the WIS station at Buoy 45007 and the measurements taken by the buoy was found to be -0.008 meters with a standard deviation of 0.057 meters in an apparently normal distribution. In the northern basin, the error distribution between the model and the buoy measurements also appeared close to normal, with a mean of 0.050 meters and a standard deviation of 0.075 meters.

The nearshore WIS station in the southern basin predicted waves between 0.48 and 0.74 meters in height. The model suggested that the mean difference in the annual mean wave heights at the position of Buoy 45007 and the nearshore station was 0.21 meters.

For the WIS dataset, the full-year (all heights) time series was analyzed, shown in Figure 3.4. At the northern basin station, the range of whole year mean wave height was 0.719 to 0.959 meters. In the southern basin, the whole year mean wave heights

ranged from 0.767 to 0.984 meters. At the southern basin nearshore location, only three years (1984, 1985, and 2013) had May-October annual wave height means that were smaller than the entire year means. The mean difference between the nearshore station May-October annual mean wave height and the entire year was -0.077 meters.

At Buoy 45007's location, for all but two years (2001 and 2012), the WIS model's annual mean including the entire year exceeds the May-October subset mean described above. The mean difference between the entire year means and the May-October mean is 0.076 meters. At Buoy 45002's position in the northern basin, however, for 29 out of the 36 years the May-October year mean exceeds the whole year mean. The mean difference between the whole year and May-October mean in the series was -0.023 meters.

Significant trends were not found at the buoy locations or the nearshore station 94463 in the full year, all heights annual mean series of the WIS data.

For a lake-scale analysis, the Theil-Sen regression slope of the annual mean of waves larger than 0.25 meters was also applied to all of the nearshore stations that the USACE WIS website makes available for Lake Michigan. Figure 3.5 shows decreasing trends in wave heights along two stretches of the lakes western coast. The magnitude of these trends is consistent with that found by Buoy 45007, in the southern basin. Stations in gray showed no significant trend during the period of available data.

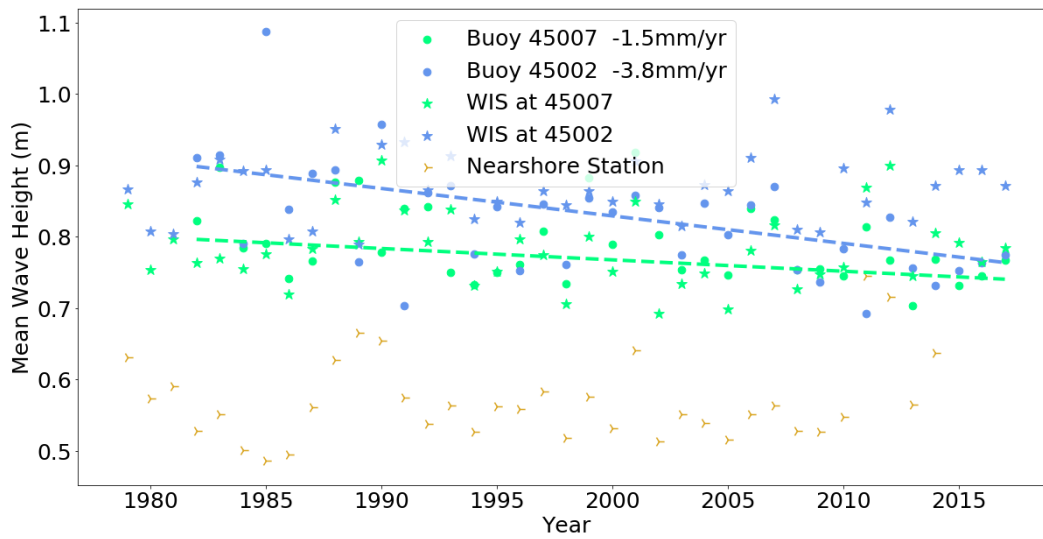


Figure 3.3. Yearly mean wave heights for waves $\geq 0.25m$. Buoy and WIS series restricted to the months of May-October. Significant trends, found only in the buoy series, are depicted. [37, 38]

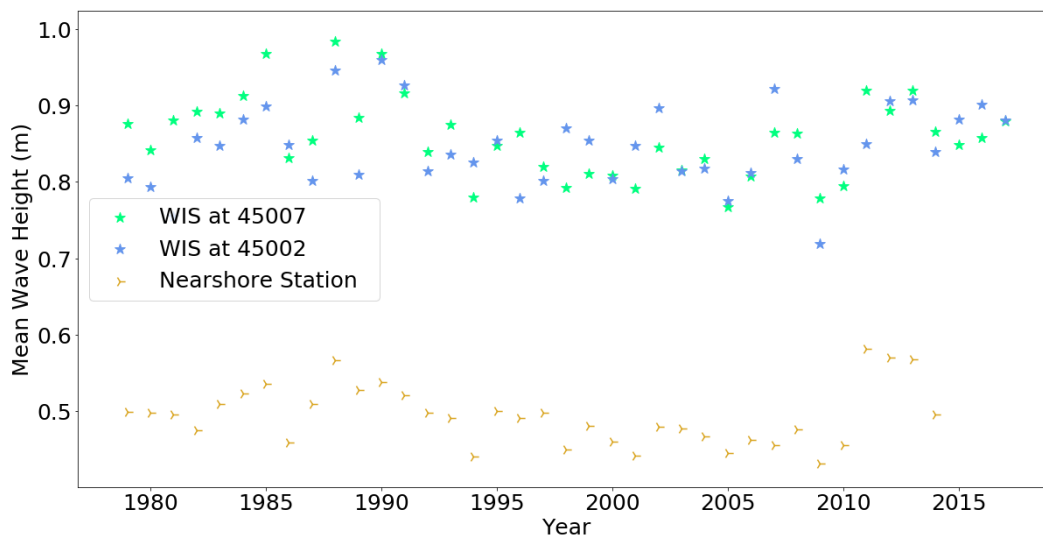


Figure 3.4. Yearly mean wave heights for complete WIS hindcast series. No significant trends were detected. [38]

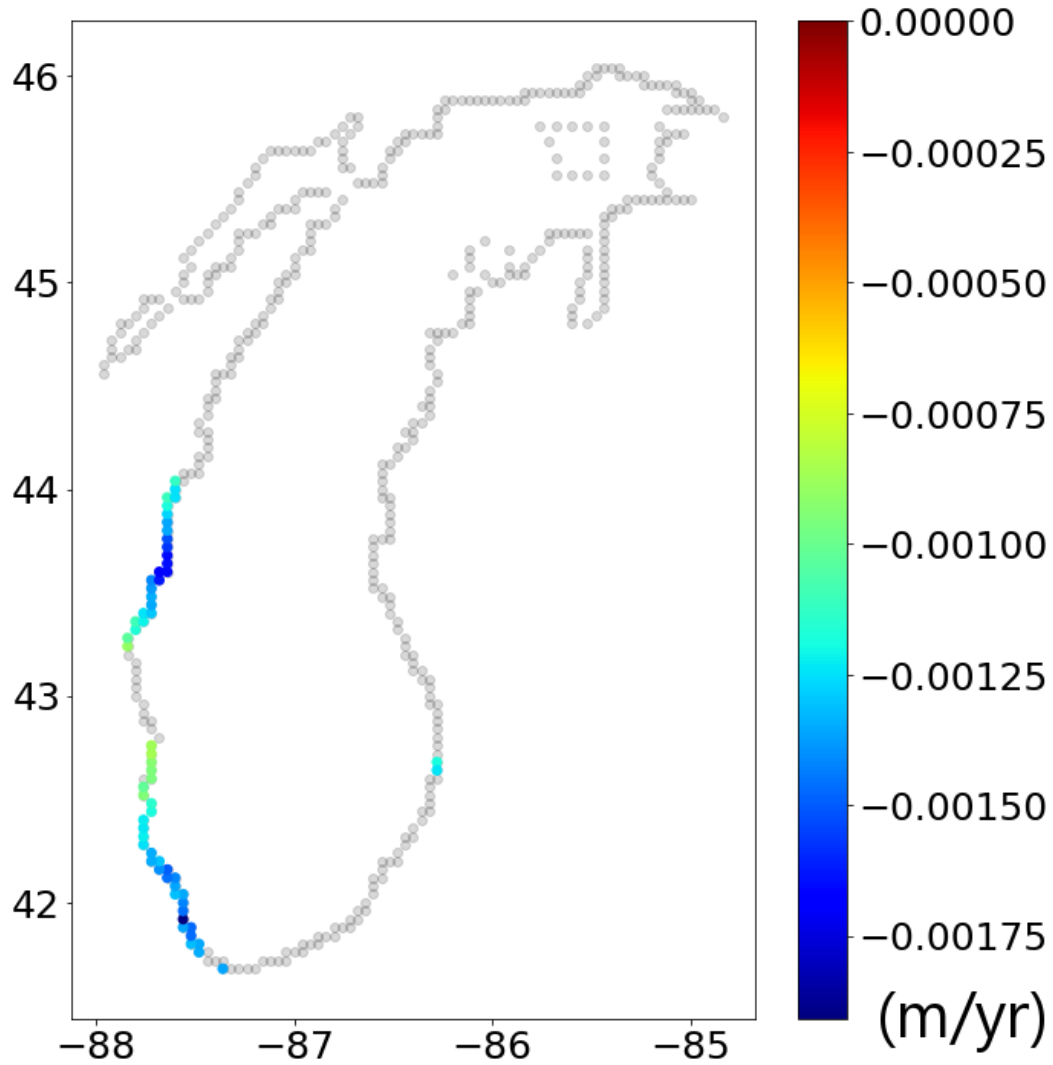


Figure 3.5. Trends in the annual mean of hourly significant wave heights (1979-2014) including full year and waves of all sizes) at all of the WIS nearshore stations on Lake Michigan [38]. Stations in gray do not have significant Theil-Sen regression slopes.

Table 3.1. Summary of trends. Format: Median(95%CI)

	Buoy 45007	Buoy 45002	WIS at 45007	WIS at 45002	Station 94463
Mean (Months 5-10, $H_s > 0.25$)	-0.002(-0.003,-0.0)	-0.004(-0.005,-0.002)	-0.0(-0.002,0.001)	0.0(-0.001,0.002)	0.0(-0.001,0.002)
Mean (All waves)	n/a	n/a	-0.001(-0.003,0.0)	0.001(-0.001,0.002)	-0.001(-0.002,0.0)
Mean of Largest 5 Waves(Months 5-10, $H_s > 0.25$)	-0.005(-0.02,0.008)	-0.005(-0.015,0.008)	0.003(-0.007,0.016)	0.001(-0.009,0.011)	nan(0.002, nan)
Mean of Largest 5 Waves(All waves)	n/a	n/a	-0.014(-0.026,0.0)	-0.005(-0.015,0.003)	-0.0(-0.002,0.001)
Mean of Deseasoned Waves(Months 5-10, $H_s > 0.25$)	-0.0003(-0.0009,0.0004)	nan(-0.001,0.0012)	-0.0(-0.0004,0.0003)	0.002(-0.0006,0.004)	nan(0.008, nan)
Mean of Deseasoned Waves(All waves)	n/a	n/a	nan(0.0023, nan)	nan(0.0031, nan)	-0.003(-0.0099,0.002)
Mean Storm Length (Threshold = 2m, Months 5-10)	0.018(-0.051,0.084)	-0.063(-0.114,-0.007)	-0.007(-0.097,0.077)	-0.026(-0.088,0.056)	nan(0.177, nan)
Total Storming Time (Threshold = 2m, Months 5-10)	-0.942(-4.545,3.0)	-3.814(-7.36,0.182)	0.133(-1.167,1.421)	0.136(-1.542,1.2)	0.222(-0.167,0.692)
Number of Storms (Threshold = 2m, Months 5-10)	-0.068 (-0.417,0.25)	-0.275(-0.667,0.111)	0.0(-0.118,0.148)	0.0(-0.13,0.133)	0.037(0.0,0.1)
Storm Peak Wave Mean (Threshold = 2m, Months 5-10)	-0.001(-0.005,0.003)	-0.003(-0.008,0.002)	0.001(-0.005,0.008)	0.0(-0.006,0.005)	nan(0.01, nan)
Mean Storm Length (Threshold = 2m, All year)	n/a	n/a	-0.085(-0.13,-0.045)	-0.006(-0.042,0.027)	-0.001(-0.004,0.002)
Total Storming Time (Threshold = 2m, All year)	n/a	n/a	-2.606 (-6.071,1.1)	0.514(-2.939,4.276)	-1.143(-2.323,0.4)
Number of Storms (Threshold = 2m, All year)	n/a	n/a	0.25(0.0,0.517)	0.115(-0.214,0.343)	0.038(-0.111,0.174)
Storm Peak Wave Mean (Threshold = 2m, All year)	n/a	n/a	-0.005(-0.008,-0.002)	-0.001(-0.004,0.002)	-0.006(-0.015,0.002)
Mean Storm Length (Threshold = 3m, Months 5-10)	nan(-0.083,0.122)	0.0(-0.08,0.083)	nan(0.296, nan)	nan(0.01,0.208)	nan(nan, nan)
Total Storming Time (Threshold = 3m, Months 5-10)	-0.159(-1.185,0.696)	-0.667(-1.387,0.143)	0.0(-0.25,0.421)	0.091(-0.273,0.667)	0.0(0.0,0.0)
Number of Storms (Threshold = 3m, Months 5-10)	0.0 (-0.143,0.176)	-0.118(-0.3,0.0)	0.0(-0.04,0.059)	0.0(-0.059,0.0)	0.0(0.0,0.0)
Storm Peak Wave Mean (Threshold = 2m, Months 5-10)	nan(-0.011,0.012)	-0.001(-0.01,0.009)	nan(0.035, nan)	nan(-0.001,0.015)	nan(nan, nan)
Mean Storm Length (Threshold = 3m, All year)	n/a	n/a	-0.094(-0.152,-0.038)	-0.020(-0.057,0.0164)	nan,(-0.053,0.792)
Total Storming Time (Threshold = 3m, All year)	n/a	n/a	-1.5(-2.653,-0.333)	-0.4054(-1.5,0.612)	-0.578(-1.047,0.0)
Number of Storms (Threshold = 3m, All year)	n/a	n/a	0.0(-0.125,0.133)	0.0(-0.166,0.153)	-0.054(-0.105,0.0)
Storm Peak Wave Mean (Threshold = 3m, All year)	n/a	n/a	-0.007(-0.014,-5e-05)	-0.002(-0.005,0.001)	nan(-0.0003,0.099)
EVD (10yr, Growing Window)	n/a	n/a	-0.012(-0.014,-0.012)	-0.001(-0.002,0.002)	-0.003(-0.004,-0.003)
EVD (10yr, Moving Window)	n/a	n/a	-0.025(-0.027,-0.022)	-0.024(-0.027,-0.013)	-0.011(-0.012,-0.008)
EVD (12yr, Growing Window)	n/a	n/a	-0.014(-0.015,-0.013)	-0.002(-0.003,-0.001)	-0.004(-0.005,-0.003)
EVD (12yr, Moving Window)	n/a	n/a	-0.011(-0.012,-0.01)	0.006(0.004,0.008)	-0.001(-0.001,-0.001)
EVD (15yr, Growing Window)	n/a	n/a	-0.013(-0.015,-0.012)	-0.004(-0.005,-0.003)	-0.006(-0.006,-0.003)
EVD (15yr, Moving Window)	n/a	n/a	-0.021(-0.026,-0.02)	-0.011(-0.013,-0.009)	-0.008 (-0.011, -0.007)
GPD (Threshold = 2m, 10yr, Growing Window)	n/a	n/a	-0.0003(-0.0003,-0.0002)	-0.0(-0.0001,0.0)	-0.0004(-0.0004,-0.0003)
GPD (Threshold = 2m, 10yr, Moving Window)	n/a	n/a	-0.0009(-0.001,-0.0007)	-0.0002(-0.0003,-0.0001)	-0.0009(-0.001,0.0007)
GPD (Threshold = 2m, 15yr, Growing Window)	n/a	n/a	-0.0003(-0.0003,-0.0002)	-0.0001(-0.0001,-0.0)	-0.0006(-0.0007,-0.0003)
GPD (Threshold = 2m, 15yr, Moving Window)	n/a	n/a	-0.0006(-0.0007,-0.0005)	-0.0003(-0.0003,-0.0002)	-0.001(-0.001,-0.0006)
GPD (Threshold = 3m, 10yr, Growing Window)	n/a	n/a	-0.001(-0.001,-0.001)	-0.0002(-0.0003,0.0006)	0.0003(0.0001,0.0005)
GPD (Threshold = 3m, 10yr, Moving Window)	n/a	n/a	-0.0021(-0.0024,-0.0019)	-0.0005(-0.0009,0.0002)	-0.0008(-0.0011,0.0001)
GPD (Threshold = 3m, 15yr, Growing Window)	n/a	n/a	-0.0014(-0.0014,-0.001)	-0.0004(-0.0004,-0.0001)	-0.0005(-0.0009,0.0005)
GPD (Threshold = 3m, 15yr, Moving Window)	n/a	n/a	-0.0019(-0.0026,-0.0017)	-0.0011(-0.0012,-0.0006)	-0.0012(-0.0013,0.0001)

3.2.2 Mean of Largest Five Independent Wave Heights

Figure 3.6 shows the annual mean of the five largest independent waves measured by the NDBC buoys and calculated by the WIS hindcast for the May-October period. No trends were found in the annual means of the five largest waves for the buoy data or the three WIS points. Results for these trends are summarized in table 3.1.

When the WIS model is tested, selecting waves from the entire yearly series, the mean of the five largest waves is consistently larger than the May-October subset, seen in Figure 3.7. The mean of the five largest waves was 0.998 and 1.365 meters higher in the northern and southern basins, respectively. The annual mean of the five largest waves ranged from 3.566 to 4.955 and 3.623 to 5.676 meters in the northern and southern basins, respectively. At the southern basin's nearshore station, the range in annual mean of the five largest wave heights occurring over the entire year was 2.03 to 2.446 meters. The mean difference between the full year mean and the May-October subset was 0.055 meters.

The larger annual mean of the five largest waves was split exactly 50% between Buoy 45007 and 45002 in the buoy-measured waves with the average difference between Buoy 45002 and 45007 being -0.020 meters. In the north, the WIS model has a mean prediction 0.250 meters larger than the waves measured at the buoy in a left skewed distribution (standard deviation: 0.404 meters). In the south, the WIS model has a mean prediction 0.071 meters smaller than the waves measured at the buoy in a uniformly shaped distribution (standard deviation: 0.400 meters). The WIS model consistently predicted smaller waves at station 94463 than at Buoy 45007 with a mean difference of 1.073 meters.

Theil-Sen regressions on the annual means of the five largest independent waves series were applied to all of Lake Michigan's nearshore WIS stations in Figure 3.8. No significant trends in the annual large wave means were found anywhere along the lake's coast.

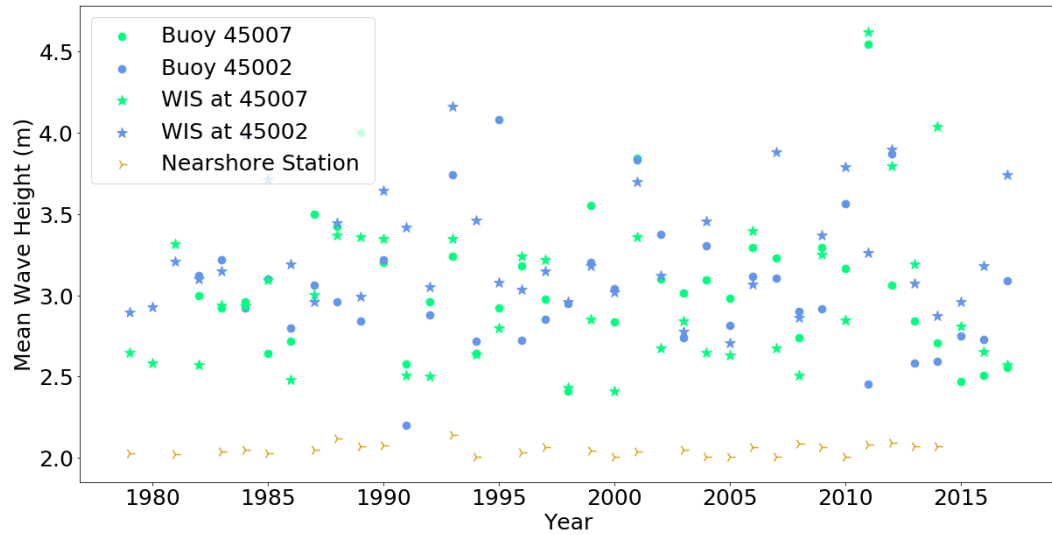


Figure 3.6. The annual series of the mean of the five largest independent wave heights was tested for trends using Theil-Sen regression slopes. No significant trends were detected in the data. For compatibility between series all data was limited to waves $\geq 0.25m$, occurring between May and October. [37,38].

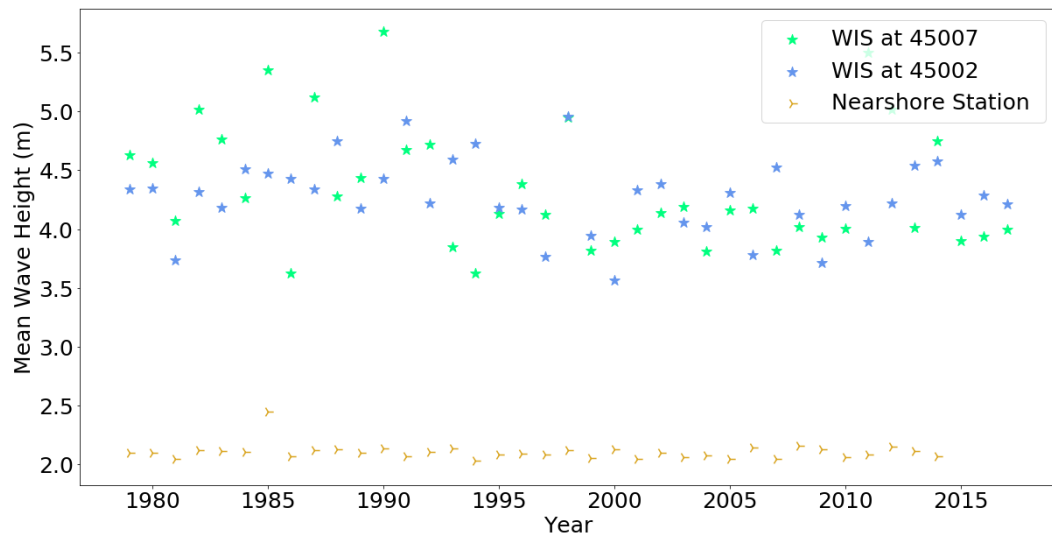


Figure 3.7. The annual series of the mean of the five largest independent wave heights was tested for trends using Theil-Sen regression slopes. No significant trends were detected in the data. This analysis of the WIS data did not limit the series by height or season. [38].

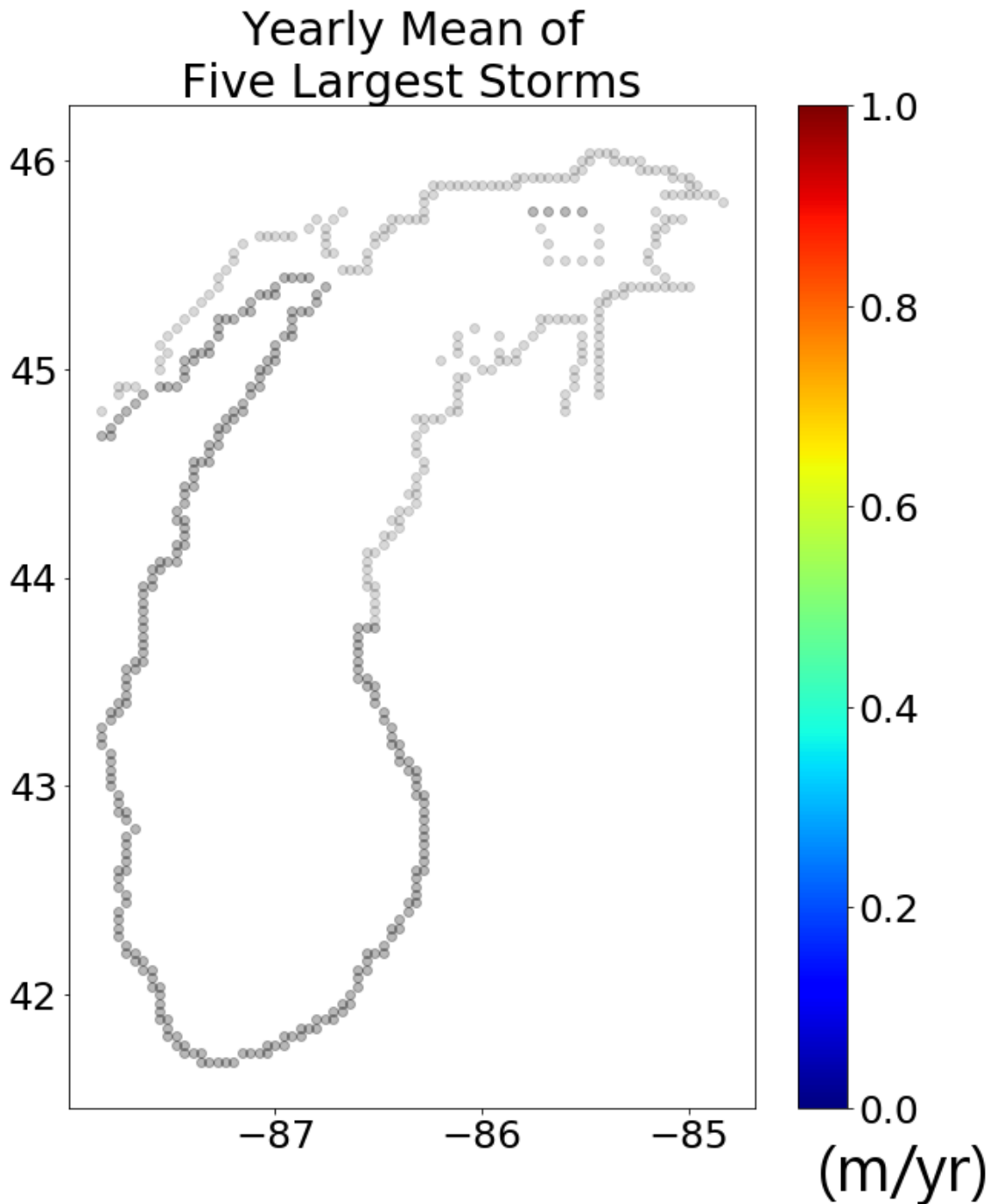


Figure 3.8. Trends in the annual mean of the five largest independent wave heights (1979-2014) at all of the WIS nearshore stations [38]. Stations in gray do not have significant Theil-Sen regression slopes. This analysis of the WIS data did not limit the series by height or season. No significant trends were detected.

3.2.3 Mann-Kendall Test Results on Monthly Wave Height Means

Hamed and Rao's (1998) modified Mann-Kendall test was applied to the monthly means of the WIS model at the locations of Buoy 45007 and 45002. The Mann-Kendall test, modified for autocorrelated data like the monthly series in Figure 3.9, did not find a significant long-term trend at either location. Figure 3.10 shows the results of the modified Mann-Kendall test applied to all of the WIS nearshore stations. No significant trends were detected at any location.

Figure 3.11 shows the results for the seasonal Mann-Kendall test applied to a series of monthly means taken at all of the publicly available WIS nearshore stations.

3.2.4 Seasonal Dependence in Wave Height

The periodograms in Figure 3.12 show both the northern- and southern-basin wave heights as having a peak frequency in the monthly mean wave heights at $1/12$, indicating a 12-month cycle. The autocorrelation function for monthly mean wave heights indicated a 12 step or 12-month periodicity in the series. This indicates a within-series dependence on the time of year, or seasonality in wave height. A within-series dependence can be a confounding factor in the previous analysis of wave height means, leading to erroneous results.

3.2.5 Removing Seasonality from Wave Height Data

To apply the results from 3.12, the 12-month season was used to generate new datasets in which the hourly wave heights were subtracted from the wave height one year prior. These "deseasoned" datasets were then used to develop "deseasoned" annual means and test the corresponding Theil-Sen regression slopes.

The annual means of the seasonally differenced wave height series and corresponding Theil-Sen regression of the deseasoned datasets were also plotted and are shown in Figure 3.13. To make WIS data comparable to the buoy-collected series, all data was

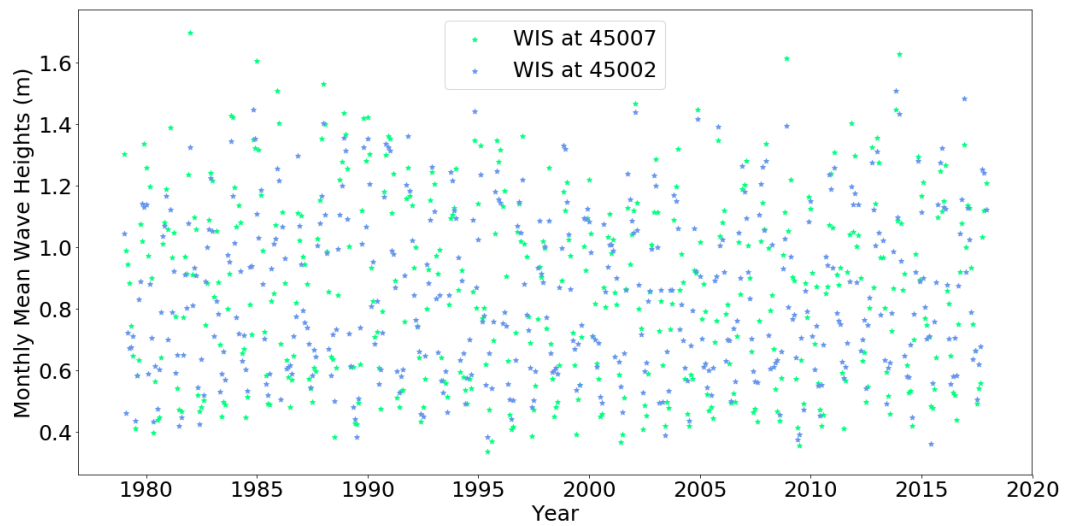


Figure 3.9. Monthly mean wave heights from the WIS model at Lake Michigan’s buoy locations. No monotonic trends were detected by the modified Mann-Kendall statistic for autocorrelated series [38].

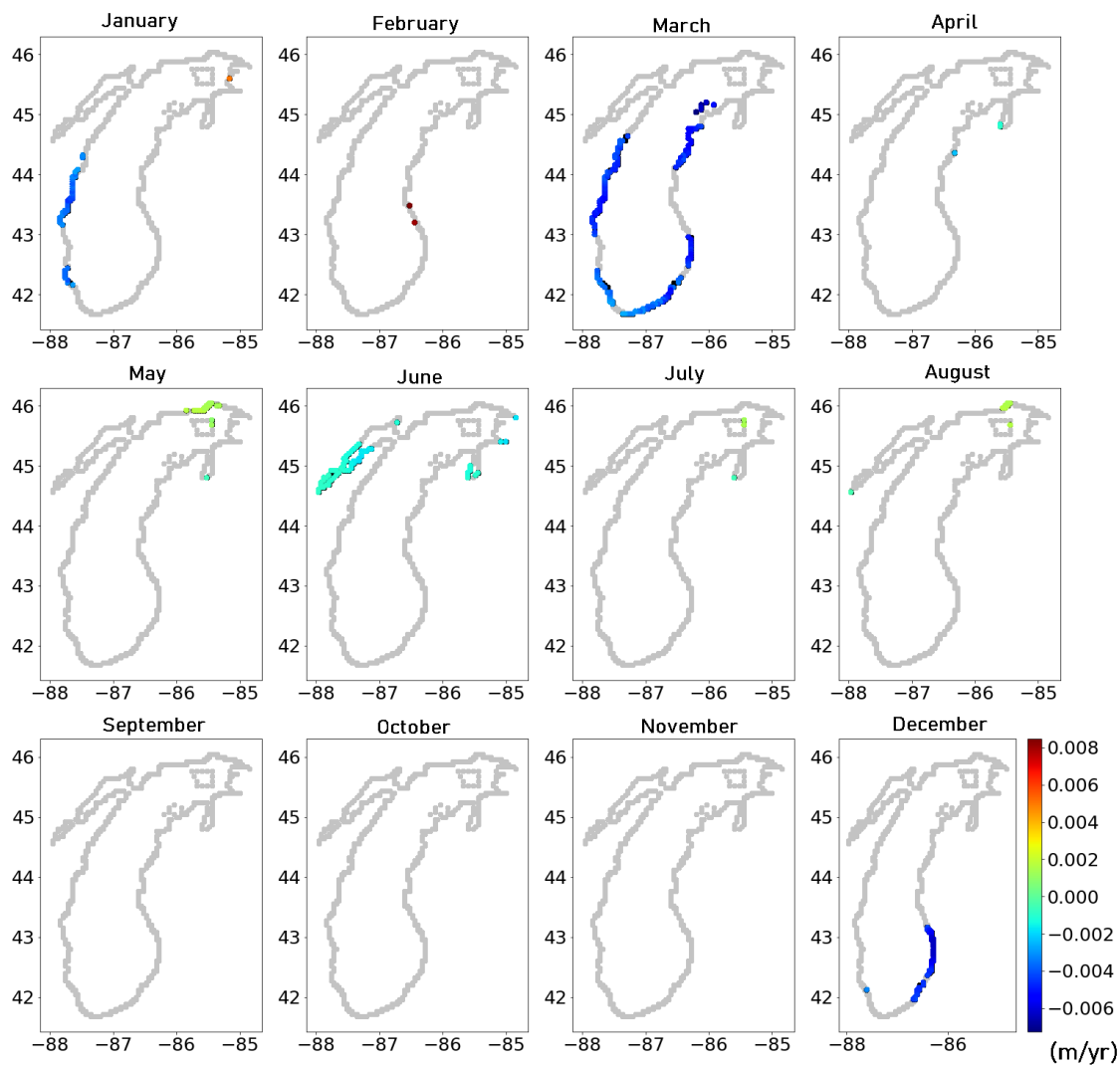


Figure 3.11. Seasonal Mann-Kendall test results for monotonic trends in the monthly mean wave heights at all Lake Michigan nearshore stations. [38].

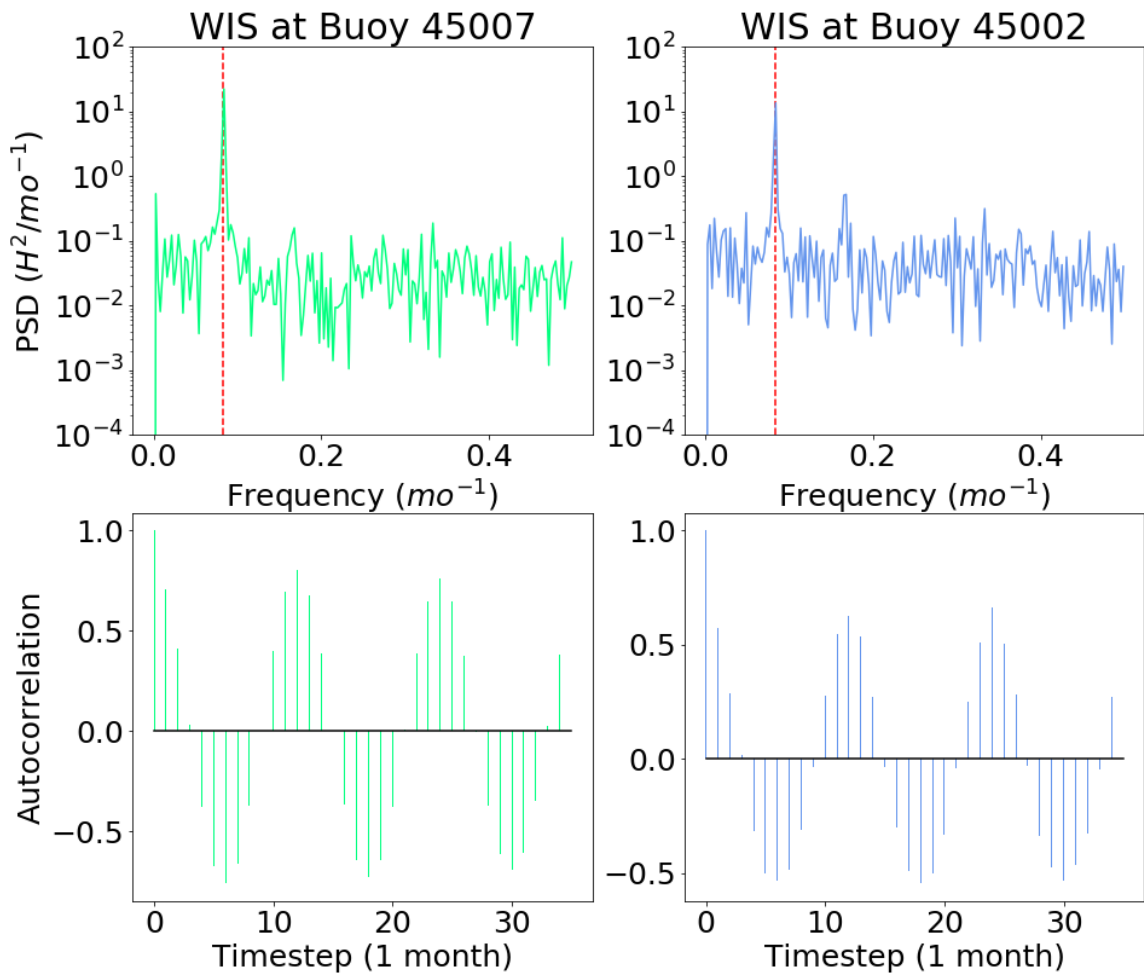


Figure 3.12. Periodograms and autocorrelation results indicate a 12-month seasonal pattern in the WIS wave model [38]. The periodograms were performed on the monthly means of the entire WIS dataset and show a peak frequency of $1/12$. The autocorrelation function was taken of the monthly means and shows a 12-step or 12-month period. These results indicate seasonal dependence in wave height series.

limited to May-October and wave heights greater than 0.25 meters before seasonal differencing. Figure 3.14 shows the results for the WIS data using the entire year and no limitation set on wave height. No significant trends were found in any of the differenced series. Results for these trends are summarized in table 3.1.

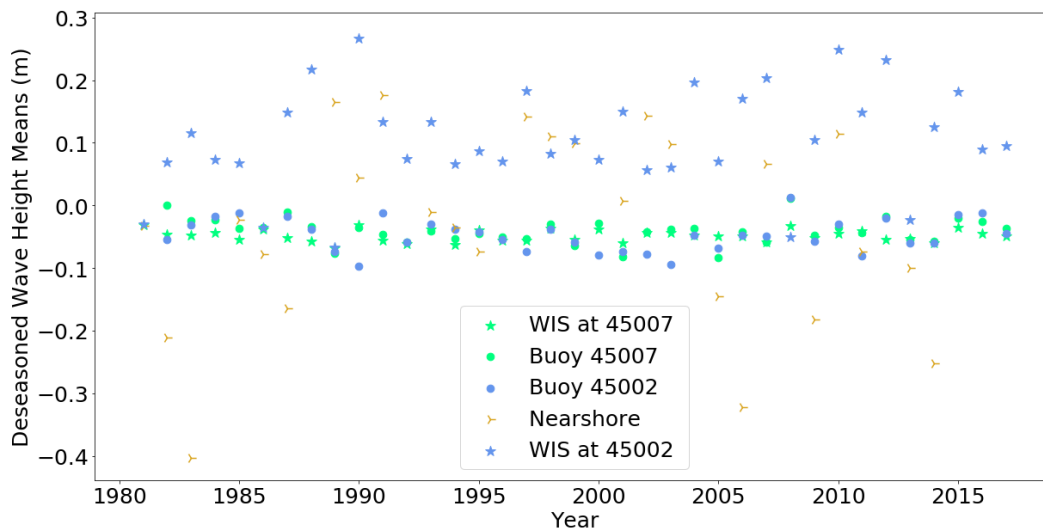


Figure 3.13. Yearly mean wave heights of hourly deseasoned data (May-October, $H_s > 0.25\text{m}$). Series were tested for trends using 95% confidence interval of Theil-Sen regression slopes. No significant trends were detected. [37, 38]

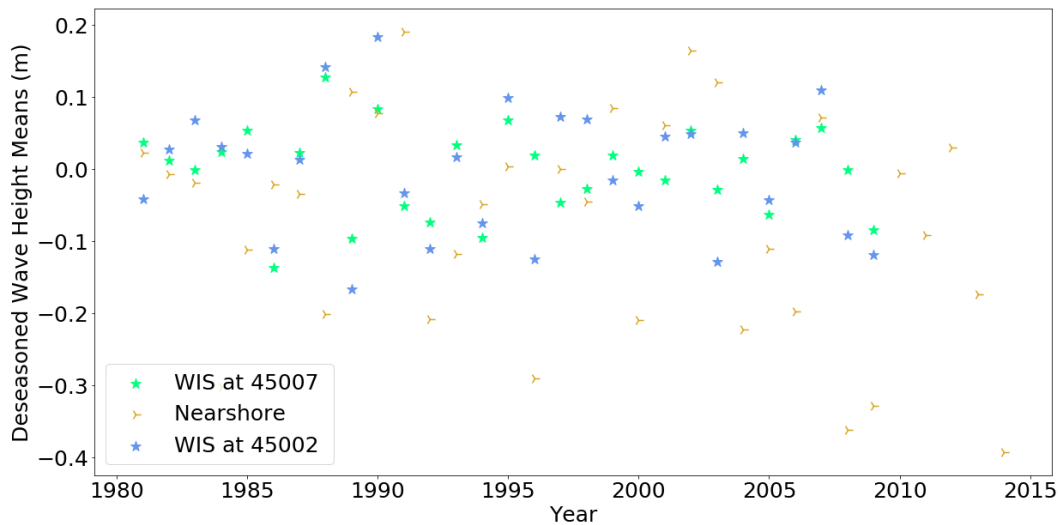


Figure 3.14. Yearly mean wave heights of hourly deseasoned data (all year, all heights). Series were tested for trends using 95% confidence interval of Theil-Sen regression slopes. No significant trends were detected. [38]

3.2.6 Removing Temporal and Spatial Dependence from Wave Height Data

Annual and monthly means were tested using Theil-Sen Confidence intervals, adjusted and traditional Mann-Kendall results monthly (monthly and annual series, respectively), and deseasoned Theil-Sen Confidence intervals in Figures 3.15 and 3.16, respectively, at all publicly available nearshore WIS stations. These results show the relative conservatism of each test as well as any spatial patterns in coastal wave height trends that may exist.

Due to the possible within-series dependence in wave direction within Lake Michigan, the comparison was also made with annual and monthly wave series separated into 30-degree directional bins. Figures 3.17 and 3.18 show the annual and monthly results, respectively. To study the effect of latitudinal and longitudinal stretch on the enclosed water body, an identical analysis was performed on publicly available WIS nearshore stations in Lake Ontario as well, shown in Figures 3.19 and 3.20

Results of the seasonal Mann-Kendall test on 10-degree directional bins can be found in Appendix D.

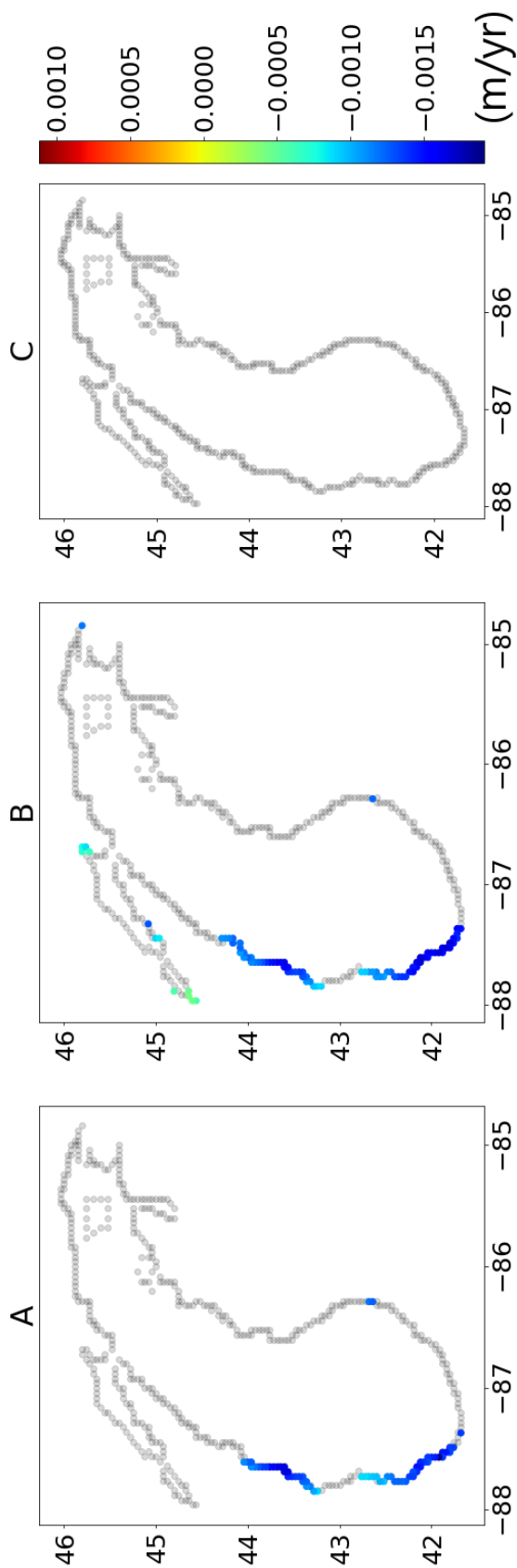


Figure 3.15. Comparison of wave-height trend results for annual means using (A) Theil-Sen regression confidence intervals, (B) Mann-Kendall test with Theil-Sen regression, and (C) seasonally differenced series with Theil-Sen confidence intervals on WIS nearshore stations [38]. Significant trends were not detected at stations shown in gray.

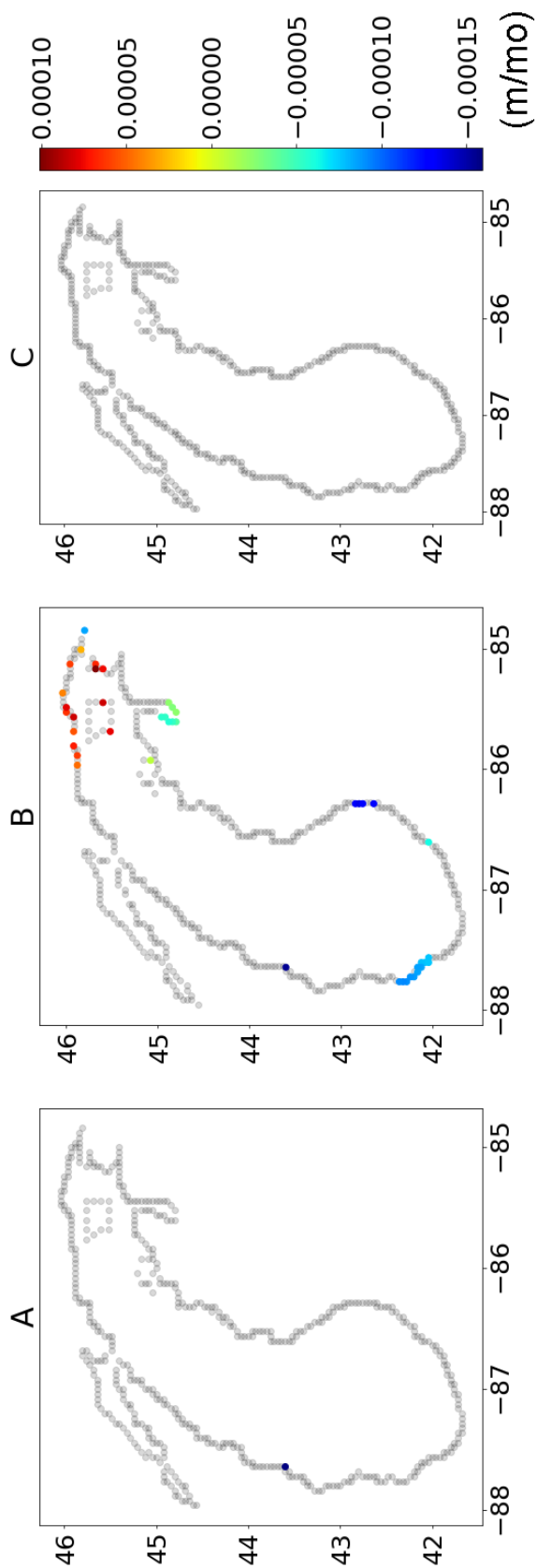


Figure 3.16. Comparison of wave-height trend results for monthly means using (A) Theil-Sen regression confidence intervals, (B) adjusted Mann-Kendall test with Theil-Sen regression, and (C) seasonally differenced series with Theil-Sen confidence intervals on WIS nearshore stations [38]. Significant trends were not detected at stations shown in gray.

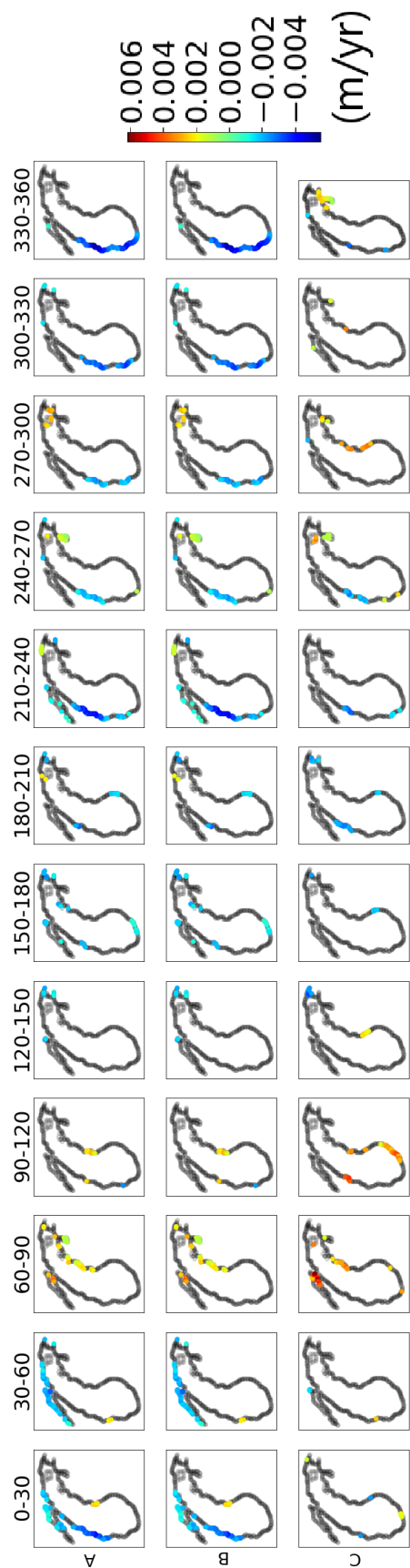


Figure 3.17. Comparison of wave-height trend results for annual means separated into 30-degree bins using (A) Theil-Sen regression confidence intervals, (B) Mann-Kendall test with Theil-Sen regression, and (C) seasonally differenced series with Theil-Sen confidence intervals on WIS nearshore stations [38]. Significant trends were not detected at stations shown in gray.

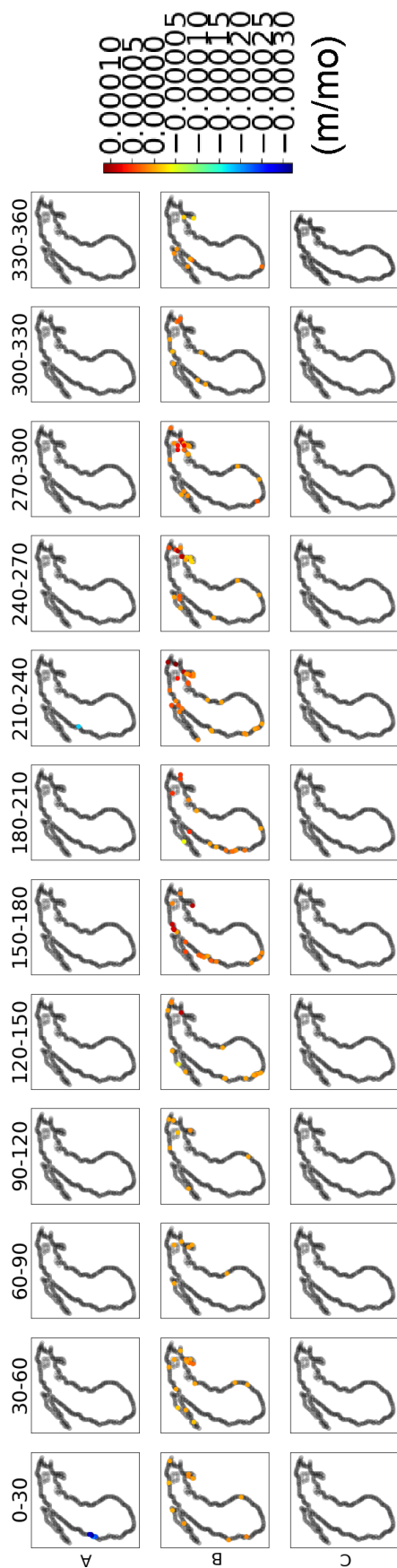


Figure 3.18. Comparison of wave-height trend results for monthly means separated into 30-degree bins using (A) Theil-Sen regression confidence intervals, (B) adjusted Mann-Kendall test with Theil-Sen regression, and (C) seasonally differenced series with Theil-Sen confidence intervals on WIS nearshore stations [38]. Significant trends were not detected at stations shown in gray.

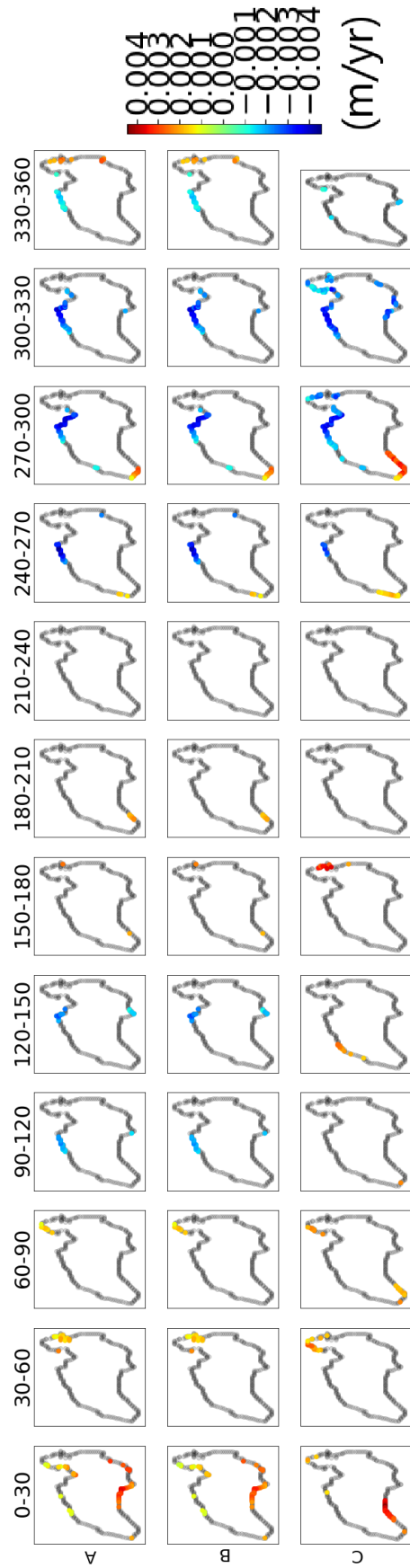


Figure 3.19. Comparison of Lake Ontario wave-height trend results for annual means separated into 30-degree bins using (A) Theil-Sen regression, (B) modified Mann-Kendall test with Theil-Sen regression, and (C) seasonally differenced series with Theil-Sen confidence intervals on WIS nearshore stations [38]. Significant trends were not detected at stations shown in gray.

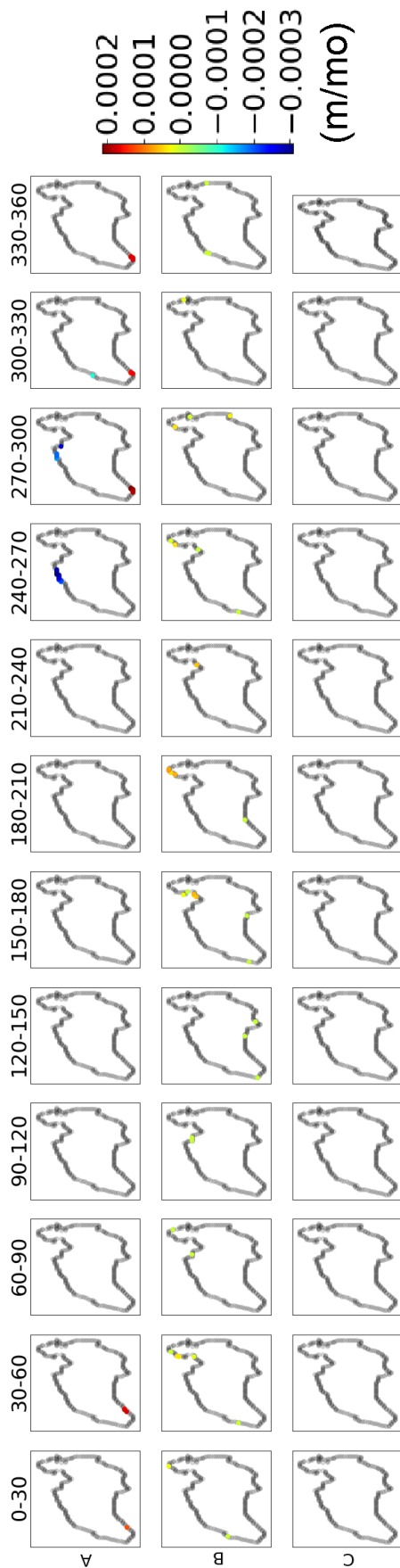


Figure 3.20. Comparison of Lake Ontario wave-height trend results for monthly means separated into 30-degree bins using (A) Theil-Sen regression, (B) modified Mann-Kendall test with Theil-Sen regression, and (C) seasonally differenced series with Theil-Sen confidence intervals on WIS nearshore stations [38]. Significant trends were not detected at stations shown in gray.

3.3 Has storm frequency or duration increased over the 36-year NDBC record?

3.3.1 Trends in Storm Metrics

The annual results of the storm criteria are plotted in Figure 3.21. The WIS model at Buoy 45007's location shows decreasing trends, -0.085hrs/yr (95% CI: $-0.1299 - -0.0451$ hrs/year) and -0.005m/yr (95% CI: $-0.0084 - -0.002\text{m/yr}$) in the mean storm length and mean storm peak metrics, respectively. The nearshore WIS station in the southern basin showed a nearly identical long-term trend as the nearby point, WIS at 45007, with -0.1042hrs/yr (95% CI: $-0.1821 - -0.0015$ hrs/yr).

In order to determine if the field-collected buoy data reflected the WIS model, the determination of the storm criteria was performed again, but this time only taking data in the WIS model for the May-October period covered by the buoys. The results of the summer-limited dataset are shown in Figure 3.22. With the data limited to the summer months, neither the buoy nor the WIS model show 95% confidence in non-zero Theil-Sen slopes for the trends detected in the full-year analysis above. This could indicate that the buoy data coverage may not be sufficient to reveal long-term trends in these annual storm metrics.

The data collected from Buoy 45002 showed a significantly decreasing trend in mean storm length (May-October period only), -0.0632hrs/yr (95% CI: $-0.1146 - -0.007$ hrs/yr). This finding, however, was not confirmed by the WIS model for the same May-October period. Results for these trends are summarized in table 3.1.

These metrics were also applied to all of the nearshore WIS stations available for Lake Michigan. Figure 3.23 indicates that the coast of Lake Michigan's southern basin may be experiencing a decrease in the mean storm duration and the yearly total storm time.

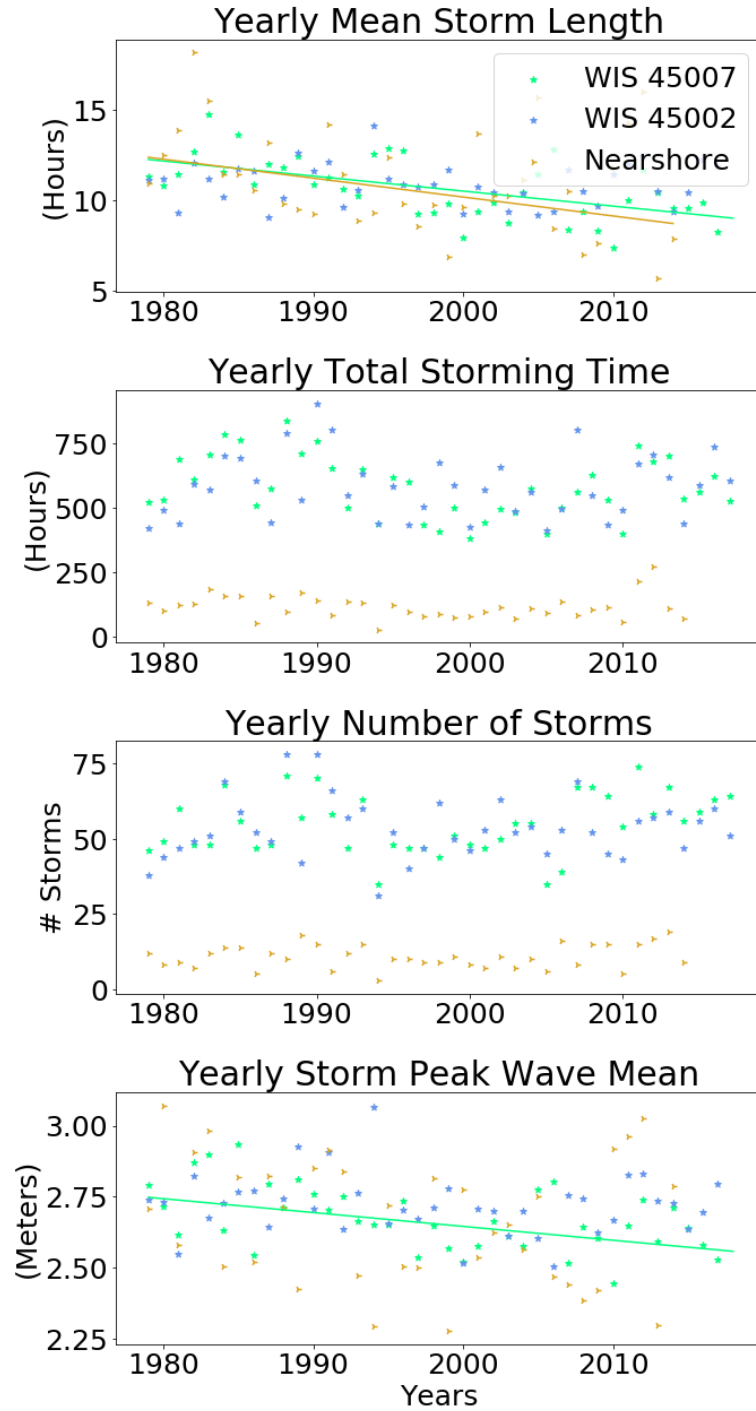


Figure 3.21. Annual storm parameter values using the WIS model at Lake Michigan buoy locations applied to entire year of WIS data. Tested for long term trends using 95% Theil-Sen slope confidence intervals. [38]

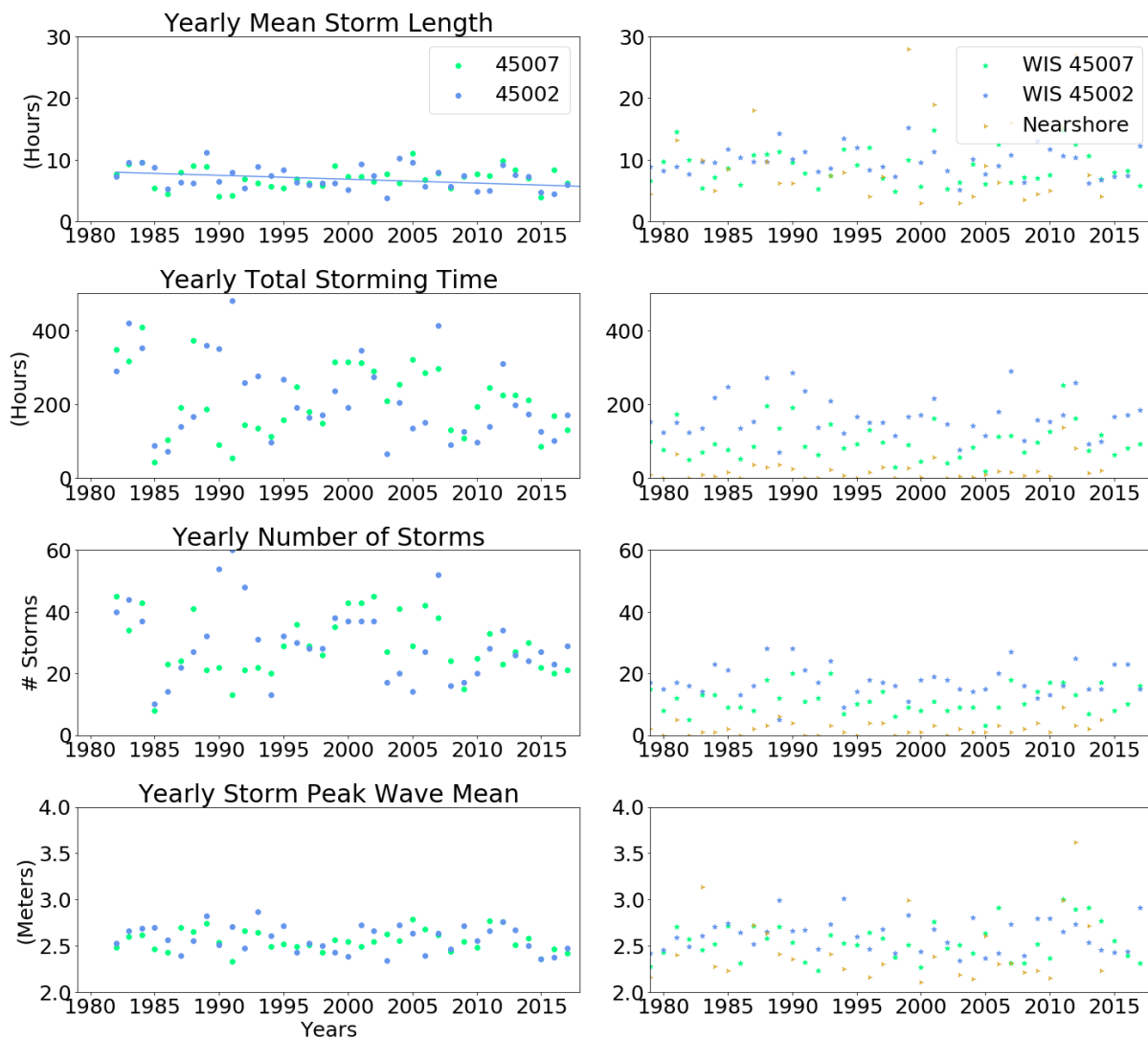


Figure 3.22. Annual storm parameter values using the WIS model at Lake Michigan buoy locations applied to May-October series of buoy and WIS data. Tested for long term trends using 95% Theil-Sen slope confidence intervals. [37, 38]

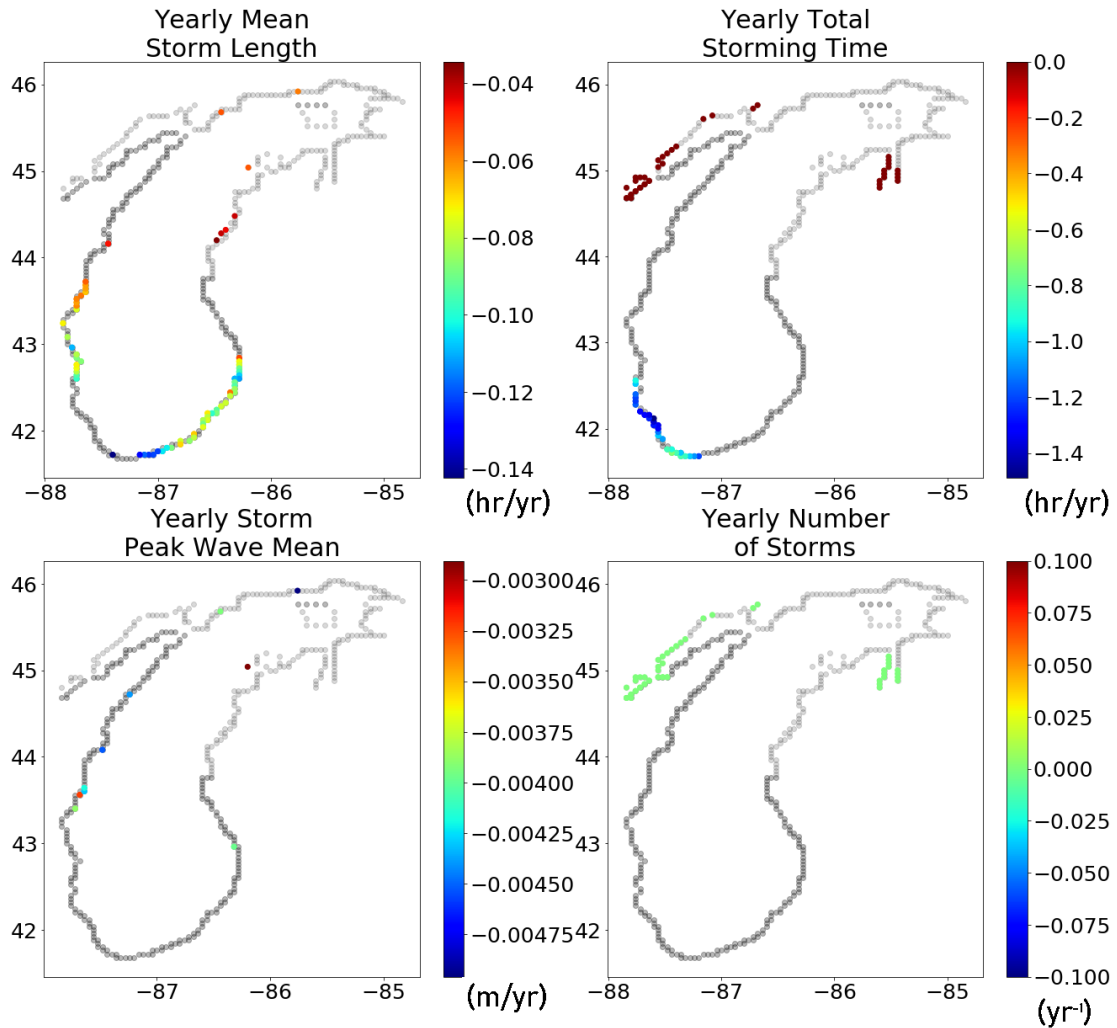


Figure 3.23. Annual storm parameter values using all Lake Michigan WIS nearshore stations applied to entire year of WIS data. Tested for long term trends using 95% Theil-Sen slope confidence intervals. Significant trends were not detected at stations shown in gray. [38].

3.3.2 Shifting Extreme Value Distribution

The WIS model at buoy locations 45007 and 45002 and nearshore station 94463 in the southern basin was subjected to a growing window analysis of the GEVD. If the 95% confidence interval of the slope did not include zero, the median Theil-Sen slope was depicted in Figure 3.24. Both series in the southern basin (WIS at 45007 and nearshore station 94463) are shown to have significant decreasing trends in the annual probability of receiving a wave greater than 5 meters in height.

If it is assumed that the process generating waves is changing, a moving window of annual wave-height maxima is more appropriate. The results of the moving window analysis is shown in Figure 3.25. All three locations show significantly decreasing trends in the probability of receiving a wave greater than 5 meters in height.

Figure 3.26 shows the results of the same analysis using the entire WIS Lake Michigan model. In the region of the southern basin, the results of the GEVD indicate that the probability of receiving a wave 6 meters or larger is decreasing at a rate of -0.0126 yr^{-1} (95% CI: $-0.0137 - -0.0119 \text{ yr}^{-1}$). A similar trend is seen in the nearshore WIS station, located in the southern basin where the probability of receiving an identical extreme wave is decreasing at a rate of -0.0031 yr^{-1} (95% CI: $-0.0039 - -0.0026 \text{ yr}^{-1}$). Results for these trends are summarized in table 3.1.

Figure 3.27 shows the results of the analysis with moving window, eliminating the assumption of the constant wave generation process. A similar spatial pattern and trends are seen in both the northern and southern basins with the value of the slopes increasing by double or more. Results for these trends are summarized in table 3.1.

The north-south orientation of Lake Michigan may be related to the distinct pattern shown in Figures 3.26 and 3.27. To further examine the effect of fetch and lake orientation the WIS model, results were analyzed in an identical manner. The results for the growing window and the moving window probability distributions can be seen in Figures 3.28 and 3.29.

Figures C.1 and C.2 from Appendix C repeat the previous analysis using only WIS data from May to October, similar to what is available to NOAA's NDBC buoys. This limitation on the data removes the trends seen previously when the entire year is considered. Some trends may exist, but they are much more limited in spatial scope and severity of the Theil-Sen slope. Also May-October trends are not found in the location of the buoys, indicating that their utility in backing up these results is limited.

Finally, the analysis with the growing window was repeated on the WIS nearshore stations in Figure 3.30. These stations reflect a similar spatial pattern to those seen in the full WIS model.

Appendix C show plots for the growing and moving window analysis that include the 95% confidence intervals of the integrated probabilities. Due to the size of these confidence intervals, an alternative peaks-over-threshold approach was taken to reduce the size of the confidence intervals. Appendix C also contains GEVD plots for 12 and 15 year windows. Changing the GEVD window size had little impact on the direction of the trends at each location, except for the WIS at Buoy 45002 data series which showed no trend, an increasing trend, and a decreasing trend in the 10-, 12-, and 15-year growing window analyses, respectively. All results are summarized in table 3.1.

Using the greater-than 2-meter peaks-over-threshold data sets generated for the storm parameters a GPD was fit to the first decade's peaks-over-threshold data sets with each subsequent year's data set added to examine the changing trend. Each GPD was integrated from 3 to 6 meters (to account for the 2 meter difference required by the Pareto distribution) to generate an equivalent 5- to 8-meter wave probability to the Gumbel approach above.

The growing window analysis show in Figure 3.31 shows a long-term decreasing probability of receiving a 5- to 8-meter wave, similar to the GEVD results for the same data series. The 95% confidence intervals on the probabilities integrated GPD

are smaller than those from the GEVD, but they remain large enough to cast doubt on the significance of the detected trends.

The probability of receiving a wave larger than 5 meters in height integrated from a GPD developed from a moving decadal window of peaks-over-threshold data sets is shown in Figure 3.32. This analysis again compares favorably with the results of the GEVD analysis for the moving window: all three locations show a significantly decreasing Theil-Sen trends, with improved 95% confidence intervals.

To test the dependence on the window size the analysis was also run using a 15-year moving and growing windows as well. The significance of the decreasing trend at the location of Buoy 45007 and the nearshore station in the southern basin were maintained. The results in northern basin were more impacted by the window size, showing increasing trends as the window increased from 10 years in length. These results can be seen in table 3.1 and Appendix C.

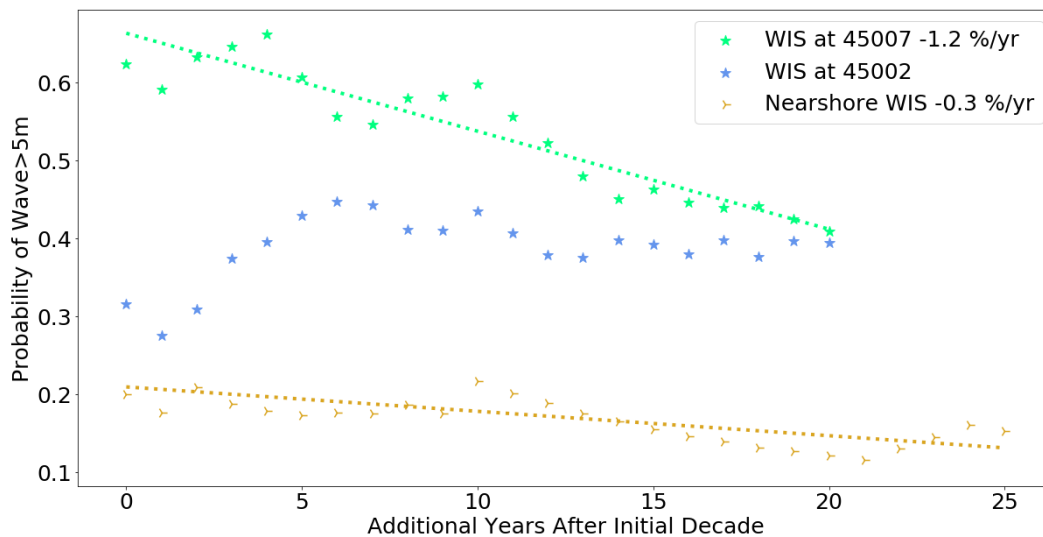


Figure 3.24. Probability of receiving a wave 5m or greater at the three WIS sites in a year, from the generalized extreme value distribution determined by a growing window of annual maxima after the first decade [38].

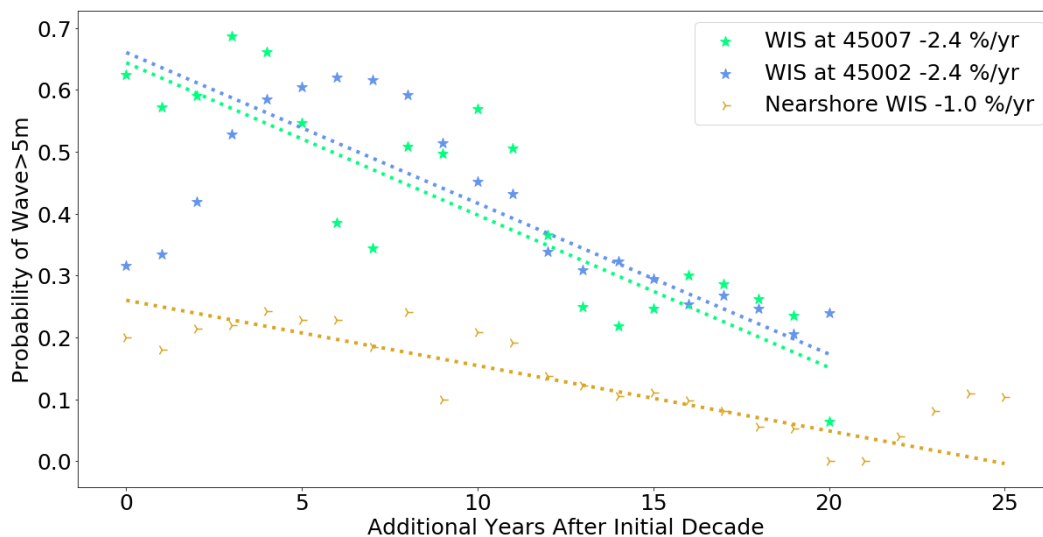


Figure 3.25. Probability of receiving a wave 5m or greater at the three WIS sites in a year, from the generalized extreme value distribution determined by moving decadal window of annual maxima [38].

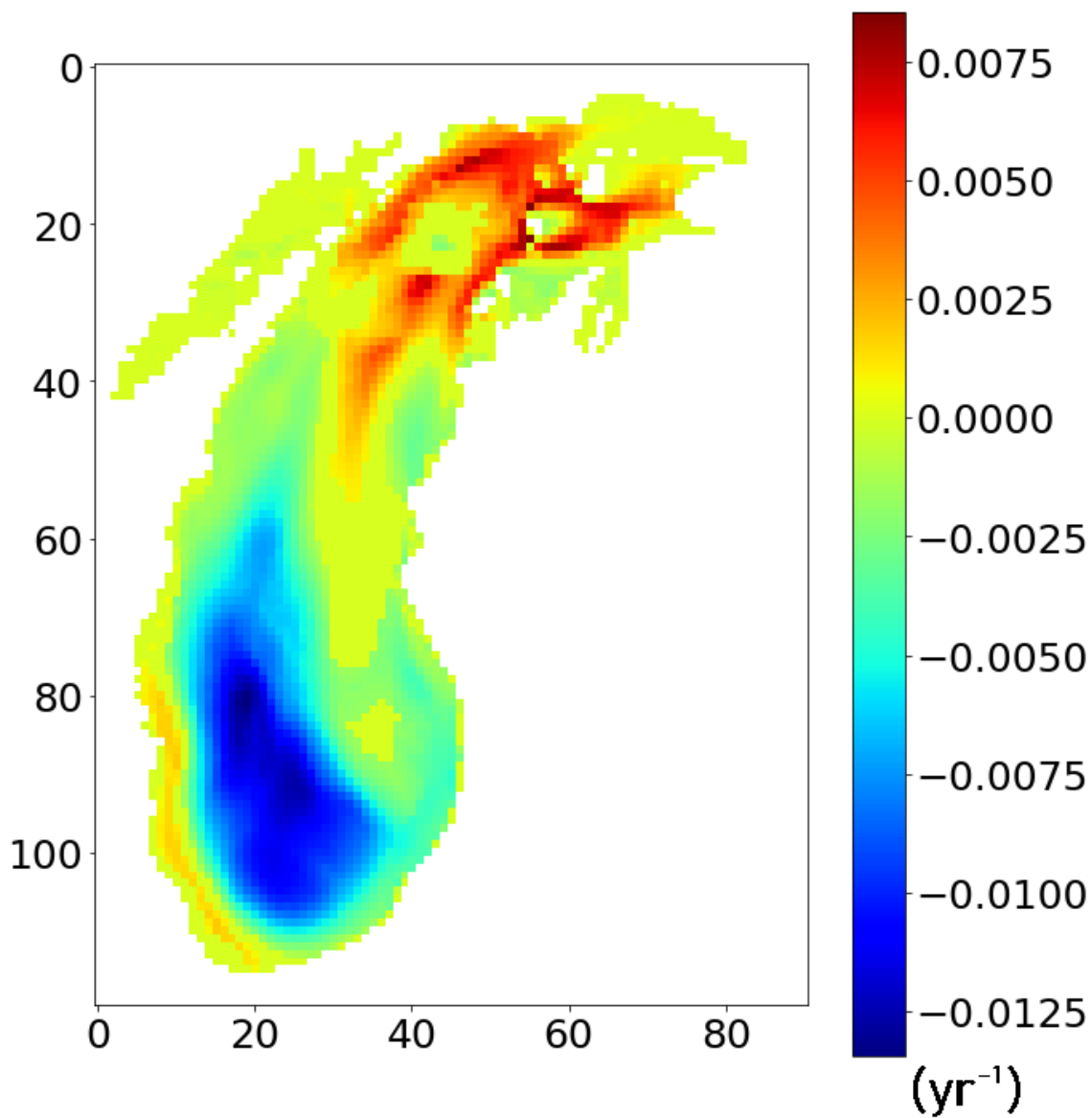


Figure 3.26. Slope of Theil-Sen regression on probability of receiving a wave larger than 5m for full WIS model of Lake Michigan [38]. Probabilities determined from an extreme value distributions generated from a growing window of yearly maxima.

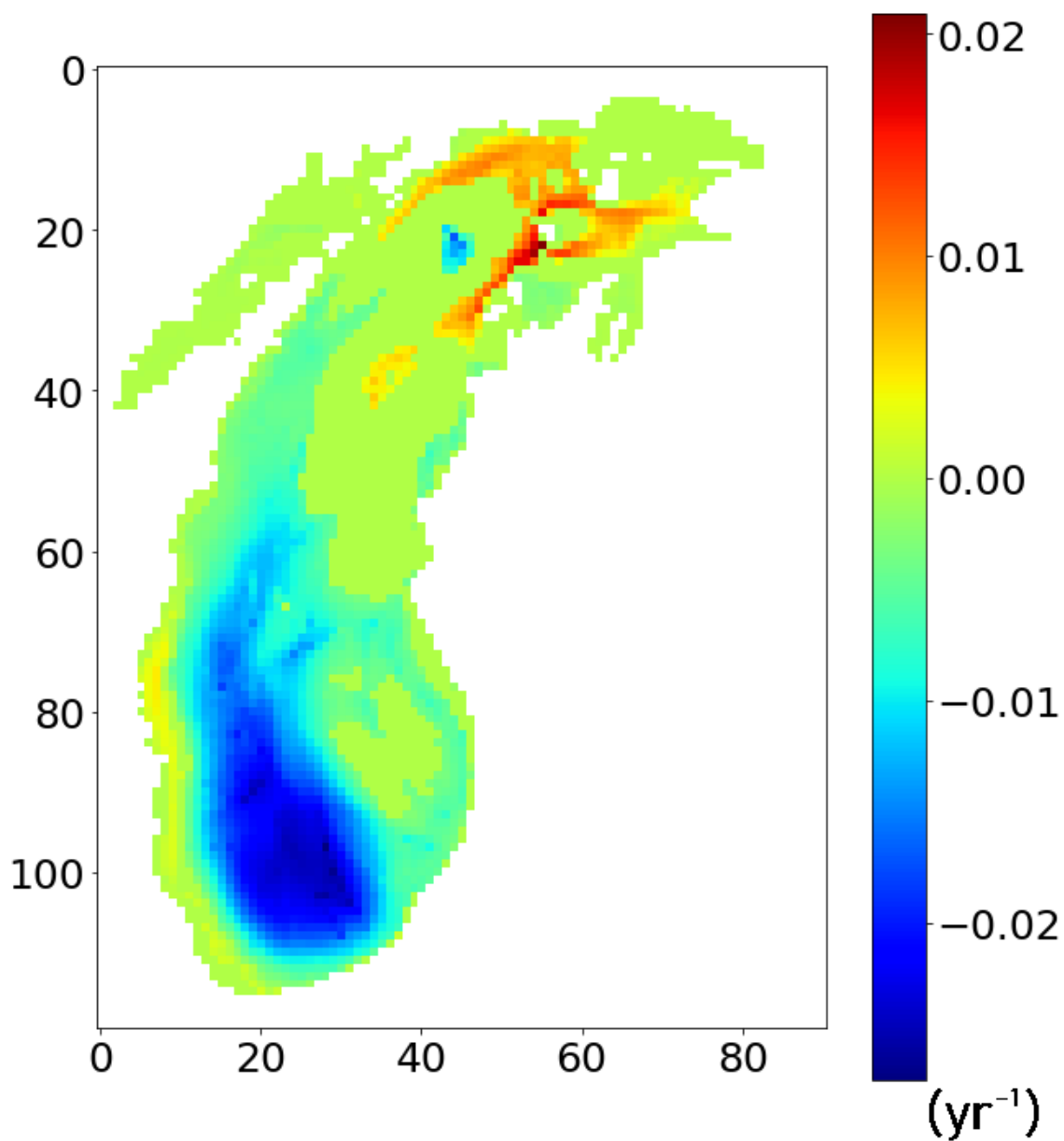


Figure 3.27. Slope of Theil-Sen regression on probability of receiving a wave larger than 5m for full WIS model of Lake Michigan [38]. Probabilities determined from an extreme value distributions generated from a moving window of yearly maxima.

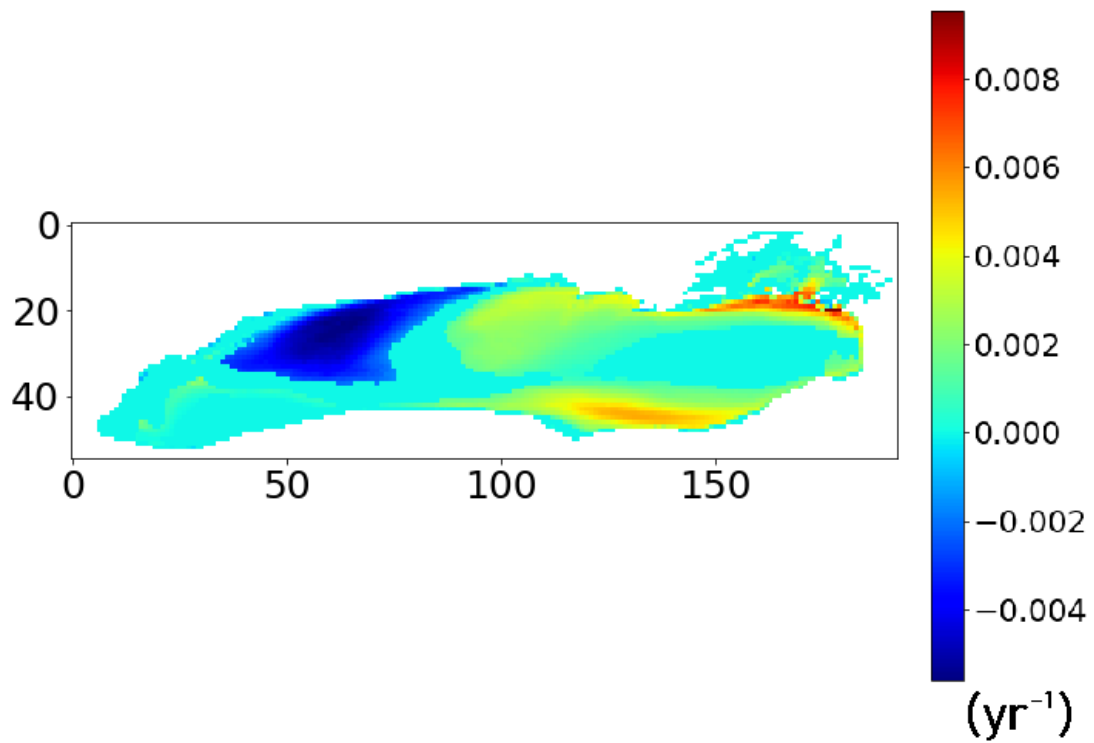


Figure 3.28. Slope of Theil-Sen regression on probability of receiving a wave larger than 5m for full WIS model of Lake Ontario [38]. Probabilities determined from an extreme value distributions generated from a growing window of yearly maxima.

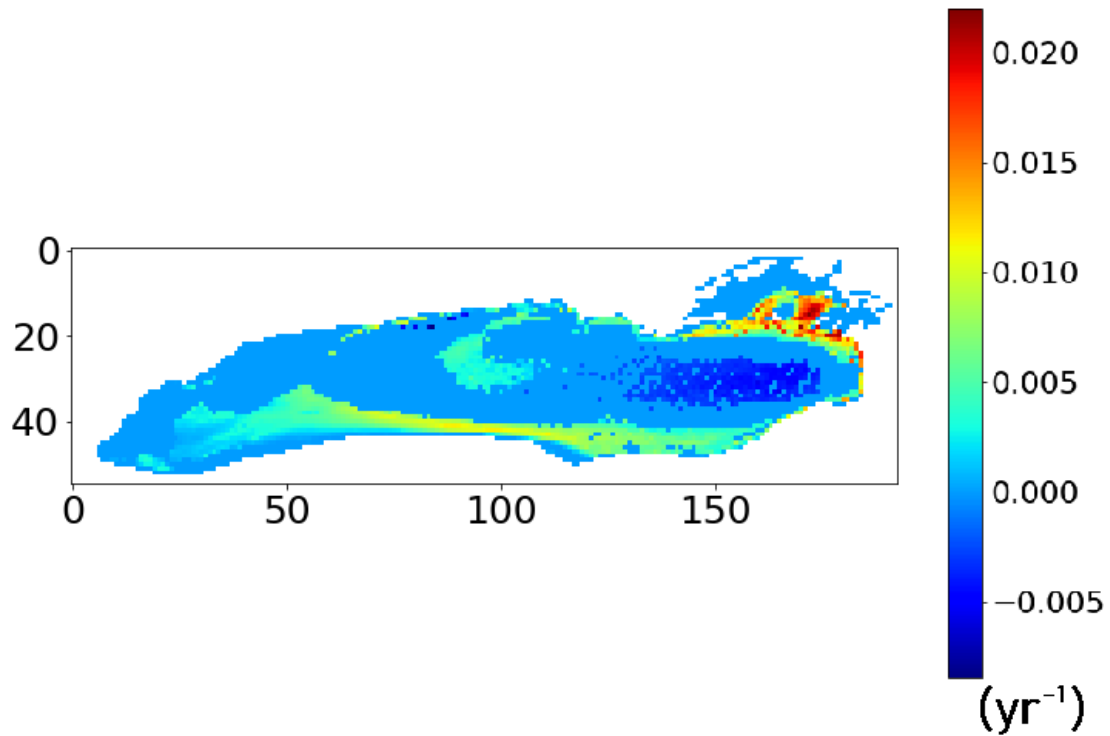


Figure 3.29. Slope of Theil-Sen regression on probability of receiving a wave larger than 5m for full WIS model of Lake Ontario [38]. Probabilities determined from an extreme value distributions generated from a moving window of yearly maxima.

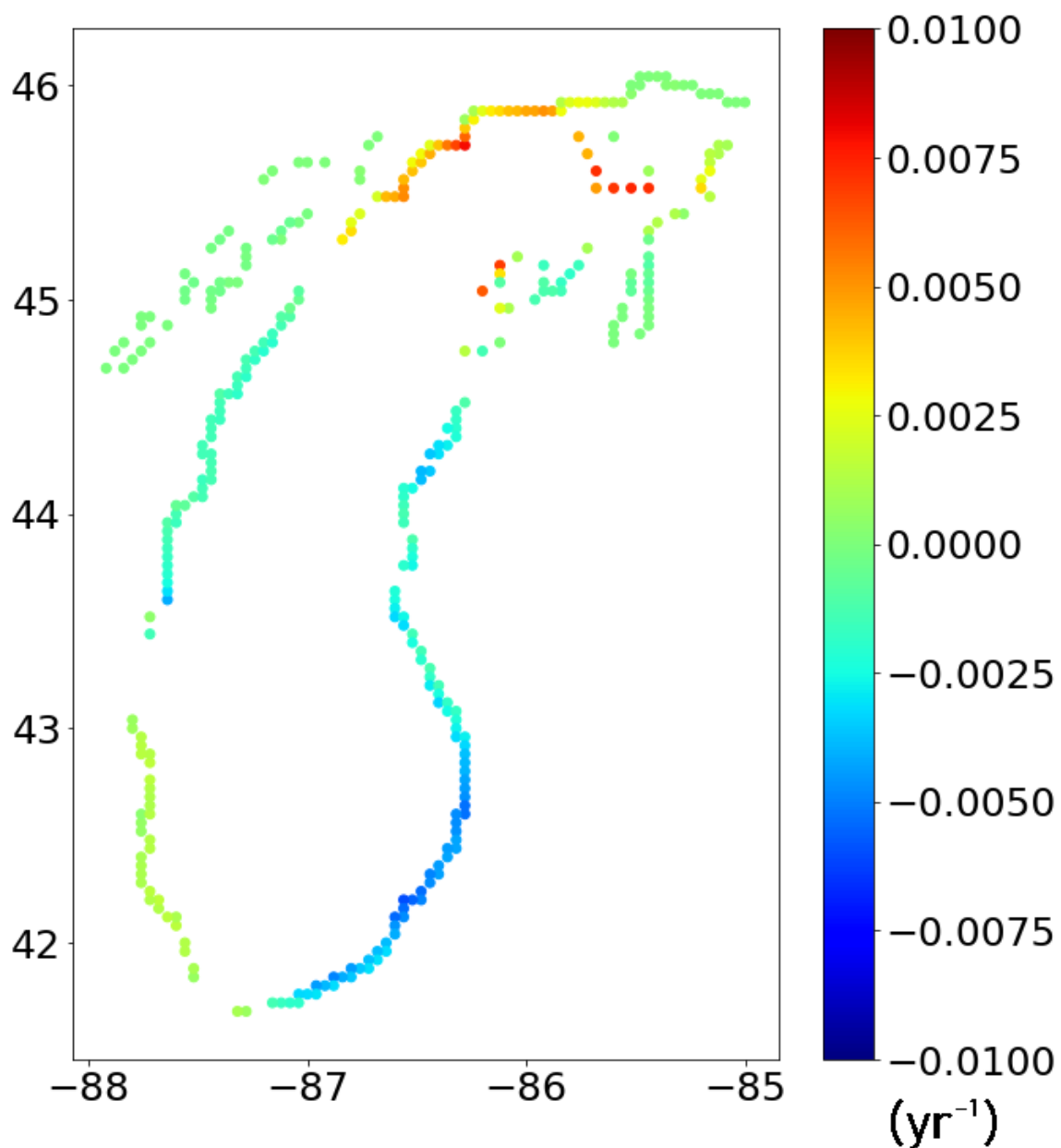


Figure 3.30. Slope of Theil-Sen regression on probability of receiving a wave larger than 5m for publicly available WIS wave model nearshore stations in Lake Michigan [38]. Probabilities determined from an extreme value distributions generated from a growing window of yearly maxima.

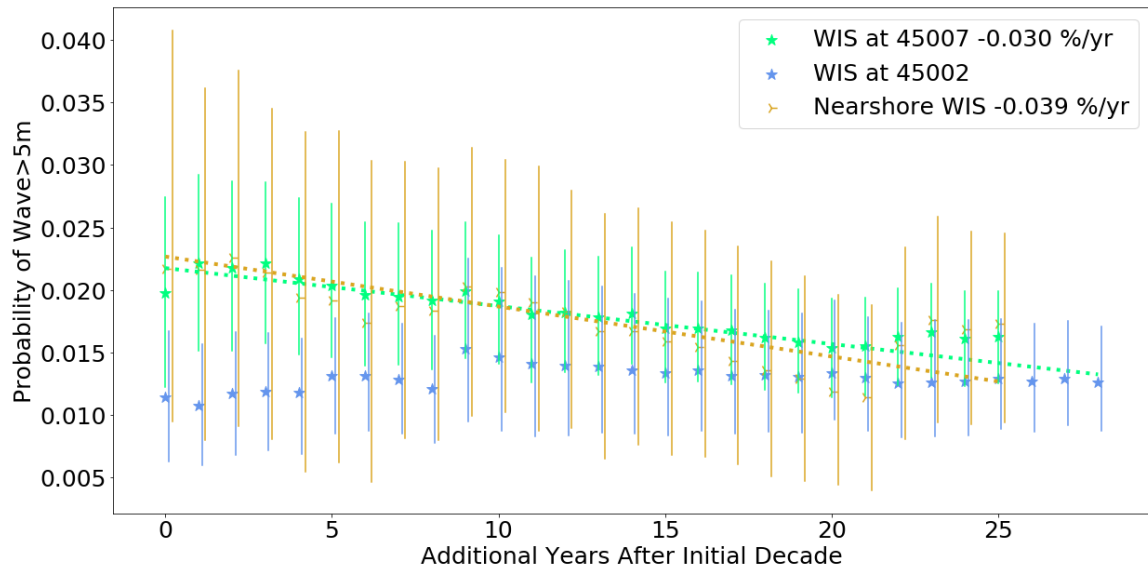


Figure 3.31. Slope of Theil-Sen regression on probability of receiving a wave larger than 5m using WIS model at buoy locations and a southern basin nearshore station [38]. Probabilities determined from Pareto distributions generated from a growing yearly window of peak $> 2m$ event heights. 95% confidence intervals developed by bootstrapping.

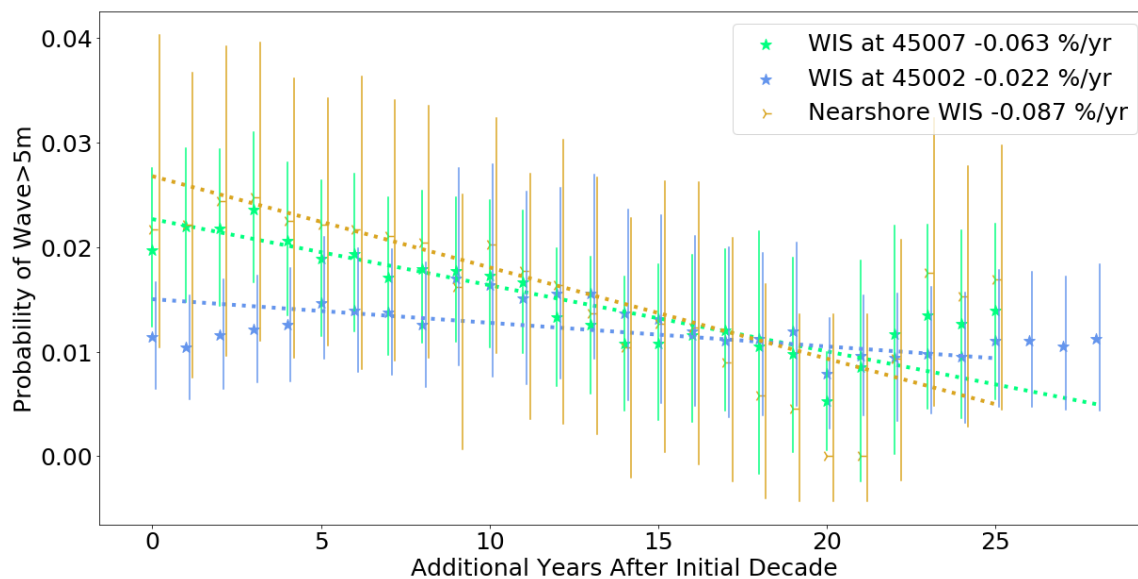


Figure 3.32. Slope of Theil-Sen regression on probability of receiving a wave larger than 5m using WIS model at buoy locations and a southern basin nearshore station [38]. Probabilities determined from Pareto distributions generated from a moving decadal window of peak $> 2m$ event heights. 95% confidence intervals developed by bootstrapping.

3.4 Has the direction of the waves changed?

3.4.1 Trends in Annual Wave Frequency by Direction

Figure 3.33 shows an arrangement of plots depicting the annual time spent with waves coming from the compass direction of their position on the circle. In the northeast corner, there are significant increasing trends, suggesting that there is an increasing number of waves approaching annually from that direction. In the southeast region, significant decreasing trends were detected.

Figure 3.34 shows an identically arranged plot. Here, the WIS data show a decreasing trend in waves approaching from the southeast.

The same analysis using a 10-degree bin size can be seen in the Appendix A. The 10-degree bins show the same spatial pattern of significant trends in wave direction described above, indicating stability.

This analysis was applied to all of the Lake Michigan WIS nearshore stations and the magnitude of the slopes of the significant Theil-Sen regressions are depicted by color in the 36 directional plots shown in Figure 3.35. Waves approaching from the northeast show increasing time in the south and southwest coast. As the wave approach direction becomes more easterly, we can see that the region of change moves west and northwards along the coast in response.

Waves approaching from the southeast show increasing time on the west and northwest coast. As the wave approach direction becomes more southerly, we can see that the region of changes moves north along the coast in response.

The same analysis was repeated using the Lake Ontario WIS nearshore stations and is seen in Figure 3.36. The Lake Ontario results reveal waves approaching from the southwest decreasing in frequency along the northwest coast and waves approaching from the east increasing in frequency along the eastern coast.

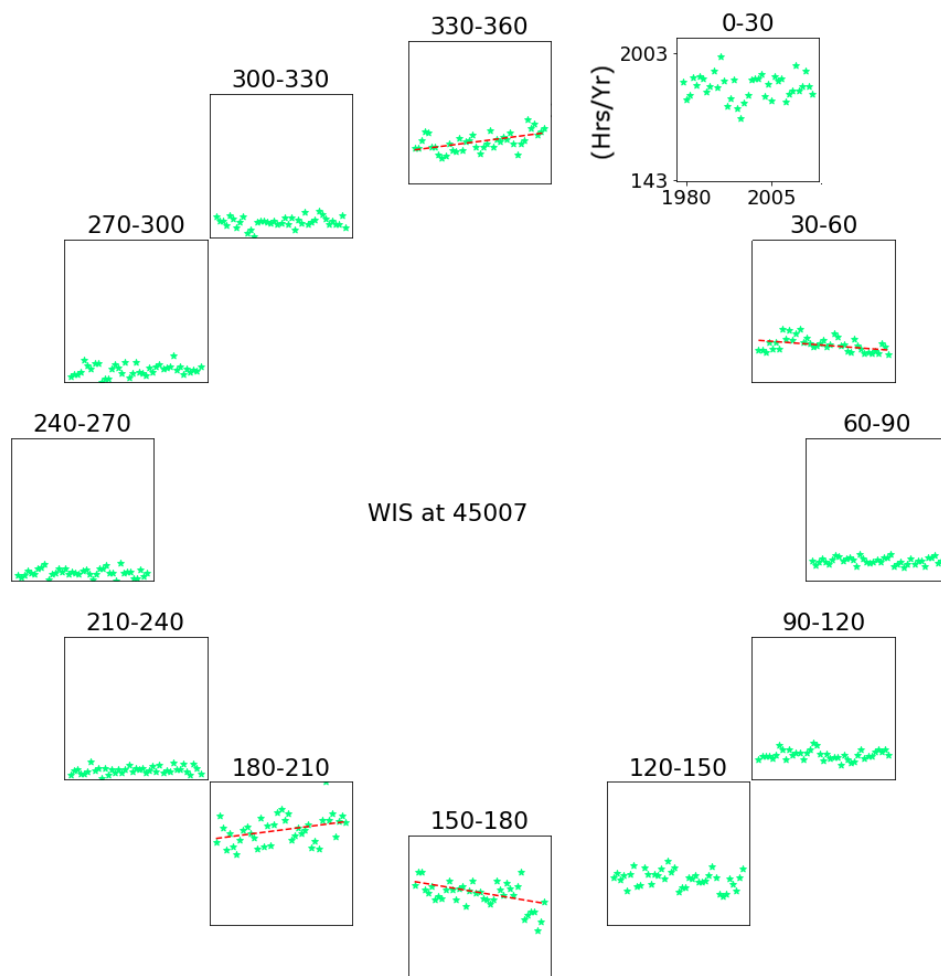


Figure 3.33. Annual trends in hourly frequency for wave approach direction in 30-degree bins from the WIS model at Buoy 45007. Significant Theil-Sen trends are indicated by depicting the slope as a red line. [38]

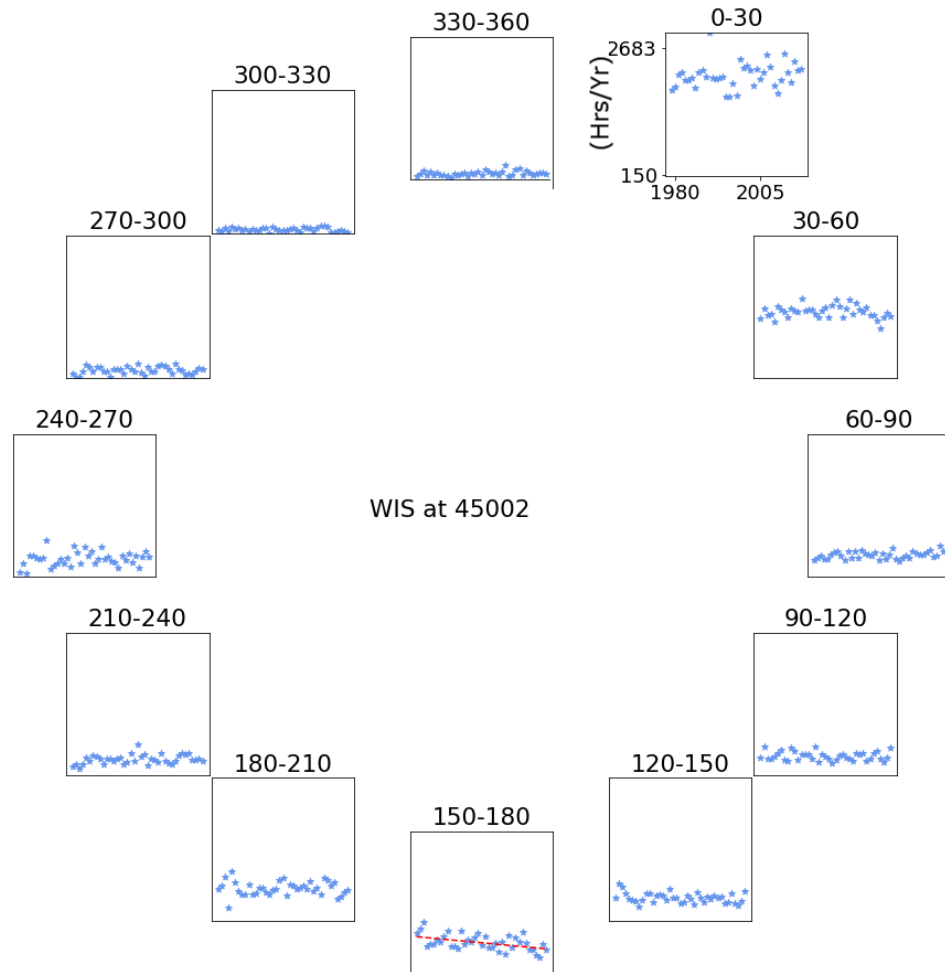


Figure 3.34. Annual trends in hourly frequency for wave approach direction in 30-degree bins from the WIS model at Buoy 45002. Significant Theil-Sen trends are indicated by depicting the slope as a red line. [38]

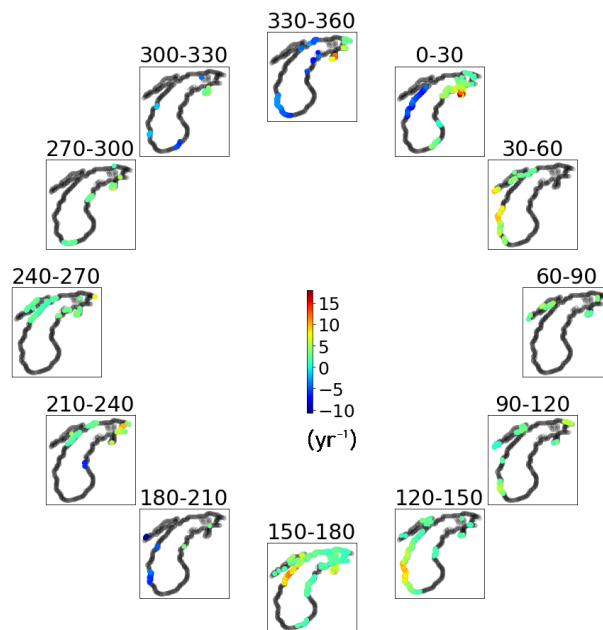


Figure 3.35. Annual trends in hourly frequency for wave approach direction in 30-degree bins from the WIS model at all WIS nearshore stations. [38]

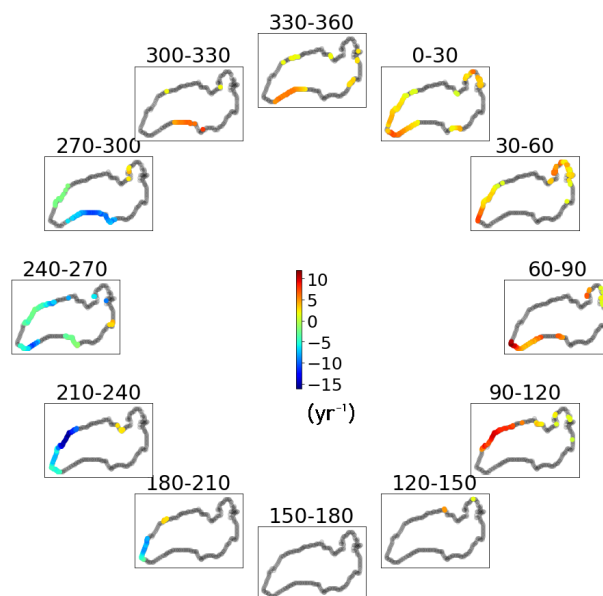


Figure 3.36. Annual trends in hourly frequency for wave approach direction in 30-degree bins from the WIS model at all WIS nearshore stations in Lake Ontario. [38]

3.4.2 Kernel Density Estimates of Wave Direction

Figure 3.37 shows monthly wave direction PDFs generated using data from the first and last three years of directional wave data collection in Buoy 45007. The kernel density estimates for the PDF suggest that there has been a shift since 1992 in wave direction. In the later part of the year (August-October), there is an increase in the probability of waves arriving from 0 to 180 degrees.

The estimated PDF can be integrated from 45 to 135 degrees to determine the probability of receiving a wave from the east for any month or year. The results of this analysis are shown in Figure 3.38. No significant annual trends were discovered in the monthly probabilities of eastern waves. The difference in the probability distribution functions seen previously in Figure 3.37 are driven by the most recent few years and not by an ongoing trend.

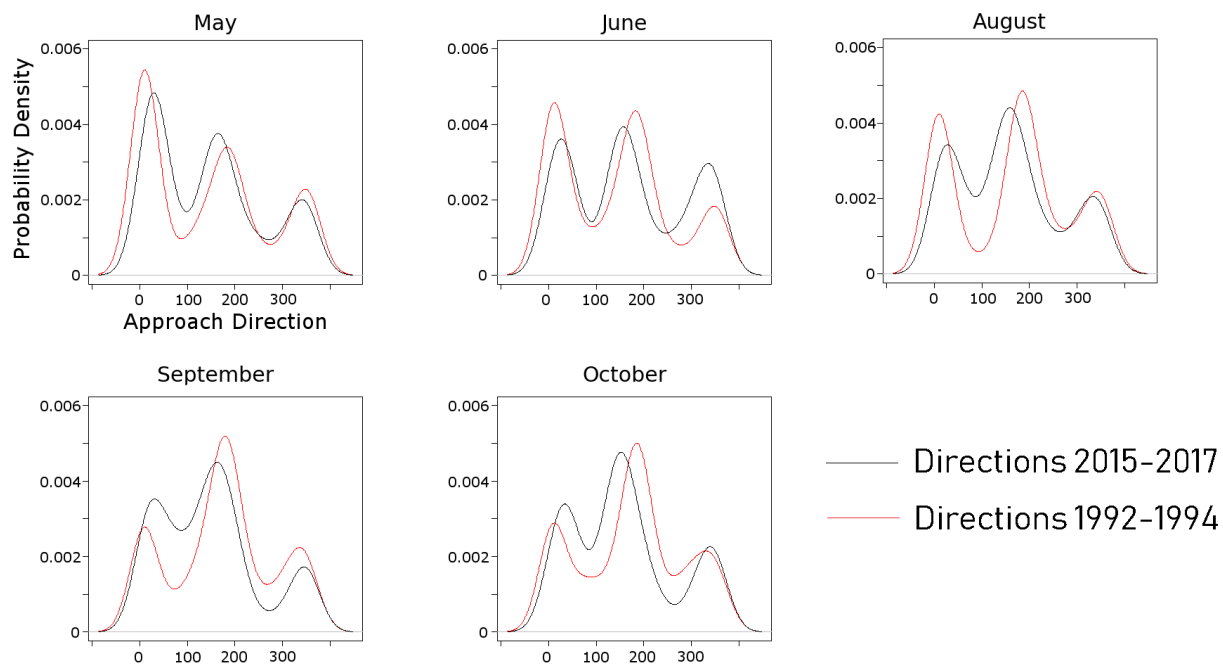


Figure 3.37. Kernel-Density Estimate of probability distributions functions of wave directions for Buoy 45007, divided by month. A 40% data completeness threshold was required to generate a plot.

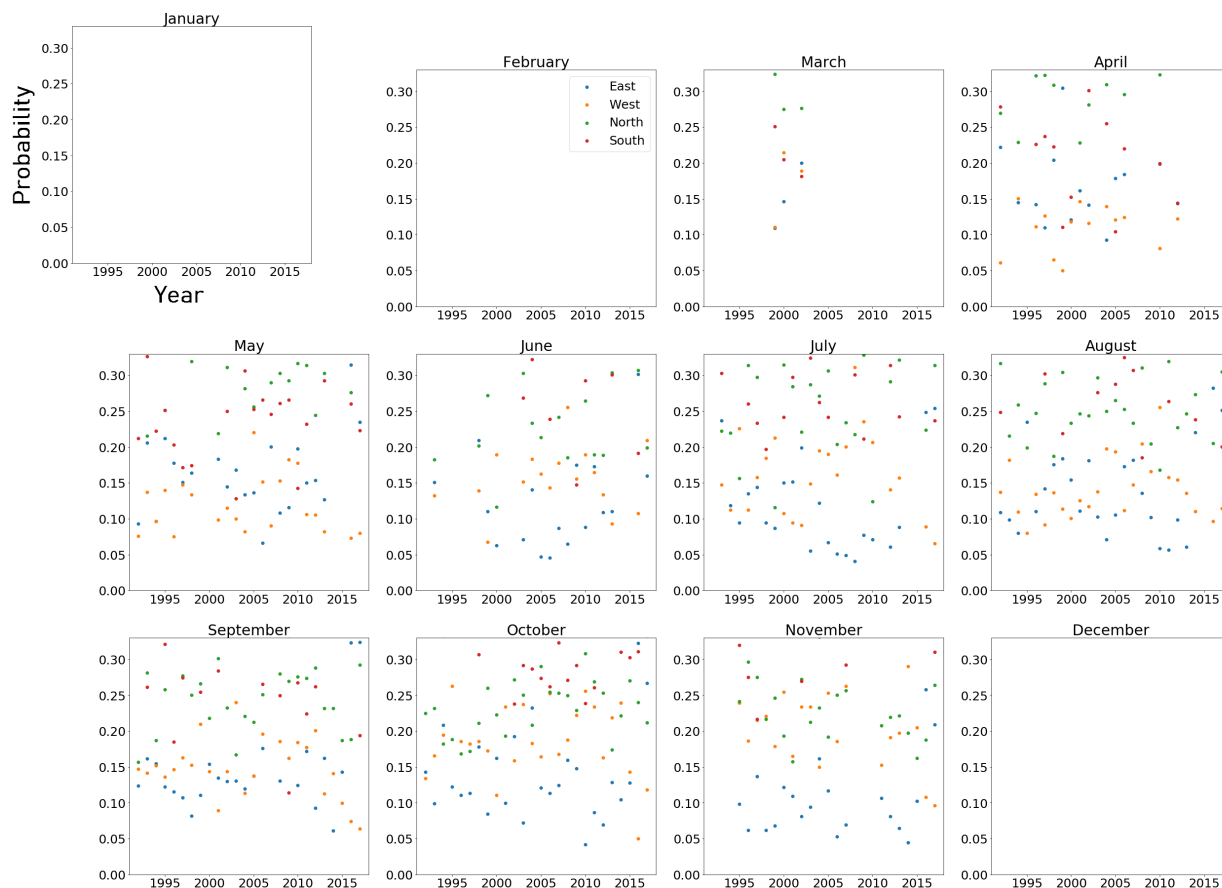


Figure 3.38. Integration of annual PDFs of wave approach direction to determine the annual trends in Buoy 45007's probability of receiving a wave from 90-degree bins centered on the four cardinal directions. No significant trends were detected. A 40% data completeness threshold within a month was required to generate a point.

3.5 Is the increasing lake level related to the size of the waves?

Using the same 60-month moving average applied by Meadows et. al (1997) to updated buoy and WIS data, shown in Figure 3.39, a significant correlation coefficient of 0.5378 was calculated. This value is comparable to their results. The smoothing effect of the 60-month moving average can be seen in Figure 3.40. A correlation coefficient was also calculated between the monthly wave height maxima and the lake level. While significant as well, this coefficient was -0.1418. These series are shown in Figure 3.41.

To investigate the effect of the window size on the moving average, the correlation coefficient between the two series was plotted against the window size in years in Figure 3.42.

Figure 3.42 indicates that a longer window resulted in higher correlations between the lake level and mean wave-height series. By choosing a five year moving window Meadows et. al may have over-smoothed both series, resulting in an arbitrarily high correlation coefficient. This result is not unexpected, given that the limiting case of the lowest possible low-pass filter would result in a perfect correlation.

Both the periodogram and the autocorrelation function suggest a 12-month cycle in lake level. This result is similar to what was seen earlier in the wave-height records and was expected from a visual inspection of raw data plots.

After applying a 12-month differencing routine to both data series to eliminate the annual cycle, the stationarity of the new series was checked using the augmented Dickey-Fuller test. This test showed that the previously non-stationary series was now stationary ($p < 0.05$).

A low correlation (-0.107) with p value greater than 0.05 indicated little relationship between the deseasoned monthly data series.

However, if the monthly wave height dataset is constructed using the deseasoned maximum monthly wave height there is a significant ($p < 0.05$) moderate anti-correlation of -0.32 found between the lake level and the waves.

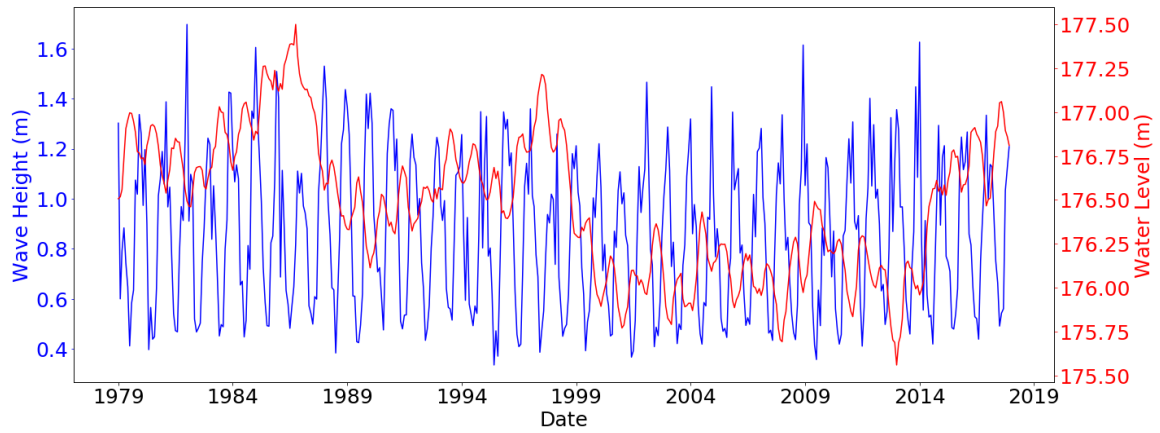


Figure 3.39. Monthly wave height means from WIS at Buoy 45007 and the USACE lake level record. [38, 43]

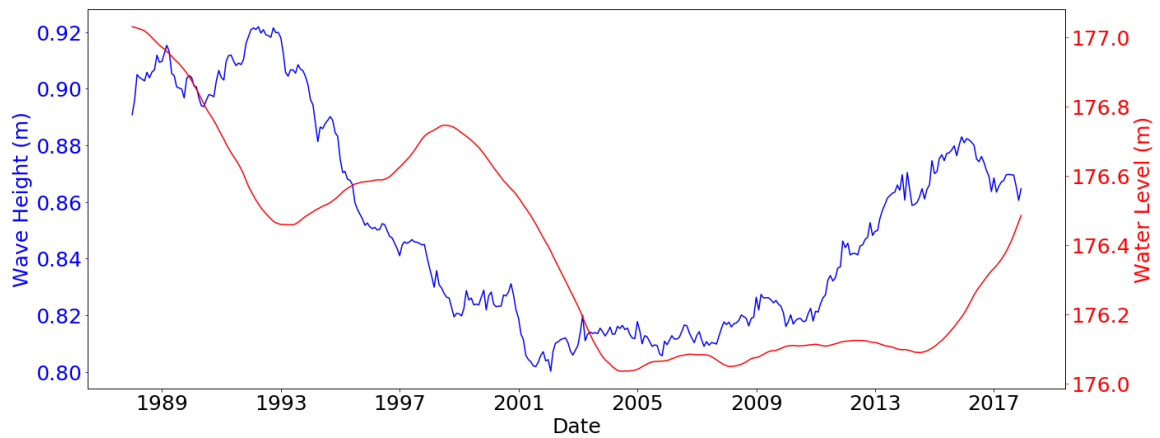


Figure 3.40. 60-month moving averages of monthly wave height mean from WIS at Buoy 45007 and the USACE lake level record. [38, 43]

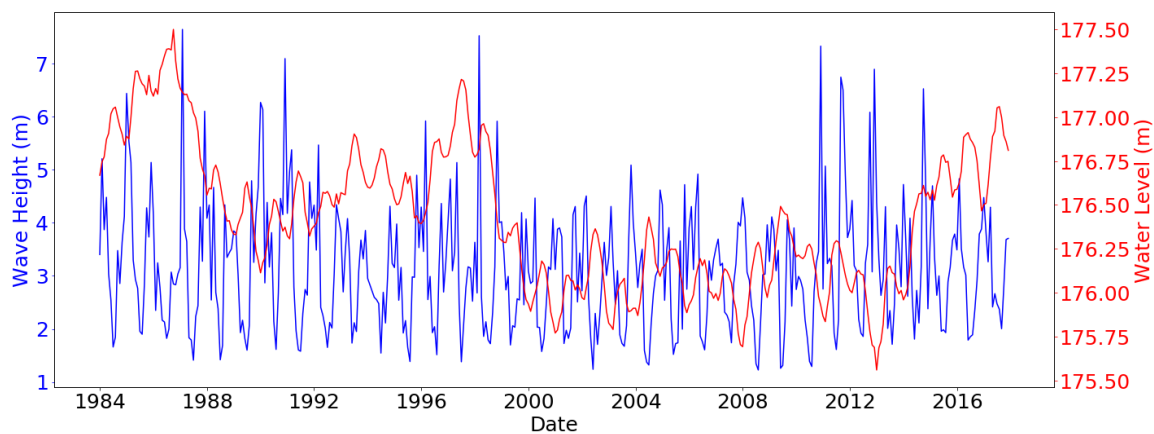


Figure 3.41. Monthly wave height maxima from WIS at Buoy 45007 and the USACE lake level record. [38, 43]

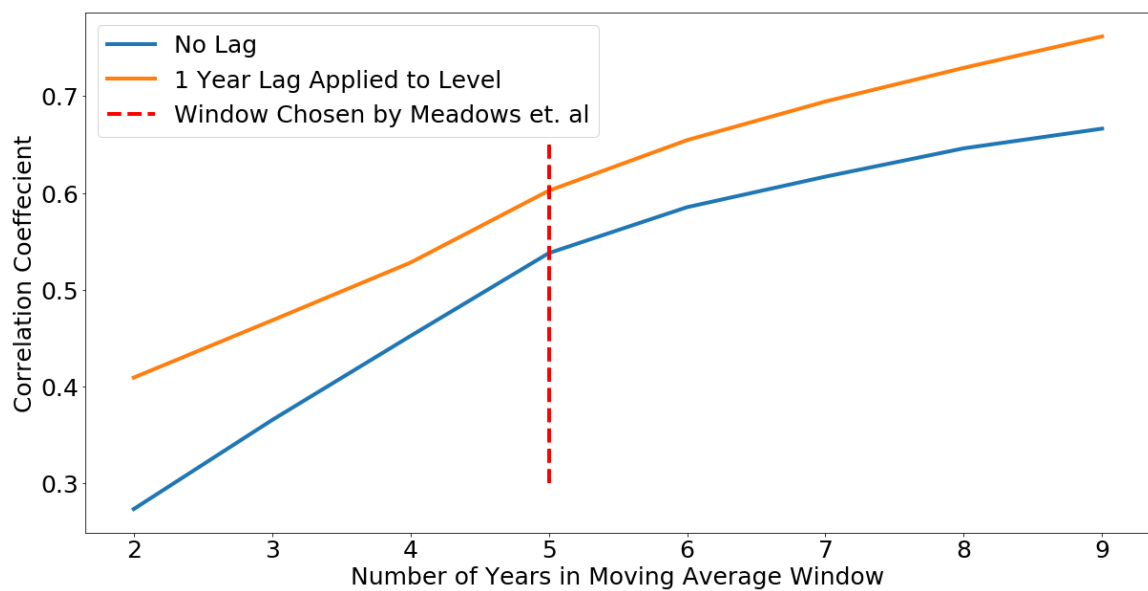


Figure 3.42. Change in Pearson's R with increasing moving average range. These coefficients were all found to be significant with $P < 0.05$.

Table 3.2. Pearson's R correlation coefficients and p values (R-value, p-value) for paired lake level and wave height series.

	No Lag	1 Year Lag
Lake Level and Monthly Mean Hs	(-0.209,0)	(-0.1691,0.0003)
Lake Level and Monthly Max Hs	(-0.1418,0.0041)	(-0.1034,0.0398)
60-Month Mean of Lake Level and Hs	(0.5378,0)	(0.6023,0)
Annually Differenced Lake Level and Mean Hs	(-0.107,0.059)	(0.0655,0.2579)
Annually Differenced Lake Level and Max Hs	(-0.318,0)	(-0.2582,0)

The maximum absolute value of deseasoned wave height had correlations that were not found to be significant as well. The correlation coefficients can be found in table 3.2.

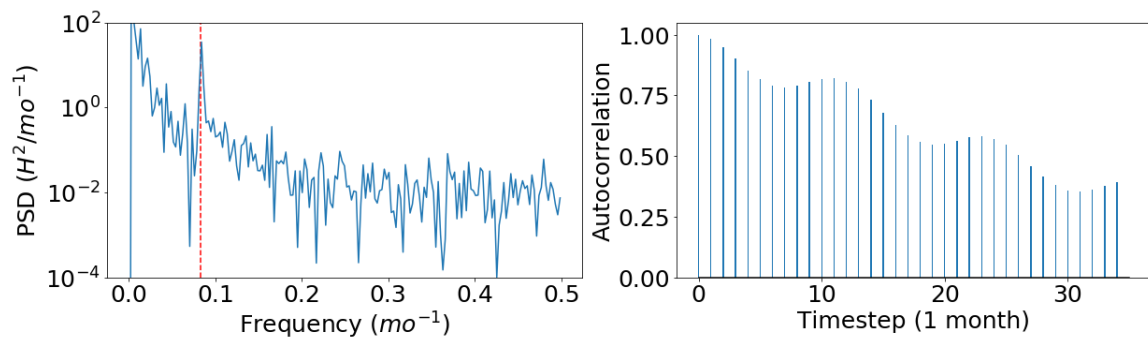


Figure 3.43. Identifying seasonality in Lake Michigan water level records using periodogram and autocorrelation function results. A peak frequency is seen at 12 months in the periodogram with lower frequency cycling. The autocorrelation function shows sinusoidal decay with a period of 12 months.

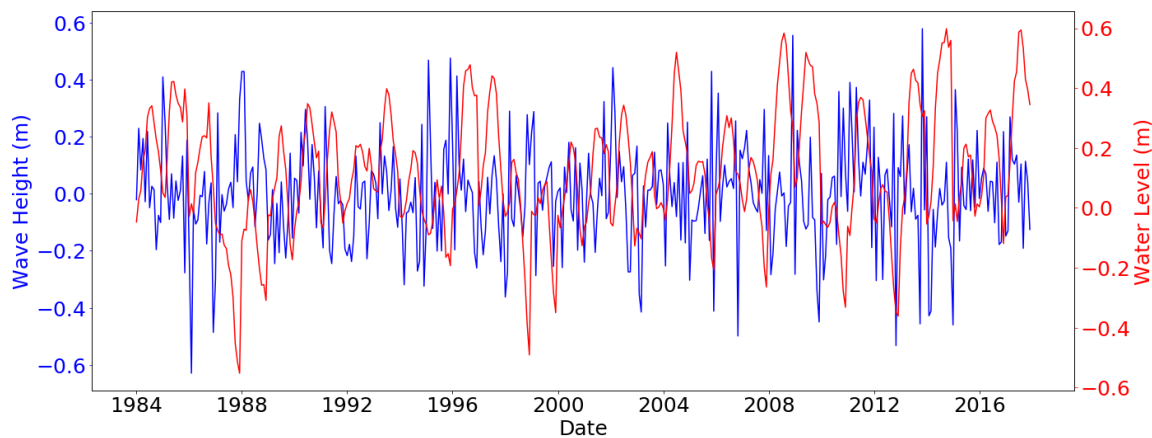


Figure 3.44. Monthly means of deseasoned wave height at Buoy 45007 and USACE lake level. Non-significant correlation of -0.1 directly, 0.06 with six-month lag. [38, 43]

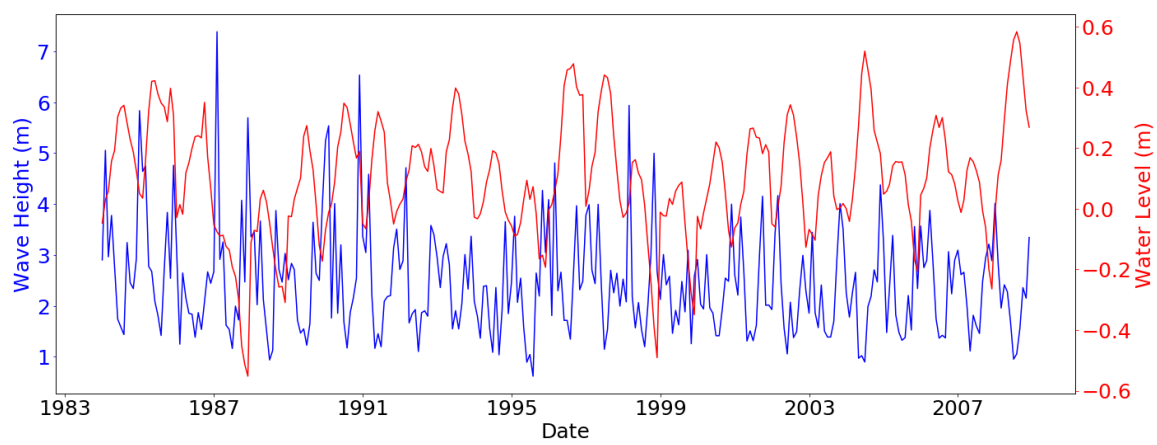


Figure 3.45. Monthly max of deseasoned wave heights and deseasoned USACE lake levels. Correlation of -0.32 directly, 0.34 with six-month lag. [38, 43]

4. DISCUSSION

To examine the wave climate of Lake Michigan, the two NOAA NDBC buoy records were subjected to relatively simple statistical techniques like annual means as well as more sophisticated methods involving seasonal differencing and maximum likelihood estimation of probability distributions to analyze changes in the lake's long-term climate trends. Alongside the field-collected buoy data, the WIS wave hindcast, produced by the USACE, was examined. The WIS hindcast allowed for the inclusion of waves occurring outside of the summer months when the buoys were not deployed. Winter waves on the Great Lakes are generally understood to be larger and it is the largest waves that drive sediment transport and hold greater importance to the coastal engineering community. Inclusion of the winter months was necessary to understanding the engineering impact of any changes in wave behavior on Lake Michigan.

4.1 Have waves in Lake Michigan increased in size over the 36-year NDBC record?

Theil-Sen slopes of the NOAA NDBC buoy annual wave height means indicated a decreasing trend in both the northern and southern basins. Data from the WIS model for the same subset of waves (May-October, $> 0.25m$) did not support these trends. When the full year of WIS data is used, significant trends are not seen in the model series. When the Theil-Sen slope of the annual means was applied to all of Lake Michigan's nearshore WIS stations significant, decreasing trends were seen along most of the western coast in the southern basin.

When the annual wave height means of the two buoy-located WIS stations were subjected to a Mann-Kendall test, the result showed a nearly identical pattern in the spatial extent of significant Theil-Sen trends. However, the Mann-Kendall test found

the coastal extent of significant decreasing trends was about 10% greater than the Theil-Sen 95% confidence interval used previously.

The monthly mean wave heights of the two buoy-located WIS stations were tested using a form of the Mann-Kendall test adjusted for within-series time dependence. Since the monthly means are positively autocorrelated, the unmodified Mann-Kendall test is more likely to find non-significant trends than the p-value suggests. The results for the monthly mean showed no significant trends in the data from the buoy locations and only a few sporadic decreasing trends in the southern basin for the nearshore stations. However, these tests indicated a slight increasing trend in monthly mean wave heights found sporadically in the northernmost portion of the lake.

When the 12-month seasonally differenced wave height data series are analyzed using means of deseasoned wave heights, none of the trends seen previously were detected in either WIS or buoy data set or at any nearshore location. While seasonal differencing has been used to study ocean waves, the complication arising from strong directional wave height dependence resulting from lake geometry was taken into account by developing directional monthly wave height means and removing seasonality from these means with the same 12-month seasonal differencing within each 90-degree directional bin. No trend in the Theil-Sen slope was found in any of the 90-degree bins as well.

It is well known that within-series time dependence can result in erroneous trend determination and it appears that this may have resulted in the magnitude or extent decreasing trends seen in the initial analysis of the annual means. Using the Lake Michigan WIS nearshore stations results from the three above methods were compared for annual and monthly means.

When the annual and monthly wave height means were broken into 30-degree directional bins, a general north-south pattern in the trend emerged. Along the south and western coast, waves approaching from the north were found to have long-term decreasing trends in height. This trend was consistent with the findings from the lumped-direction analysis. In the directional plots of the nearshore trends, the effect

of wave direction on the significantly affected coastal extent can be seen in cases like the one found on the west coast of Lake Michigan. As the wave-approach angle moves from west to northwest, the impacted portion of the coastline extends further towards the southern tip of the lake. A gap existing between regions of the affected western coast in the lumped-direction analysis was closed in the directional bins results.

There exist some discrepancies in the significance of trends between the WIS model results and those from the buoys, such as those seen in Figures 3.3 and 3.22 where trends are found in one of the data sources but not in the corresponding series. This may be a result of data missing from the buoy data within the May-October period.

When wave-height trend analyses are isolated into directional bins, many trends that were detected during the lumped analysis persist, but are seen to increase in coastal extent and trending slope. Additionally, trends that were not detected during the lumped analysis may be revealed.

Surface wave height in the Great Lakes is primarily a function of the wind speed and fetch. The fetch of any particular region of the coastline is strongly effected by the orientation of the lake's longest axis. If a shift in the direction of historically prevailing winds is occurring across a stretched body of water then adjacent regions of the coast will experience opposite trends in the local wave climate, with waves growing along coasts where the dominant wind direction's fetch is increasing and shrinking where the fetch is decreasing. Some evidence for this phenomena was seen in the results for trends wave approach direction frequency, seen in Figures 3.33 and 3.34.

Examining the USACE simplified method for predicting deep-water wave heights [44], we can see that a wave created by a constant 10m/s wind over the lake's east-west 50-mile fetch and north/south 300-mile fetch is estimated to be 1.9 and 4.6 meters, respectively, an 83% difference under fetch-limited conditions. Ocean waves are expected to be duration-limited rather than fetch-limited, but may be expected to have a more homogeneous wave climate with respect to direction due to the relatively small difference in fetch length in any particular direction.

In enclosed bodies of water like Lake Michigan, when all of these fetch lengths are combined, increasing, decreasing, and neutral trends may blur together, as well as develop the problematic features of Simpson's paradox. Simpson's paradox describes a situation when several groups of differently developed phenomena are classed together. The inappropriately grouped data can exhibit false trends that do not exist when separated into meaningful categories.

In the case of the lakes, waves approaching from different directions have developed in a different process compared to one another and may not be comparable. The likelihood of this impacting wave-height trends is made clear when the wave climate plots in Figures 3.1 and 3.2 show that wave height is strongly dependent on both direction and time of year. The in-comparability between directional bins is especially evident when considering the means of the largest five waves.

Since the largest waves are responsible for the majority of sediment transport and constrain coastal engineering design the behavior of largest waves was examined using the annual mean of the five largest independent waves. Results of testing large wave means with significance of Theil-Sen slopes, Mann-Kendall tests, and the deseasoned means were in agreement that no significant trend existed.

4.2 Has storm frequency or duration increased over the 36-year NDBC record?

The results indicated that storm behavior seemed to be weakening, particularly in the southern basin of Lake Michigan, where significant decreasing trends were detected in the storm duration, mean peak storm wave height, total yearly storm time, and in the probability of experiencing 5m or larger waves. These trends were stable across a range of storm wave height thresholds.

These results combined with the decreasing mean wave height trends seen above, indicate that a long-term trend in wave height or storm behavior is not part of the erosion seen along the western coast. Since the largest waves that have the greatest

influence over sediment transport it is necessary to understand the changing storm dynamics in Lake Michigan to make predictions regarding erosion, ecosystem health, and water quality. The changing distribution of the lake's extreme waves could exert an influence on the level of available nutrients for algae and phytoplankton.

Storm wave behavior was further studied using the extreme value distribution. Using the WIS model, a GEVD was developed from the first decade of data at the buoy locations and the nearshore station. These PDFs were integrated for wave heights 5- to 8-meters to determine the probability of receiving a wave in that range. Trends in the GEVD shape at a location was studied by adding additional wave height maxima from each subsequent year by growing the ten-year window forwards in time. Both analyses revealed significant decreasing trends in the southern basin at the buoy location and the nearshore station. A moving window, maintained at a 10-year span also showed a significant decreasing trend in regions of the northern basin location as well. While the trend in the southern basin was stable across multiple window sizes, the direction of the northern basin's trend was shown to be dependent on window length in Appendix C.

When this analysis was expanded to the entire Lake Michigan WIS model, a trend of decreasing extreme wave probability in the southern basin coupled with increasing extreme wave probability in the northern basin was revealed. With this finding revealed, the analysis was repeated using a moving decade-long window to study the GEVD rather than the growing window. The moving window study revealed a similar pattern of lake wave height extreme wave probabilities. These results are compatible with the spatial pattern of significant decreasing trends shown by the storm metrics.

If only the May-October time span is considered in the GEVD trends, some weakly increasing trends are found in the southern basin of the lake, but not in the region of Buoy 45007, indicating that the field-collected data sets may not be able to verify the trends found by the WIS model (see Appendix C for results).

Along the western coastline of the southern basin, a significant trend shows an increasing trend in the probability of receiving a 5- to 8-meter wave. This trend is contrary to the pattern seen throughout the remainder of the basin. The coastal strip of increasing probability appears to follow a common trend in pattern of winter ice that forms on the lake [45]. In 2012, Wang et al. showed that annual ice cover was decreasing on the Great Lakes [13] and it may be that decreasing ice cover along the western coastline of Lake Michigan is responsible for exposing this coast to larger, winter waves.

Decreases in the annual ice cover of Lake Michigan could lead to increases in the probability of receiving large waves because these regions of the lake, previously removed from the wave climate during winter, would now exhibit the winter wave behavior. With winter wave months, during which occur the largest of the seasonal large wave means, added to the previously ice covered regional distributions an increasing trend would be expected.

The strongly directional nature of these results led to the interest in Lake Ontario, a predominately east-west stretched lake as a counter to the north-south orientation of Lake Michigan. In Lake Ontario, the likelihood of receiving an extreme was found to be increasing in the north and south regions of the eastern part of the lake in the growing window analysis. The south to north trend in Lake Michigan and west to east trend in Lake Ontario could indicate a shifting of large wind events away from the southwest or towards the northeast. However, as a lake that generally experiences more ice coverage than Lake Michigan, Lake Ontario's extreme wave behavior might be more impacted by trends in ice cover. This may also explain the discrepancy between the growing and moving window results in Lake Ontario.

The 95% confidence intervals on the GEVD integrated probability values are large, though the spatial consistency of the trend at multiple locations may indicate some validity to the trends despite the waves' spatial dependence. To improve the confidence intervals, a similar analysis using the peaks-over-threshold dataset and the GPD was taken. In the growing window analysis, significant trends in the integra-

tion of the fitted GPD for a wave 5- to 8-meters in height were found at both the buoy location and the selected nearshore station. No significant trend was found at the location of the northern buoy. These results corroborate the previous finding using the GEVD with substantially improved confidence intervals on each integrated probability.

4.3 Has the direction of the waves changed?

When annual frequency of waves approaching from 30-degree directional bins was examined using Theil-Sen regression, significant decreases in annual hours of waves approaching from the 150- to 180-degree range was found in the WIS model data at both buoy locations in the north and south basins. In the southern basin, there was a significant increase in annual hours with waves approaching from the 330- to 360-degree range. The northern basin buoy location also showed an increasing trend in waves approaching from this directional bin, but the trend was not found to be significant. These trends were found to be stable when 10-degree bins were used as well.

This analysis was applied to all Lake Michigan WIS nearshore stations. Waves approaching from the 330- to 30-degree range were found to be significantly decreasing in frequency along the western coast of Lake Michigan. As the waves' direction becomes more easterly, the band of relatively steeper slopes moves northwards along the coast. It is notable that this directional range corresponds roughly to the longest fetch at that position. With waves coming from the direction of greatest fetch becoming less frequent, the potential for regularly occurring large waves may decrease, bringing corresponding decreases in sediment transport in southward direction.

The opposite trend is seen in southern wave approach behavior along the west coast. Waves approaching from 120 to 180 degrees show significant increasing trends in frequency along the western coast. As the wave direction becomes more easterly, the affected region moves towards the south. This again appears to roughly show that

the direction of the longest fetch, and therefore potentially the largest waves, is experiencing the highest rate of change albeit an increasing change from this directional band. This pattern further shows the possibility of decreasing sediment transport in the southward direction.

4.4 Is the increasing lake level related to the size of the waves?

Using updated data sets, similar results to the 1994 study by Meadows et al. on the relationship between lake level and wave height were found for the correlation coefficient between the series [27]. However, if the lake level and wave height series are deseasoned without the long moving average which homogenizes the data, the correlation coefficient between them becomes an order of magnitude smaller and loses significance. This holds true whether it is the mean or the maximum of monthly waves being compared. Lagging the lake level data by one year did not improve the strength of the relationship or lead to significance.

This result disagrees with Meadows et. al's 1994 findings but is similar to recent findings from USACE which showed no relationship between wave heights, or storm wave heights, and water levels [27, 28].

5. SUMMARY

The impacts of climate change have been seen in many environmental systems. This study examined the long-term wave climate in Lake Michigan using two NOAA NDBC buoys and the USACE WIS wave hindcast. Annual time series were examined for trends in mean wave height, mean large wave height, mean storm duration, total storm time, mean storm peak wave height, number of storms, and probability of receiving a 5- to 8- meter wave.

Despite increasing trends in wave height and storm behavior found throughout the world's oceans, there was little indication of that behavior in Lake Michigan. On the contrary, the results presented here show many of the wave metrics decreasing, particularly in the lake's southern basin which saw significant declines in most of the parameters tested. This study also showed that the magnitude of the trends was increased when the analysis was divided by wave direction. It was hypothesized that this was due to the fetch limitation on waves reaching full-development in the enclosed body of water. This issue may not be present in ocean wave studies where the fetch may be considered large in every direction.

The mean storm duration, peak wave height, and yearly storm time were also found to be decreasing in the southern basin. These results were substantiated by the finding that there were significant decreasing trends in the probability of receiving a wave 5- to 8-meters in height in the southern basin, a result that proved stable between the Gumbel approach and the peaks-over-threshold approach for multiple window sizes and threshold wave heights.

These decreasing trends suggest that changes in Lake Michigan's wave climate are not comparable to the changes seen in ocean wave climates. The trends' dependence on the direction of wave approach and the spatial pattern in the extreme wave analyses suggests that the relationship between wind and fetch length is responsible for the change.

6. RECOMMENDATIONS

This study indicated that long-term trends in Lake Michigan's wave climate primarily took place in winter months, during which the largest waves occur. The need to measure these waves using field instrumentation should be emphasized as the WIS model is currently the only long-term data series available for analysis. The discrepancies between the WIS hindcast and the buoy measurements in the summer, when the model can be calibrated, may lead to questions regarding its validity during the winter when it cannot. Since the larger winter waves will constrain coastal design, understanding their behavior and long-term trends should be a priority in future work.

To continue investigation into the relationship between lake level and wave height further analysis is needed to address the effect of different lag times on the monthly series correlation coefficients. Despite the flaws with the 60-month moving average analysis there appears to be a strong relationship between the two filtered series given a five-year offset. To investigate the meaningfulness of this potential relationship the correlation coefficients of the deseasoned series should be analyzed for multiple lag times, with special attention paid to the five-year time lag.

Finally the latest data from 2018 in NOAA NDBC Buoys 45007 and 45002 should be cleaned and included into analyses.

REFERENCES

- [1] D.L. Hartmann, A.M.G. Klein Tank, M. Rusticucci, L.V. Alexander, S. Brönnimann, Y. Charabi, F.J. Dentener, E.J. Dlugokencky, D.R. Easterling, A. Kaplan, B.J. Soden, P.W. Thorne, M. Wild, and P.M. Zhai. *Observations: Atmosphere and Surface*, chapter 2, page 159254. Cambridge University Press, Cambridge, United Kingdom and New York, NY, USA.
- [2] P.D. Komar and J.C. Allan. Increasing hurricane-generated wave heights along the u.s. east coast and their climate controls.(report). *Journal of Coastal Research*, 24(2), 2008.
- [3] J. Allan and P. Komar. Are ocean wave heights increasing in the eastern north pacific? *Eos, Transactions American Geophysical Union*, 81(47):561–567, 2000.
- [4] P. Ruggiero, P.D. Komar, and J.C. Allan. Increasing wave heights and extreme value projections: The wave climate of the us pacific northwest. *Coastal Engineering*, 57(5):539–552, 2010.
- [5] S. Bacon and D.J.T. Carter. Wave climate changes in the north atlantic and north sea. *International Journal of Climatology*, 11(5):545–558, 1991.
- [6] J. Gemmrich, B. Thomas, and R. Bouchard. Observational changes and trends in northeast pacific wave records. *Geophysical Research Letters*, 38(22):n/a–n/a, 2011.
- [7] R.M. Sorensen. *Basic Coastal Engineering*. Number v. 10 in Basic Coastal Engineering. Springer US, 2005.
- [8] X.L. Wang and Feng Y. *RHtestsV4 User Manual*. Climate Research Division, Atmospheric Science and Technology Directorate, Science and Technology Branch, Environment Canada, Toronto, Ontario, Canada, 2013.
- [9] E. Vanem and S.E. Walker. Identifying trends in the ocean wave climate by time series analyses of significant wave height data. *Ocean Engineering*, 61, 2013.
- [10] E.L. Venrick, J.A. McGowan, D.R. Cayan, and T.L. Hayward. Climate and chlorophyll a: long-term trends in the central north pacific ocean. *Science*, 238(4823):70–72, 1987.
- [11] S.M. Herrmann, A. Anyamba, and C.J. Tucker. Recent trends in vegetation dynamics in the african sahel and their relationship to climate. *Global Environmental Change*, 15(4):394–404, 2005.
- [12] Y. Malhi and J. Wright. Spatial patterns and recent trends in the climate of tropical rainforest regions. *Philosophical Transactions of the Royal Society of London. Series B: Biological Sciences*, 359(1443):311–329, 2004.

- [13] J. Wang, X. Bai, H. Hu, A. Clites, M. Colton, and B. Lofgren. Temporal and spatial variability of great lakes ice cover, 1973–2010. *Journal of Climate*, 25(4):1318–1329, 2012.
- [14] J.T. Waples and J.V. Klump. Biophysical effects of a decadal shift in summer wind direction over the laurentian great lakes. *Geophysical Research Letters*, 29(8), 2002.
- [15] J. Austin and S. Colman. A century of temperature variability in lake superior. *Limnology and Oceanography*, 53(6):2724–2730, 2008.
- [16] J.H. Slade, T.M. Vanreken, G.R. Mwaniki, S. Bertman, B. Stirm, and P.B. Shepson. Aerosol production from the surface of the great lakes. *Geophysical Research Letters*, 37(18):n/a–n/a, 2010.
- [17] S. Chung, B. Basarab, and T. Vanreken. Regional impacts of ultrafine particle emissions from the surface of the great lakes. *Atmospheric Chemistry and Physics*, 11(24), 2011.
- [18] C. Chen, L. Wang, R. Ji, J.W. Budd, D.J. Schwab, D. Beletsky, G.L. Fahnenstiel, H. Vanderploeg, B. Eadie, and J. Cotner. Impacts of suspended sediment on the ecosystem in lake michigan: A comparison between the 1998 and 1999 plume events. *Journal of Geophysical Research: Oceans*, 109(C10).
- [19] J.E. Evans and A. Clark. Re-interpreting great lakes shorelines as components of wave-influenced deltas: An example from the portage river delta (lake erie). *Journal of Great Lakes Research*, 37(1):64–77, 2011.
- [20] B.J. Eadie, D.J. Schwab, T.H. Johengen, P.J. Lavrentyev, G.S. Miller, R.E. Holland, G.A. Leshkevich, M.B. Lansing, N.R. Morehead, J.A. Robbins, N. Hawley, D.N. Edgington, and P.L. Van Hoof. Particle transport, nutrient cycling, and algal community structure associated with a major winter-spring sediment re-suspension event in southern lake michigan. *Journal of Great Lakes Research*, 28(3):324–337, 2002.
- [21] N. Chien and Z. Wan. *Mechanics of Sediment Transport*, volume translated under the guidance of John S. McNown. American Society of Civil Engineers, Reston, VA (US), 1999.
- [22] G. Fahnenstiel, T. Nalepa, S. Pothoven, H. Carrick, and D. Scavia. Lake michigan lower food web: Long-term observations and dreissena impact. *Journal of Great Lakes Research*, 36(3):1–4, 2010.
- [23] J.L. Mida, D. Scavia, G.L. Fahnenstiel, S.A. Pothoven, H.A. Vanderploeg, and D.M. Dolan. Long-term and recent changes in southern lake michigan water quality with implications for present trophic status. *Journal of Great Lakes Research*, 36(3):42–49, 2010.
- [24] M.D. Rowe, D.R. Obenour, T.F. Nalepa, H.A. Vanderploeg, F. Yousef, and W.C. Kerfoot. Mapping the spatial distribution of the biomass and filterfeeding effect of invasive dreissenid mussels on the winterspring phytoplankton bloom in lake michigan. *Freshwater Biology*, 60(11):2270–2285, 2015.
- [25] T. Briscoe and N. Husain. Data: Lake michigan shoreline erosion could be getting worse, research shows. *Chicago Tribune*, May 2017.

- [26] The great lakes dashboard. <https://www.glerl.noaa.gov/data/dashboard/GLD_HTML5.html>.
- [27] G.A. Meadows, L.A. Meadows, W.L. Wood, J.M. Hubertz, and M. Perlin. The relationship between great lakes water levels, wave energies, and shoreline damage. *Bulletin of the American Meteorological Society*, 78(4):675–683, 1997.
- [28] J.A. Melby, N.C. Nadal-Caraballo, Y. Pagn-Albelo, and B. Ebersole. Wave height and water level variability on lakes michigan and st clair. *Great Lakes Coastal Flood Study, 2012 Federal Inter-Agency Initiative*, 2012.
- [29] K.E. Trenberth. Changes in precipitation with climate change. *Climate Research*, 47(1-2):123–138, 2011.
- [30] Coastal Engineering Research Center. *Shore Protection Manual, Fourth Ed.*, volume 2. United States Army Corps of Engineers.
- [31] N. Nekouee, B. Ataie-Ashtiani, and S. Hamidi. Uncertainty analysis of wind-wave predictions in lake michigan. *China Ocean Engineering*, 30(5):811–820, 2016.
- [32] Buoy 45006 moored buoy events chart. Personal Communication, Candice Hall - NOAA Affiliate.
- [33] T. Hesser. Us army corps of engineers wave information studies project documentation. http://wis.usace.army.mil/wis_project_overview.html, 2010.
- [34] R.E. Jensen, M.A. Cialone, R.S. Chapman, B.A. Ebersole, M. Anderson, and Leonette T. Lake michigan storm: Wave and water level modeling (draft). *ERDC TR-12-X*, 2012.
- [35] J.M. Hubertz. User’s guide to the wave information studies (wis) wave model: Version 2.0. *WIS Report 27*, page 41, 1992.
- [36] K. Tillotson and P.D. Komar. The wave climate of the pacific northwest (oregon and washington): A comparison of data sources. *Journal of Coastal Research*, pages 440–452, 1997.
- [37] National oceanic and atmospheric administration national data buoy center. <https://www.ndbc.noaa.gov/>.
- [38] United states army corps of engineers wave information study. <http://wis.usace.army.mil/>.
- [39] Extremes for lake michigan st94405 hindcast 1960-2014. http://wis.usace.army.mil/data/mich/XTRMS/ST94405_XTRM.TXT.
- [40] K.H. Hamed and A.R. Rao. A modified mann-kendall trend test for autocorrelated data. *Journal of hydrology*, 204(1-4):182–196, 1998.
- [41] fume package for r. <https://cran.r-project.org/web/packages/fume/index.html>.
- [42] C.N. Stefanakos and G.A. Athanassoulis. Extreme value predictions based on nonstationary time series of wave data. *Environmetrics*, 17(1):25–46, 2006.
- [43] Great lakes water level data, us army corps of engineers detroit district. <https://www.lre.usace.army.mil/Missions/Great-Lakes-Information/Great-Lakes-Information-2/Water-Level-Data/>.

- [44] Coastal Engineering Research Center. *Shore Protection Manual, Fourth Ed.*, volume 1. United States Army Corps of Engineers.
- [45] Great lakes ice cover. <https://www.glerl.noaa.gov/data/ice/overview>.

A. DIRECTIONAL TRENDS

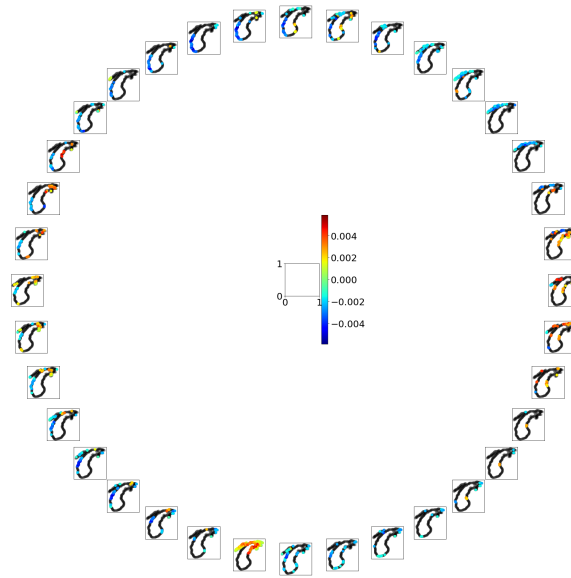


Figure A.1. Directional trends in annual wave heights at all WIS nearshore stations.

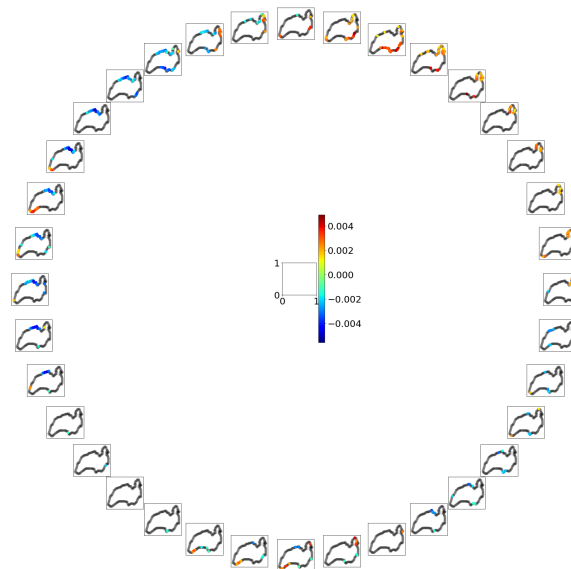


Figure A.2. Directional trends in annual wave heights at all WIS nearshore stations in Lake Ontario.

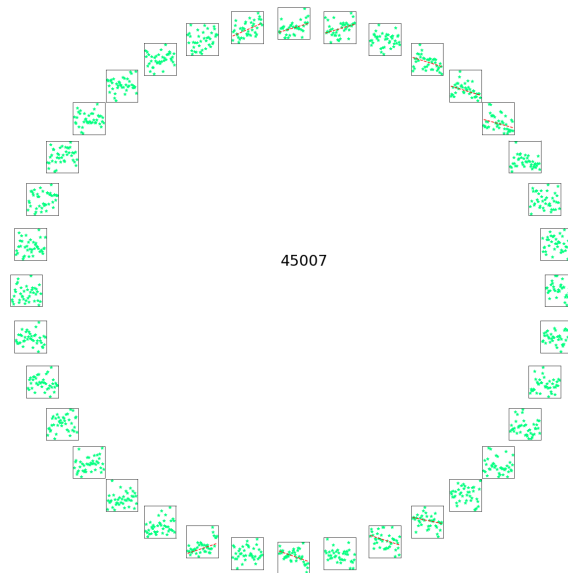


Figure A.3. Directional trends in annual wave time at buoy 45007.



Figure A.4. Directional trends in annual wave time at buoy 45002.

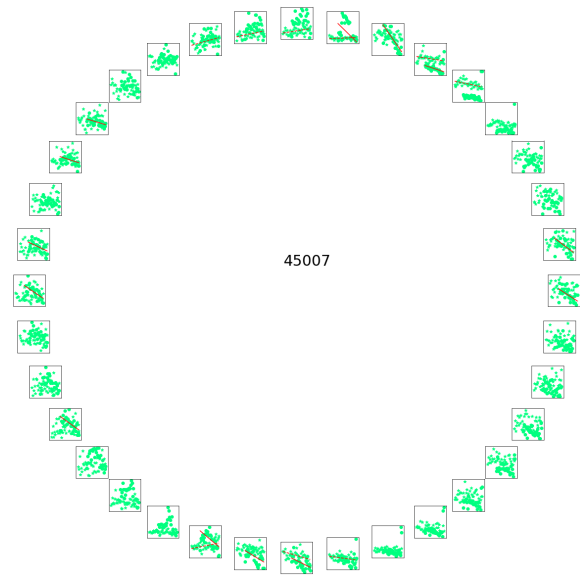


Figure A.5. Directional trends in annual wave time at buoy 45007. Summer Only.

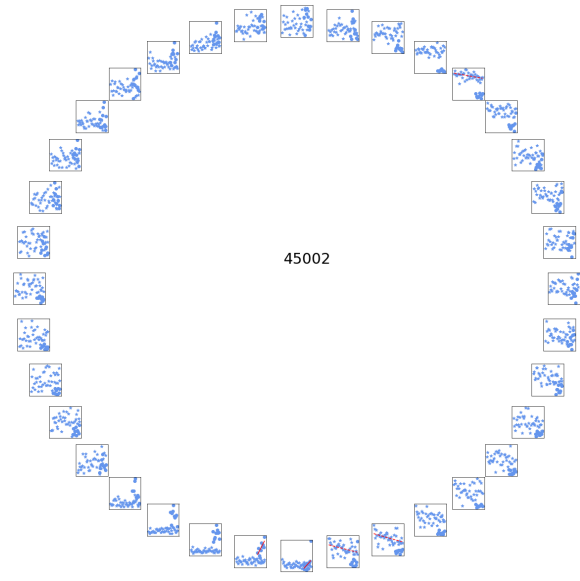


Figure A.6. Directional trends in annual wave time at buoy 45002. Summer Only.

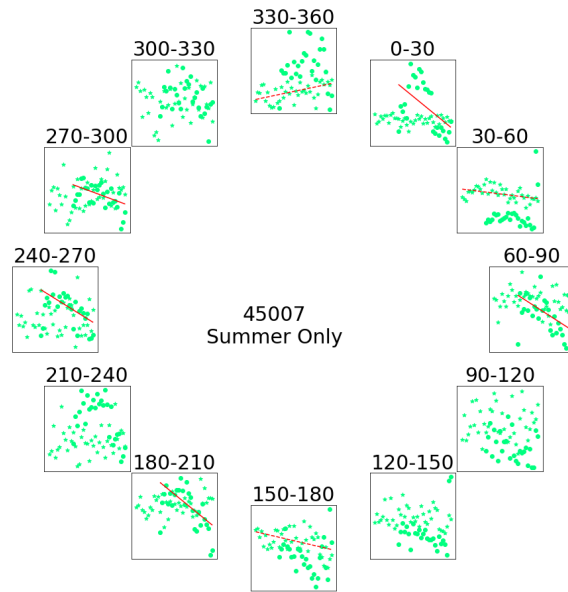


Figure A.7. Directional trends in annual wave time at buoy 45007. Summer Only.

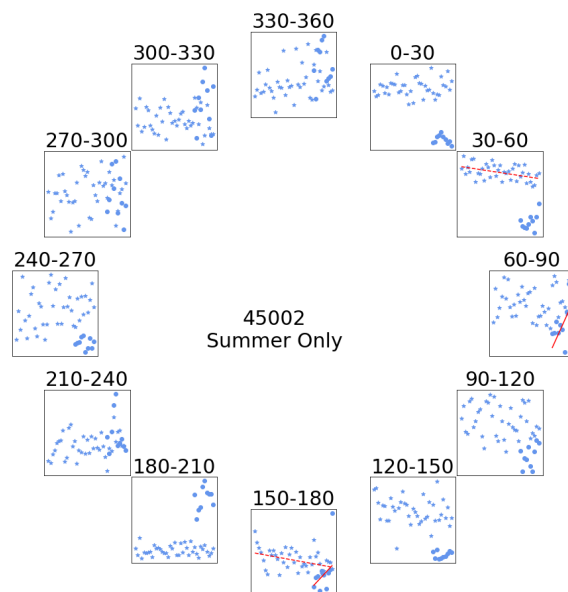


Figure A.8. Directional trends in annual wave time at buoy 45002. Summer Only.

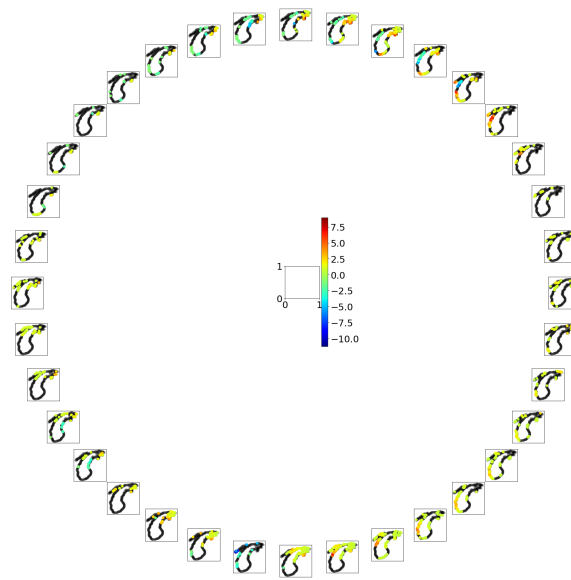


Figure A.9. Directional trends in annual wave spatial frequency at all WIS nearshore stations.

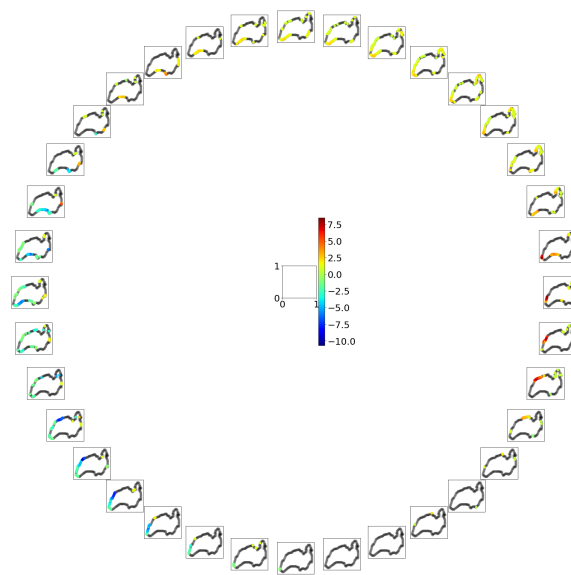


Figure A.10. Directional trends in annual wave spatial frequency at all WIS nearshore stations in Lake Ontario.

B. DATA CLEANING

Table B.1. Data removal and justification.

Year	Removed Data	Justification
1985	Initial-1453 hrs	Instantaneous zero values for water temperature.
1989	5477-Final hrs	Water temperature following air temperature closely. Possibly sampling during retrieval.
1995	Initial-515	Large fluctuations during early season temperature sampling. Many datasets with error values.
1998	6304-Final	Water temperature following air temperature closely. Possibly sampling during retrieval.
2002	Initial-307	Unusual trend in early season water temperature sampling. Other datasets include error values.
2003	Initial-38	Unusual trend in early season water temperature sampling. Other datasets include error values.
2004	Initial-6 / 6510-Final	Water temperature following air temperature closely. Possibly sampling during deployment and retrieval.
2007	Initial-37	Large fluctuations during early season water temperature sampling, including values close to air temperature.
2008	Initial-4	Water temperature following air temperature closely. Possibly sampling during deployment.
2009	Initial-6	Water temperature following air temperature closely. Possibly sampling during deployment.
2010	Initial-933 / 5107-Final	Large fluctuations during early and late season temperature sampling. Many datasets with error values.
2011	Initial-219	Anomalously high values and large fluctuations during early season water temperature sampling.
2012	Initial-70 / 5970-Final	Water temperature following air temperature closely. Possibly sampling during deployment and retrieval.
2013	Initial-618 / 5289-Final	Unusual to see air temperatures without water temperature.
2014	Initial-180 / 5018-Final	Water temperature following air temperature closely. Possibly sampling during deployment and retrieval.
2015	Initial-255	Anomalously high values and large fluctuations during early season water temperature sampling.
2016	Initial-5 / 5380-Final	Water temperature following air temperature closely. Possibly sampling during deployment and retrieval.

Table B.2. Value ranges of raw data.

Year	Air Temp.	Water Temp.	Wind Direction	Wind Speed	Gust Speed	Wave Height	Dominant Wave Period	Average Wave Period	Mean Wave Direction
1981	-1.6-999.0	6.3-999.0	0.0-999.0	0.0-99.0	0.0-99.0	0.0-99.0	2.0-99.0	2.2-99.0	999.0-999.0
1982	-6.8-999.0	1.3-999.0	0.0-999.0	0.0-99.0	0.0-99.0	0.0-99.0	2.0-99.0	2.0-99.0	999.0-999.0
1983	-3.0-999.0	2.9-999.0	0.0-999.0	0.0-99.0	0.0-99.0	0.0-99.0	0.0-99.0	0.0-99.0	999.0-999.0
1984	-1.6-999.0	1.6-24.9	0.0-999.0	0.0-99.0	0.0-99.0	0.0-99.0	0.0-99.0	0.0-99.0	999.0-999.0
1985	-14.0-999.0	0.0-999.0	0.0-999.0	0.0-99.0	0.0-99.0	0.0-99.0	2.5-99.0	0.0-99.0	999.0-999.0
1986	-9.7-999.0	3.1-999.0	0.0-999.0	0.0-99.0	0.0-99.0	0.0-99.0	2.5-99.0	2.5-99.0	999.0-999.0
1987	-3.2-999.0	2.6-999.0	0.0-999.0	0.0-99.0	0.0-99.0	0.0-99.0	2.5-99.0	2.5-99.0	999.0-999.0
1988	-2.9-999.0	2.0-999.0	0.0-999.0	0.0-99.0	0.0-99.0	0.0-99.0	0.0-99.0	0.0-99.0	999.0-999.0
1989	-4.3-999.0	2.0-999.0	0.0-999.0	0.0-99.0	0.0-99.0	0.0-99.0	0.0-99.0	0.0-99.0	999.0-999.0
1990	1.7-999.0	3.2-999.0	0.0-999.0	0.0-99.0	0.0-99.0	0.0-99.0	0.0-99.0	0.0-99.0	999.0-999.0
1991	1.0-999.0	2.7-999.0	0.0-360.0	0.0-13.7	0.0-99.0	0.0-99.0	0.0-99.0	0.0-99.0	0.0-999.0
1992	-2.3-999.0	2.6-999.0	2.0-999.0	0.0-99.0	0.0-99.0	0.0-99.0	0.0-99.0	0.0-99.0	0.0-999.0
1993	-3.0-999.0	2.4-999.0	2.0-999.0	0.0-99.0	0.0-99.0	0.0-99.0	0.0-99.0	0.0-99.0	0.0-999.0
1994	-2.4-999.0	0.9-999.0	2.0-999.0	0.0-99.0	0.0-99.0	0.0-99.0	0.0-99.0	0.0-99.0	0.0-999.0
1995	-8.8-999.0	-1.9-999.0	2.0-999.0	0.0-99.0	0.0-99.0	0.0-99.0	0.0-99.0	0.0-99.0	0.0-999.0
1996	-4.5-999.0	0.8-999.0	2.0-999.0	0.0-99.0	0.0-99.0	0.0-99.0	0.0-99.0	0.0-99.0	0.0-999.0
1997	-6.1-999.0	2.0-999.0	2.0-999.0	0.0-99.0	0.0-99.0	0.0-99.0	0.0-99.0	0.0-99.0	0.0-999.0
1998	-0.4-999.0	1.6-999.0	2.0-999.0	0.0-99.0	0.0-99.0	0.0-99.0	0.0-99.0	0.0-99.0	0.0-999.0
1999	-1.1-999.0	3.0-999.0	2.0-999.0	0.0-99.0	0.0-99.0	0.0-99.0	0.0-99.0	0.0-99.0	0.0-999.0
2000	-8.9-999.0	4.0-999.0	2.0-999.0	0.0-99.0	0.0-99.0	0.0-99.0	0.0-99.0	0.0-99.0	0.0-999.0
2001	-7.2-999.0	2.4-999.0	2.0-999.0	0.1-99.0	0.1-99.0	0.0-99.0	0.0-99.0	0.0-99.0	0.0-999.0
2002	-19.8-999.0	0.1-999.0	2.0-999.0	0.0-99.0	0.0-99.0	0.0-99.0	0.0-99.0	0.0-99.0	0.0-999.0
2003	-4.2-999.0	2.1-999.0	2.0-999.0	0.1-99.0	0.1-99.0	0.0-99.0	0.0-99.0	0.0-99.0	0.0-999.0
2004	-1.2-999.0	2.4-999.0	2.0-360.0	0.0-17.1	0.1-99.0	0.0-99.0	0.0-99.0	0.0-99.0	0.0-999.0
2005	-8.1-999.0	2.7-999.0	2.0-999.0	0.0-99.0	0.0-99.0	0.0-99.0	0.0-99.0	0.0-99.0	0.0-999.0
2006	-6.7-999.0	2.7-999.0	2.0-360.0	0.0-17.9	0.0-99.0	0.0-99.0	0.0-99.0	0.0-99.0	0.0-999.0
2007	-4.9-999.0	3.2-999.0	2.0-999.0	0.0-99.0	0.0-99.0	0.0-99.0	0.0-99.0	0.0-99.0	0.0-999.0
2008	1.5-999.0	3.2-999.0	2.0-360.0	0.0-15.8	0.0-99.0	0.01-99.0	2.5-99.0	2.65-99.0	0.0-999.0
2009	3.1-24.4	3.1-999.0	2.0-360.0	0.0-17.9	0.0-99.0	0.01-99.0	2.56-99.0	2.65-99.0	0.0-999.0
2010	-19.0-999.0	-0.4-999.0	2.0-999.0	0.0-99.0	0.0-99.0	0.0-99.0	2.5-99.0	0.0-99.0	0.0-999.0
2011	-2.0-999.0	-0.3-999.0	1.0-360.0	0.0-19.8	0.0-99.0	0.0-99.0	2.25-99.0	2.22-99.0	1.0-999.0
2012	-2.0-999.0	3.3-999.0	1.0-999.0	0.0-99.0	0.2-99.0	0.02-99.0	2.35-99.0	2.24-99.0	1.0-999.0
2013	-20.4-999.0	-0.4-999.0	1.0-360.0	0.0-17.5	0.0-99.0	0.01-99.0	2.35-99.0	2.23-99.0	1.0-999.0
2014	-11.5-999.0	-0.4-999.0	1.0-999.0	0.0-99.0	0.0-99.0	0.01-99.0	2.35-99.0	2.26-99.0	1.0-999.0
2015	-2.6-999.0	2.9-999.0	1.0-999.0	0.0-99.0	0.0-99.0	0.01-99.0	2.35-99.0	2.26-99.0	1.0-999.0
2016	-10.8-999.0	-0.4-999.0	1.0-999.0	0.0-99.0	0.0-99.0	0.01-99.0	2.25-99.0	2.28-99.0	1.0-999.0

Table B.3. Value ranges of data with officially recognized error values removed.

Year	Air Temp.	Water Temp.	Wind Direction	Wind Speed	Gust Speed	Wave Height	Dominant Wave Period	Average Wave Period	Mean Wave Direction
1981	-1.6-24.5	6.3-23.2	0.0-359.0	0.0-13.9	0.0-20.3	0.0-4.8	2.0-9.1	2.2-6.6	999.0-999.0
1982	-6.8-23.9	1.3-23.3	0.0-360.0	0.0-18.3	0.0-27.1	0.0-4.9	2.0-9.1	2.0-6.4	999.0-999.0
1983	-3.0-27.5	2.9-25.5	0.0-360.0	0.0-15.1	0.0-19.4	0.0-5.3	0.0-10.0	0.0-7.3	999.0-999.0
1984	-1.6-25.9	1.6-24.9	0.0-360.0	0.0-16.3	0.0-22.5	0.0-4.8	0.0-10.0	0.0-6.6	999.0-999.0
1985	-14.0-24.5	0.0-22.9	0.0-350.0	0.0-19.0	0.0-24.0	0.0-3.1	2.5-8.3	2.5-6.4	999.0-999.0
1986	-9.7-25.2	3.1-25.3	0.0-350.0	0.0-15.0	0.0-18.0	0.0-3.2	2.5-8.3	2.5-6.5	999.0-999.0
1987	-3.2-27.4	2.6-26.1	0.0-360.0	0.0-16.0	0.0-23.0	0.0-4.8	2.5-10.0	2.5-7.2	999.0-999.0
1988	-2.9-29.2	2.0-26.6	0.0-360.0	0.0-18.2	0.0-23.2	0.0-4.4	0.0-10.0	0.0-7.0	999.0-999.0
1989	-4.3-25.8	2.0-25.0	0.0-360.0	0.0-17.8	0.0-25.3	0.0-5.6	0.0-10.0	0.0-7.8	999.0-999.0
1990	1.7-25.8	3.2-23.1	0.0-360.0	0.0-18.5	0.0-22.5	0.0-3.9	0.0-9.1	0.0-6.3	999.0-999.0
1991	1.0-27.1	2.7-25.1	0.0-360.0	0.0-13.7	0.0-17.9	0.0-2.8	0.0-9.1	0.0-5.8	0.0-999.0
1992	-2.3-24.2	2.6-22.8	2.0-360.0	0.0-17.7	0.0-22.2	0.0-5.1	0.0-10.0	0.0-7.7	0.0-360.0
1993	-3.0-25.9	2.4-25.8	2.0-360.0	0.0-16.4	0.0-21.2	0.0-4.0	0.0-10.0	0.0-6.9	0.0-360.0
1994	-2.4-25.3	0.9-22.2	2.0-360.0	0.0-15.0	0.0-18.5	0.0-3.7	0.0-9.1	0.0-6.8	0.0-360.0
1995	-8.8-28.1	-1.9-27.4	2.0-360.0	0.0-18.1	0.0-23.5	0.0-5.2	0.0-10.0	0.0-7.6	0.0-360.0
1996	-4.5-26.1	0.8-26.6	2.0-360.0	0.0-18.7	0.0-23.7	0.0-4.04	0.0-9.09	0.0-6.98	0.0-359.0
1997	-6.1-23.6	2.0-24.4	2.0-360.0	0.0-18.5	0.0-23.7	0.0-4.5	0.0-10.0	0.0-7.06	0.0-359.0
1998	-0.4-26.5	1.6-26.2	2.0-360.0	0.0-21.2	0.0-27.7	0.0-5.93	0.0-9.09	0.0-7.57	0.0-359.0
1999	-1.1-28.2	3.0-25.8	2.0-360.0	0.0-17.2	0.0-22.8	0.0-4.82	0.0-10.0	0.0-7.35	0.0-360.0
2000	-8.9-25.3	4.0-23.9	2.0-360.0	0.0-17.6	0.0-21.9	0.0-5.22	0.0-10.0	0.0-7.49	0.0-360.0
2001	-7.2-27.7	2.4-26.6	2.0-360.0	0.1-19.0	0.1-24.3	0.0-5.16	0.0-10.0	0.0-7.61	0.0-360.0
2002	-19.8-26.0	0.1-25.9	2.0-360.0	0.0-16.6	0.0-21.9	0.0-4.2	0.0-10.0	0.0-10.12	0.0-360.0
2003	-4.2-26.1	2.1-25.0	2.0-360.0	0.1-20.1	0.1-25.8	0.0-4.66	0.0-12.5	0.0-6.86	0.0-360.0
2004	-1.2-25.6	2.4-23.7	2.0-360.0	0.0-17.1	0.1-22.3	0.0-4.4	0.0-9.09	0.0-8.37	0.0-360.0
2005	-8.1-26.8	2.7-25.1	2.0-360.0	0.0-17.5	0.0-21.8	0.0-5.31	0.0-10.0	0.0-8.42	0.0-360.0
2006	-6.7-26.7	2.7-25.0	2.0-360.0	0.0-17.9	0.0-23.3	0.0-4.37	0.0-20.0	0.0-7.57	0.0-360.0
2007	-4.9-26.5	3.2-25.9	2.0-360.0	0.0-17.3	0.0-21.1	0.0-4.31	0.0-10.0	0.0-9.48	0.0-360.0
2008	1.5-25.3	3.2-25.8	2.0-360.0	0.0-15.8	0.0-19.2	0.15-3.52	2.5-8.33	2.66-6.47	0.0-360.0
2009	3.1-24.4	3.1-23.0	2.0-360.0	0.0-17.9	0.0-23.3	0.25-3.72	2.56-9.09	2.73-6.86	0.0-360.0
2010	-19.0-26.9	-0.4-26.6	2.0-360.0	0.0-17.0	0.0-23.1	0.25-4.12	2.5-9.09	2.7-6.95	0.0-360.0
2011	-2.0-27.7	-0.3-26.4	1.0-360.0	0.0-19.8	0.0-24.0	0.25-6.97	2.25-10.0	2.33-8.47	1.0-360.0
2012	-2.0-29.5	3.3-26.5	1.0-360.0	0.0-19.4	0.2-24.6	0.25-6.56	2.35-11.43	2.44-8.42	1.0-360.0
2013	-20.4-26.9	-0.4-26.1	1.0-360.0	0.0-17.5	0.0-22.1	0.25-3.81	2.35-14.81	2.33-9.66	1.0-360.0
2014	-11.5-23.8	-0.4-24.2	1.0-360.0	0.0-20.2	0.0-26.3	0.25-6.64	2.35-14.81	2.49-8.92	1.0-360.0
2015	-2.6-25.2	2.9-23.9	1.0-360.0	0.0-17.1	0.0-22.2	0.25-3.54	2.35-13.79	2.47-8.64	1.0-360.0
2016	-10.8-27.7	-0.4-27.3	1.0-360.0	0.0-17.4	0.0-22.7	0.25-3.58	2.25-13.79	2.39-9.5	1.0-360.0

C. EXTREME VALUE AND PARETO DISTRIBUTIONS

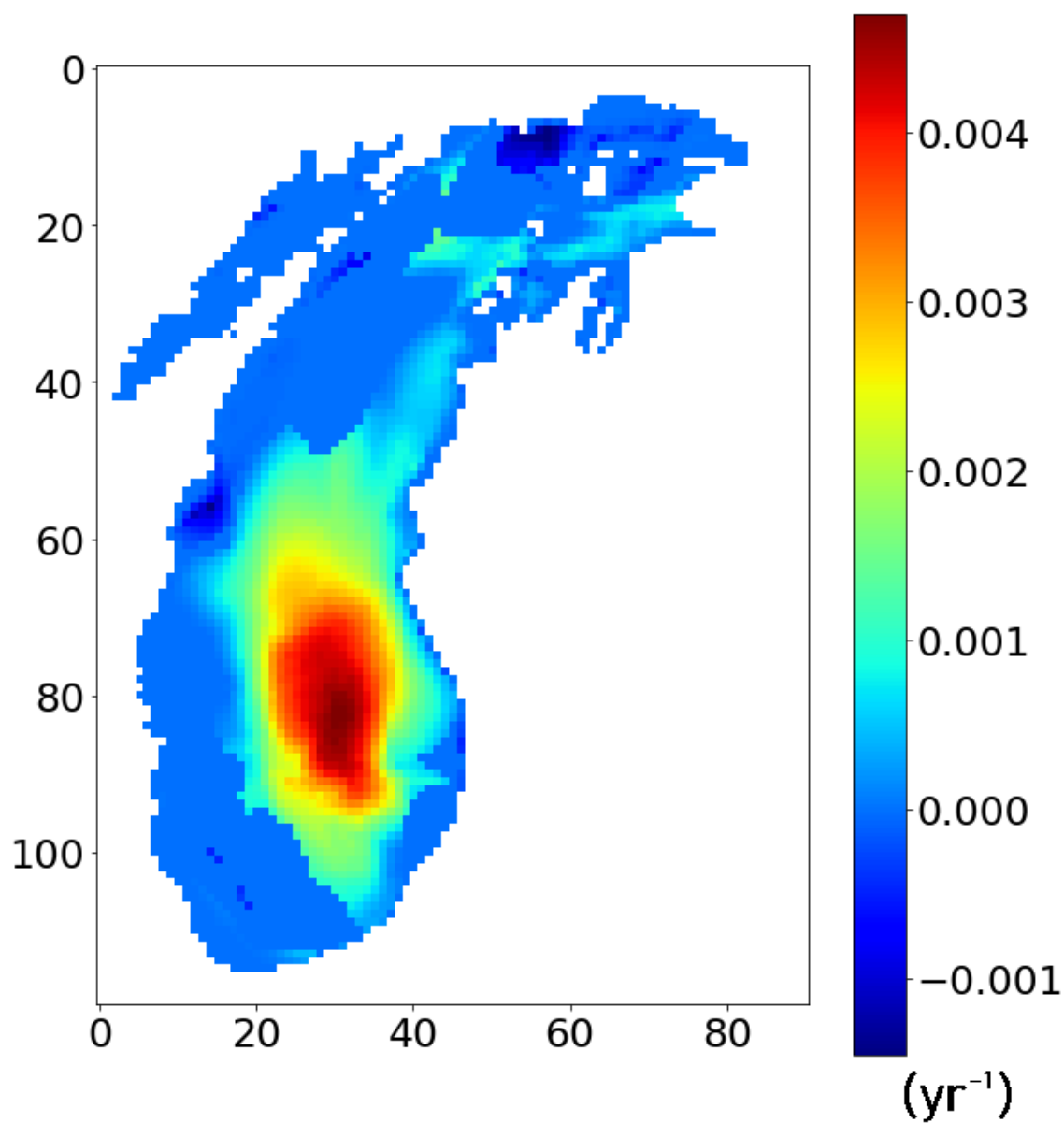


Figure C.1. Slope of Theil-Sen regression on probability of receiving a wave larger than 5m between May and October for full WIS model of Lake Michigan [38].

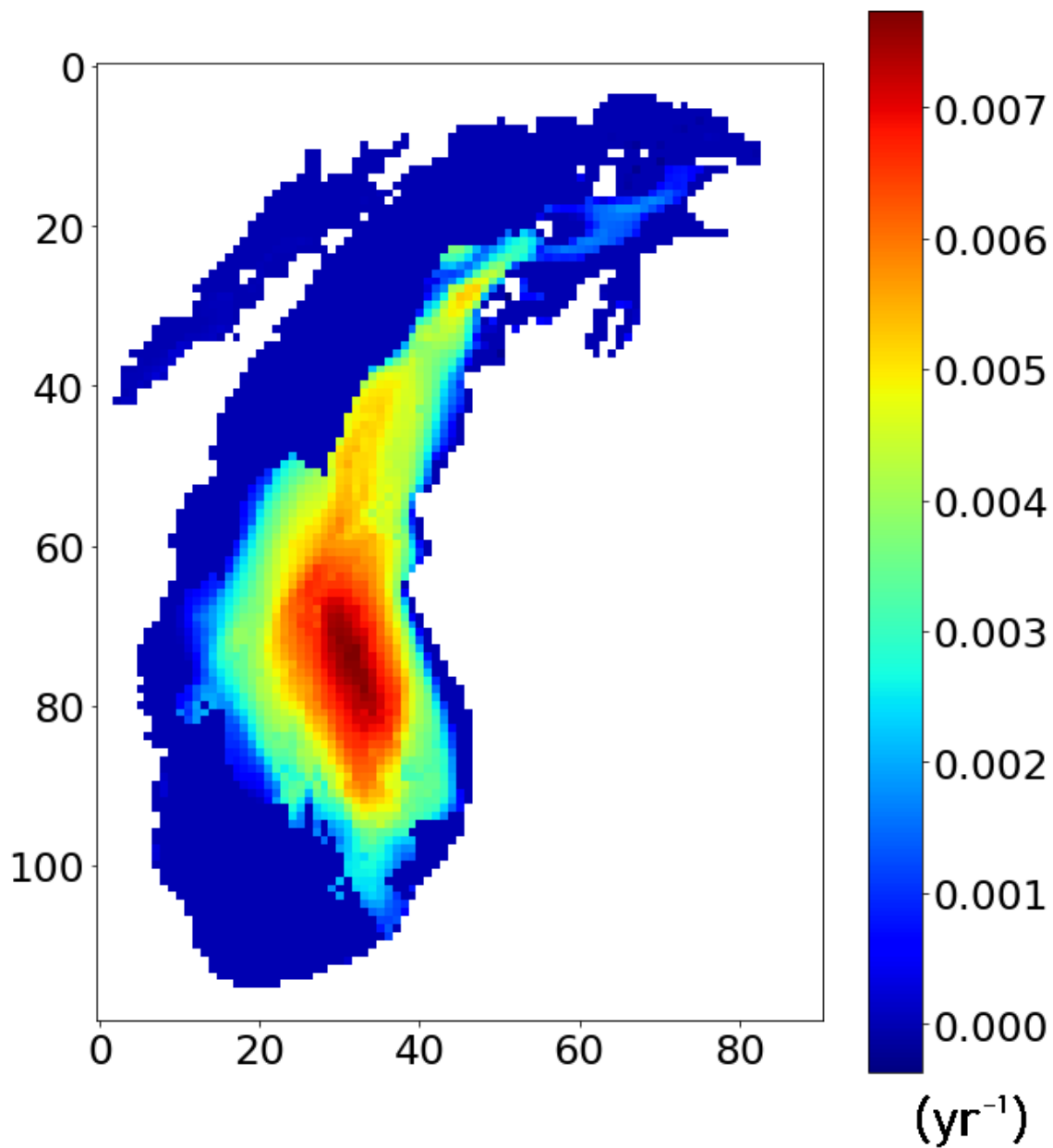


Figure C.2. Slope of Theil-Sen regression on probability of receiving a wave larger than 5m between May and October for full WIS model of Lake Michigan [38].

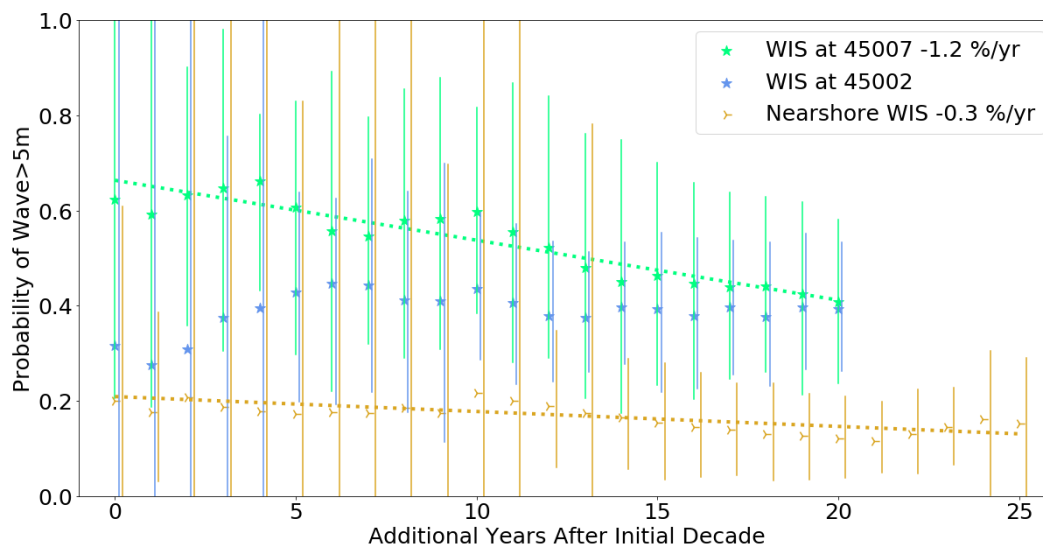


Figure C.3. Probability of receiving a wave 5m or greater at the three WIS sites in a year, from the generalized extreme value distribution determined by a growing window of annual maxima after the first 10 years [38]. Confidence intervals determined by bootstrapping from annual maxima.

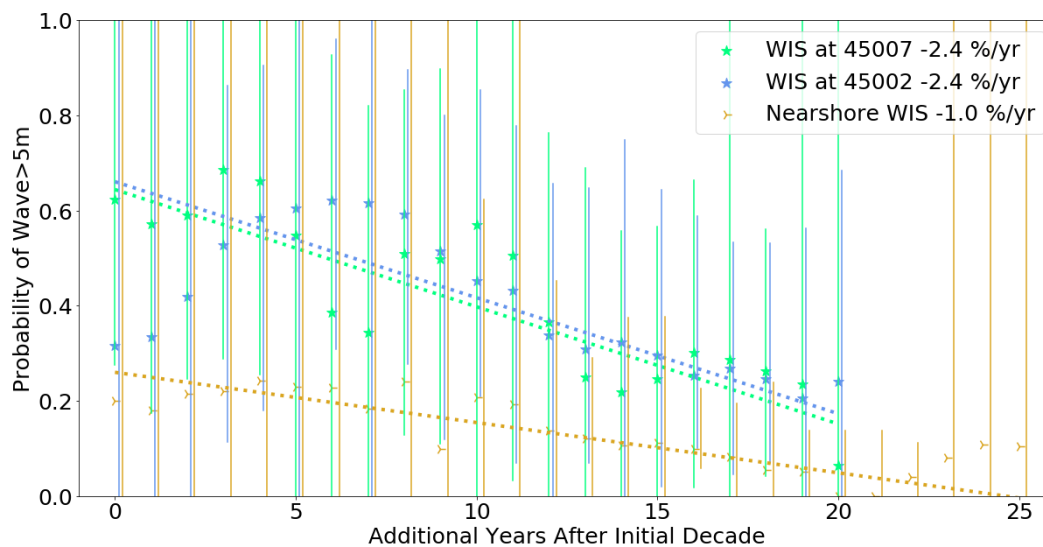


Figure C.4. Probability of receiving a wave 5m or greater at the three WIS sites in a year, from the generalized extreme value distribution determined by moving 10-year window of annual maxima [38]. Confidence intervals determined by bootstrapping from annual maxima.

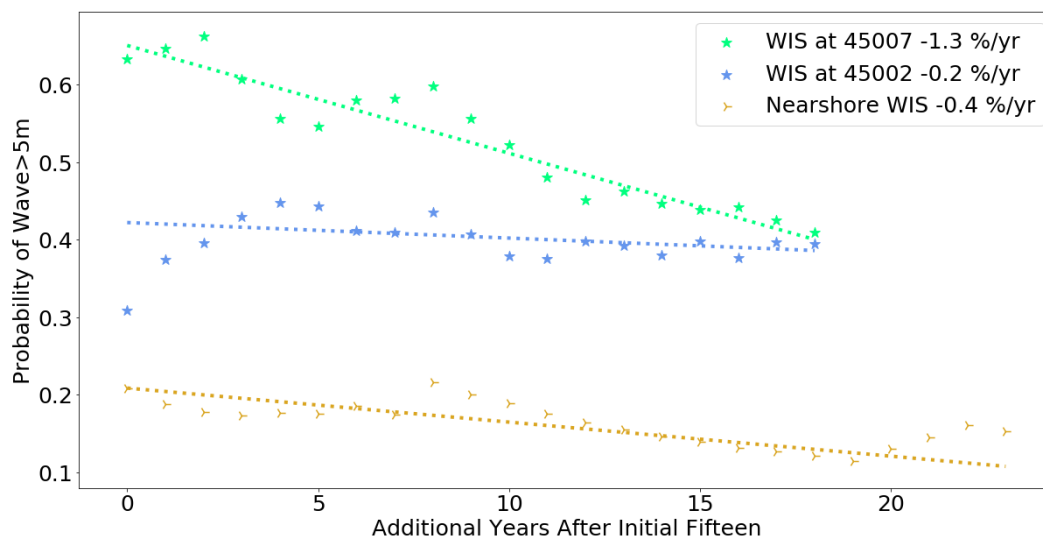


Figure C.5. Probability of receiving a wave 5m or greater at the three WIS sites in a year, from the generalized extreme value distribution determined by a growing window of annual maxima after the first 12 years [38].

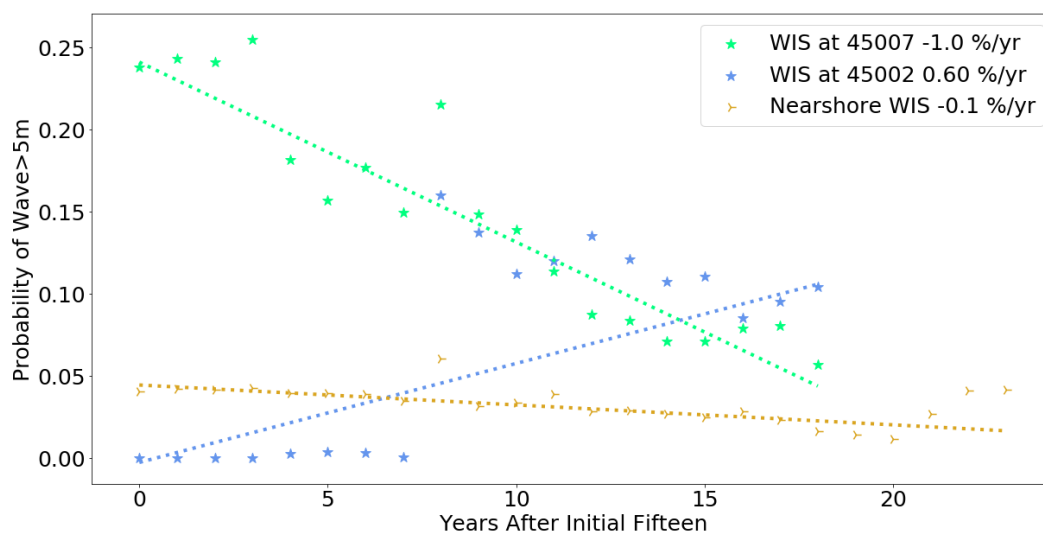


Figure C.6. Probability of receiving a wave 5m or greater at the three WIS sites in a year, from the generalized extreme value distribution determined by moving 12-year window of annual maxima [38].

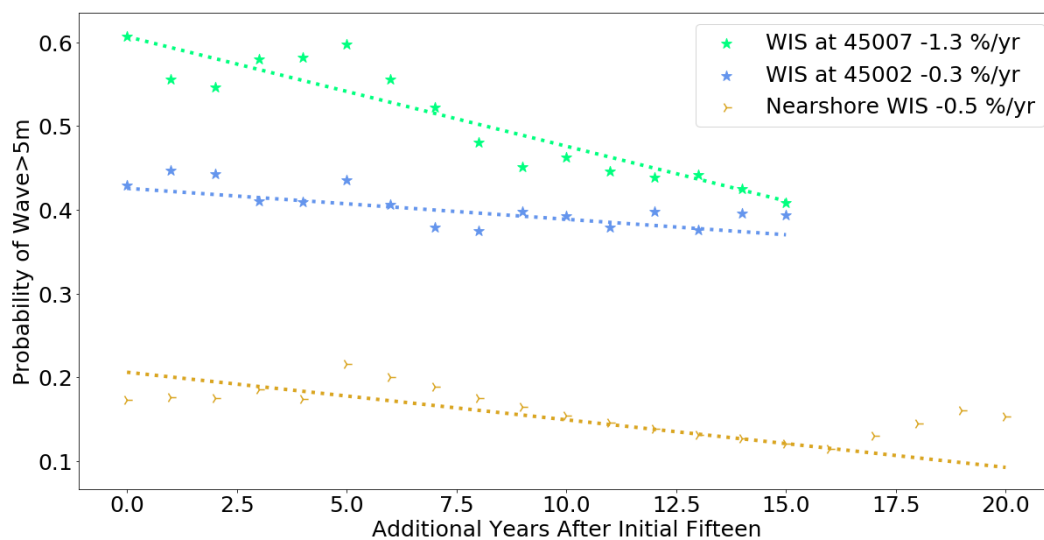


Figure C.7. Probability of receiving a wave 5m or greater at the three WIS sites in a year, from the generalized extreme value distribution determined by a growing window of annual maxima after the first 15 years [38].

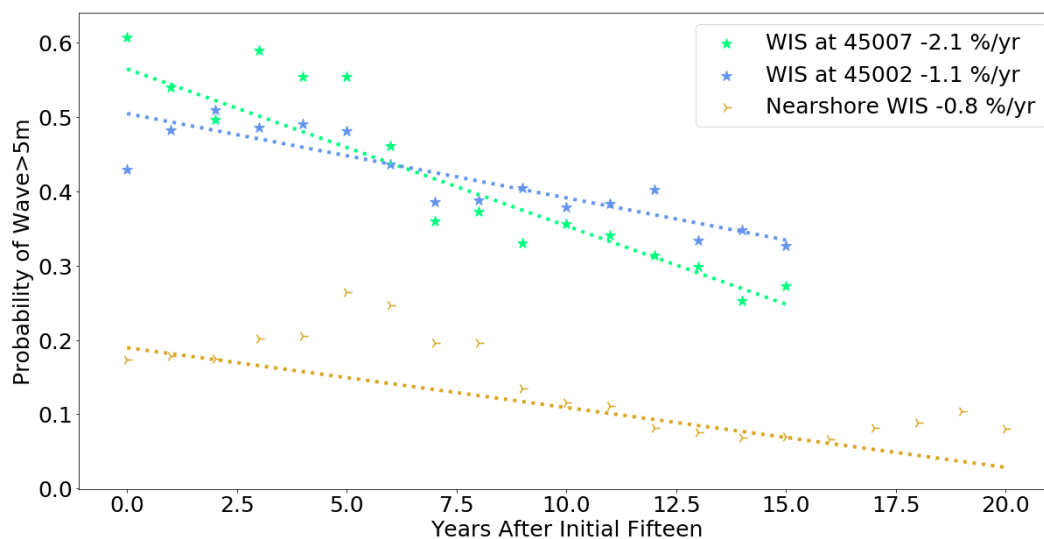


Figure C.8. Probability of receiving a wave 5m or greater at the three WIS sites in a year, from the generalized extreme value distribution determined by moving 15-year window of annual maxima [38].

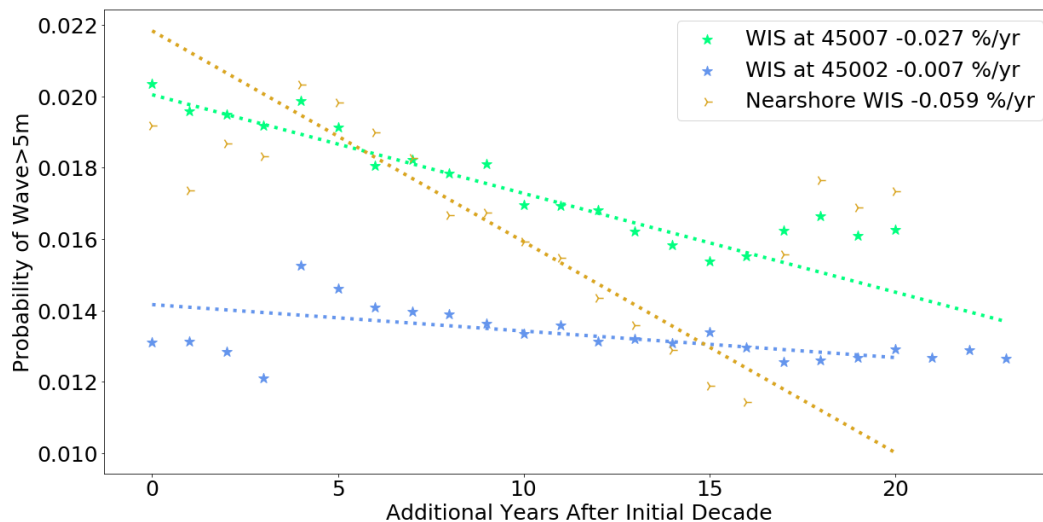


Figure C.9. Slope of Theil-Sen regression on probability of receiving a wave larger than 5m using WIS model at buoy locations and a southern basin nearshore station [38]. Generalized Pareto distributions generated from a growing yearly window of peak $> 2m$ event heights after the first 15 years.

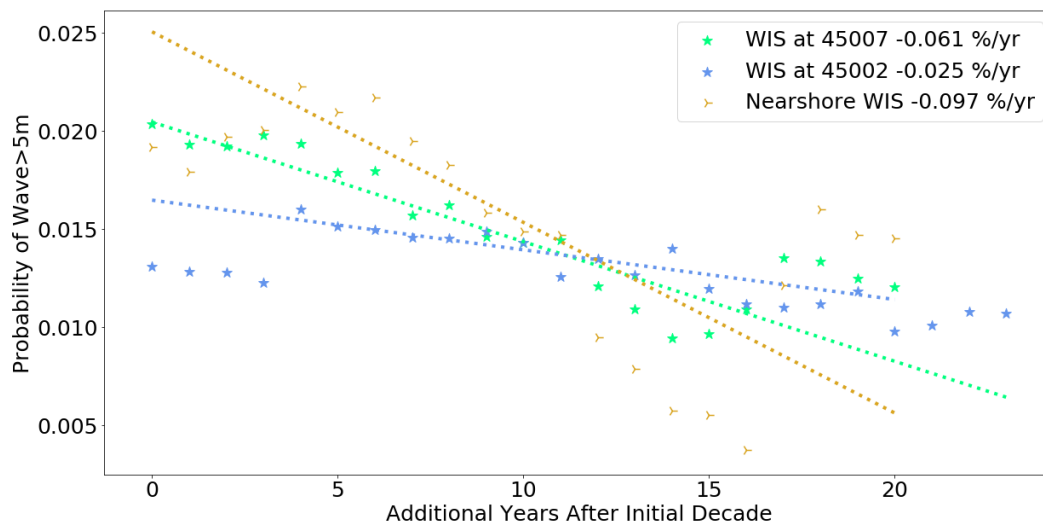


Figure C.10. Slope of Theil-Sen regression on probability of receiving a wave larger than 5m using WIS model at buoy locations and a southern basin nearshore station [38]. Generalized Pareto distributions generated from a moving 10-year window of peak $> 2m$ event heights after the first 15 years.

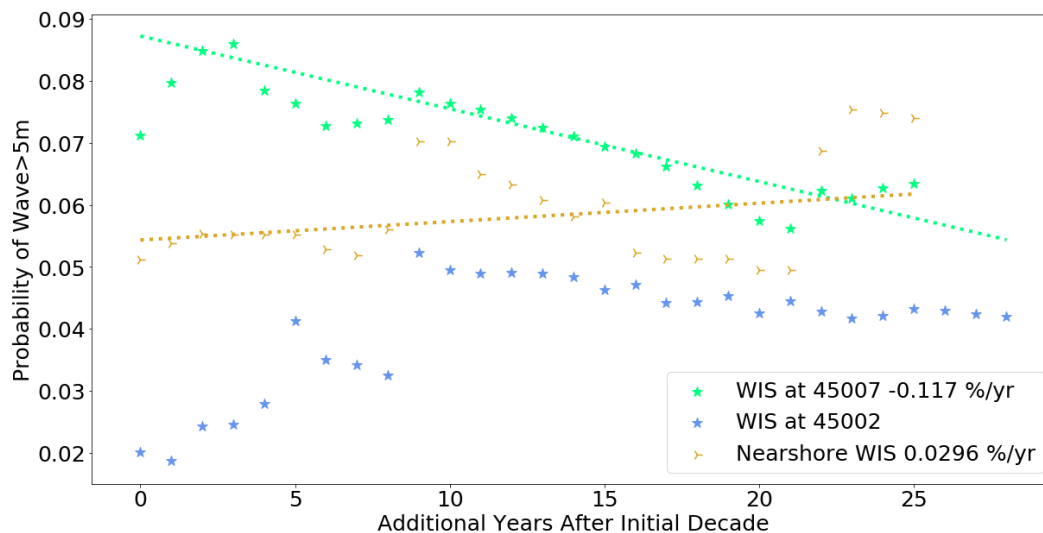


Figure C.11. Slope of Theil-Sen regression on probability of receiving a wave larger than 5m using WIS model at buoy locations and a southern basin nearshore station [38]. Generalized Pareto distributions generated from a growing yearly window of peak $> 3m$ event heights after the first 10 years.

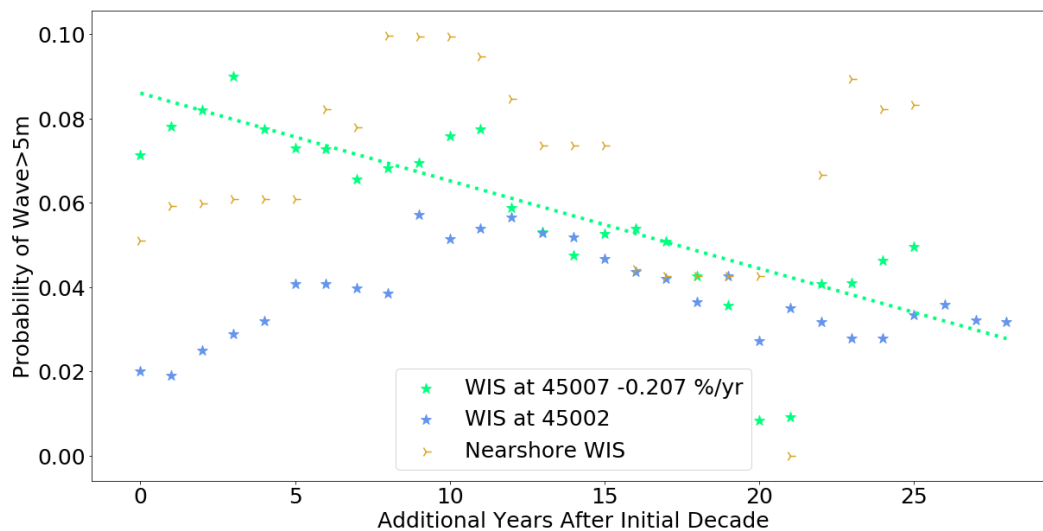


Figure C.12. Slope of Theil-Sen regression on probability of receiving a wave larger than 5m using WIS model at buoy locations and a southern basin nearshore station [38]. Generalized Pareto distributions generated from a moving 10-year window of peak $> 3m$ event heights after the first 10 years.

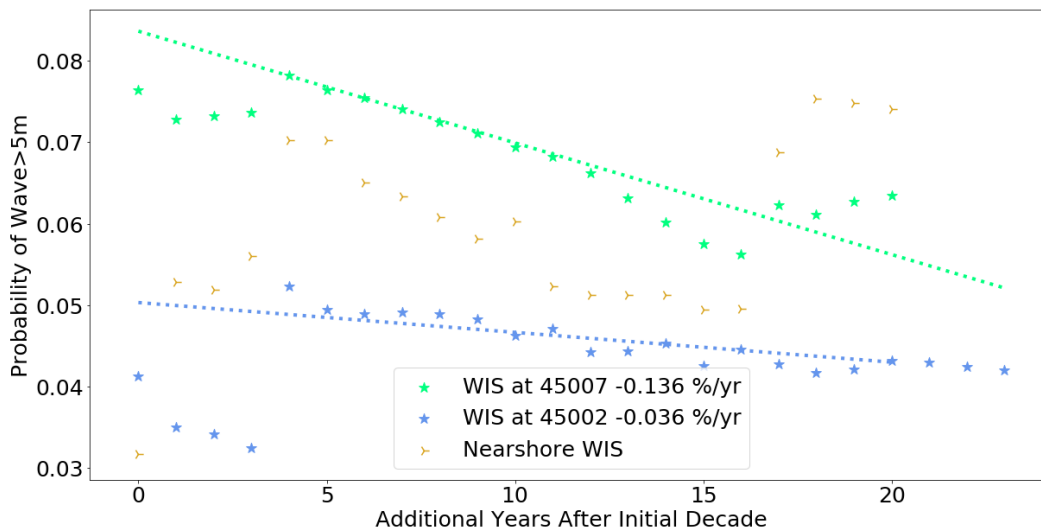


Figure C.13. Slope of Theil-Sen regression on probability of receiving a wave larger than 5m using WIS model at buoy locations and a southern basin nearshore station [38]. Generalized Pareto distributions generated from a growing yearly window of peak $> 3m$ event heights after the first 15 years.

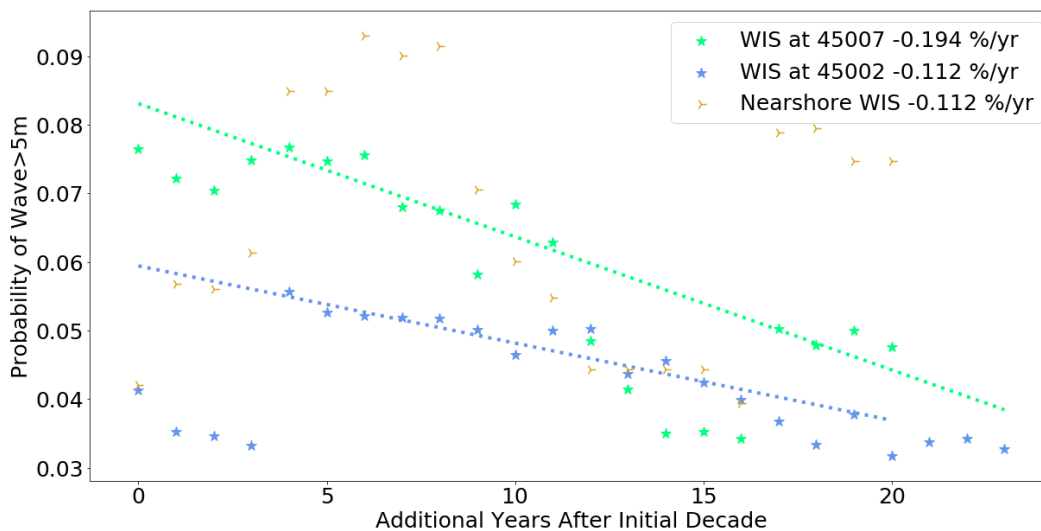


Figure C.14. Slope of Theil-Sen regression on probability of receiving a wave larger than 5m using WIS model at buoy locations and a southern basin nearshore station [38]. Generalized Pareto distributions generated from a moving 15-year window of peak $> 3m$ event heights after the first 15 years.

D. SEASONAL MANN-KENDALL RESULTS FOR DIRECTIONAL
BINS

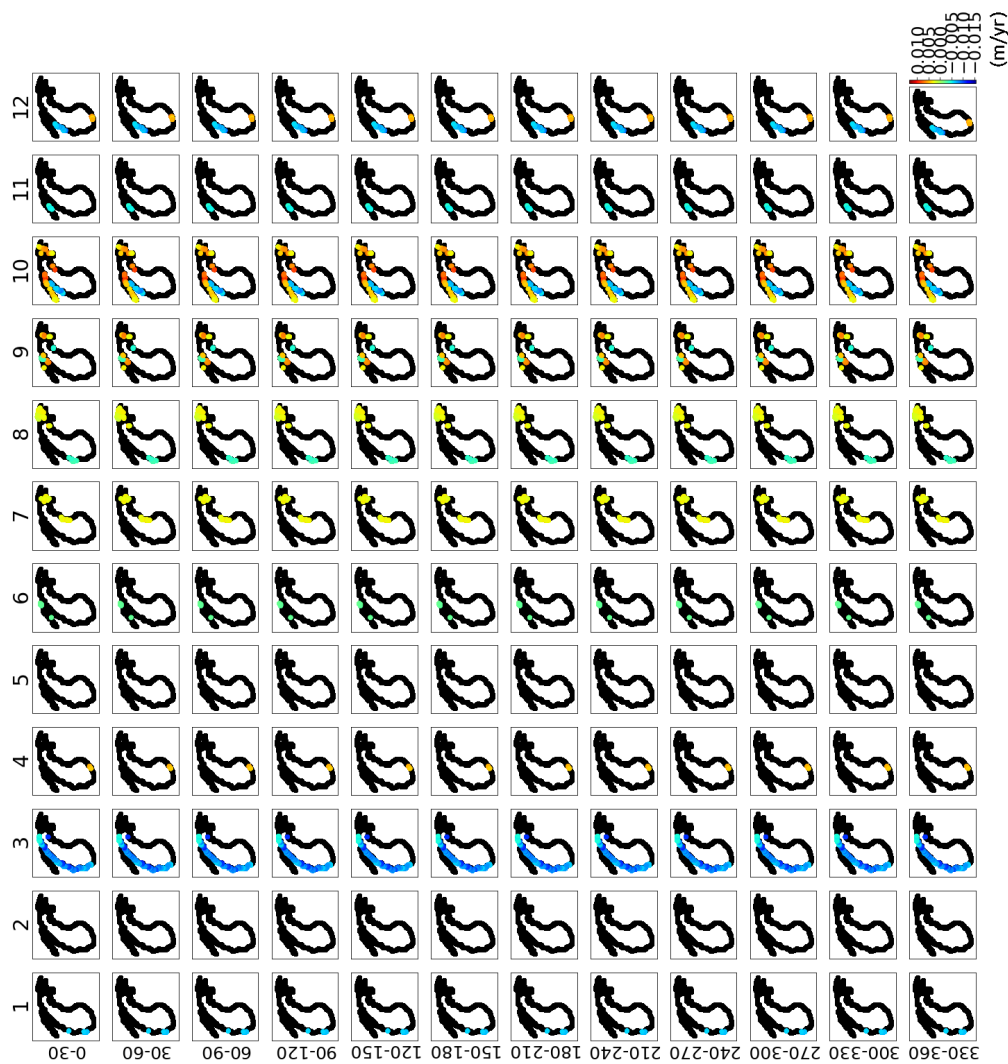


Figure D.1. Seasonal Mann-Kendall test results for monotonic trends in the monthly mean wave heights at all Lake Michigan nearshore stations for isolated 30-degree directional bins. [38].

E. TRENDS IN STORM PARAMETERS

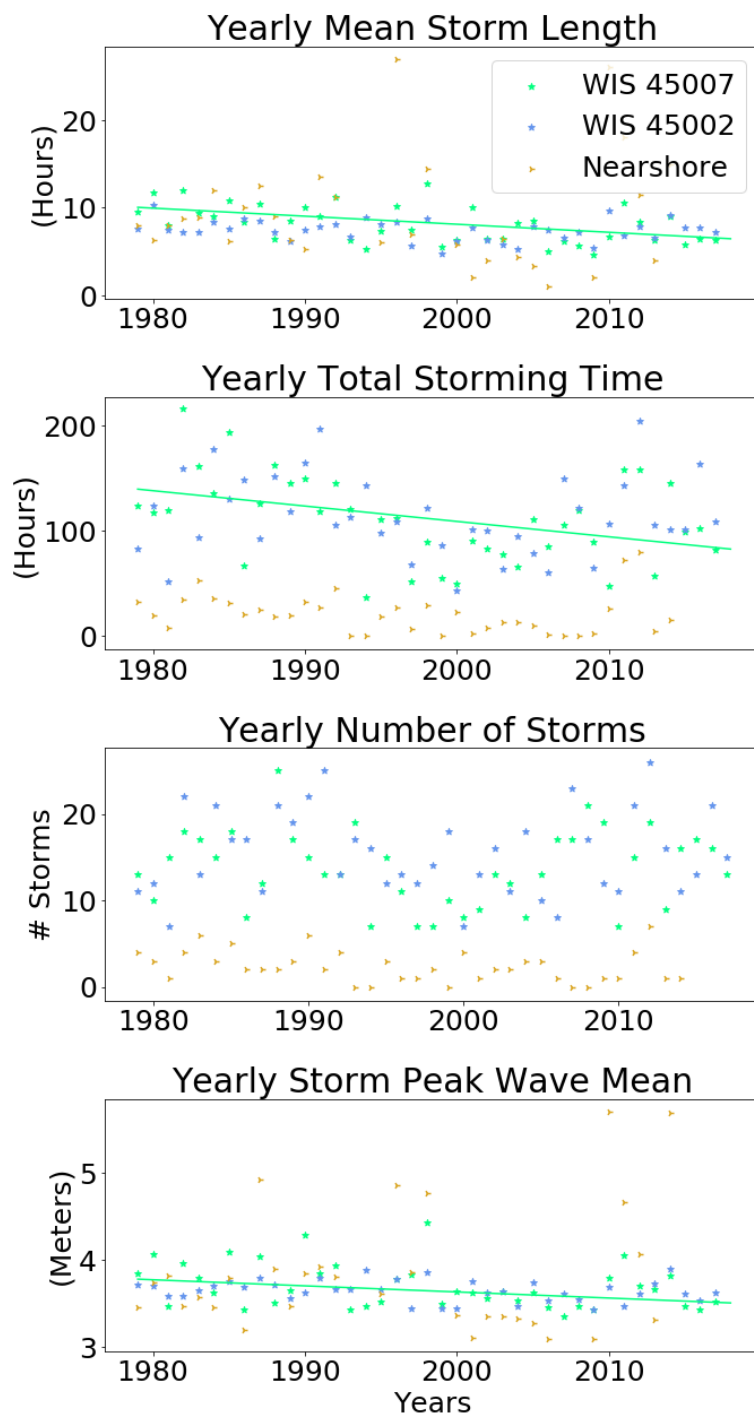


Figure E.1. Annual storm ($H_s > 3\text{m}$) parameter values from WIS model at Lake Michigan buoy locations using entire year of WIS data tested for long term trends using 95% Theil-Sen slope confidence intervals [38].